Role of astrocytic connexins in health and disease

Dissertation
zur
Erlangung des Doktorgrades (Dr. rer. nat.)
der
Mathematisch-Naturwissenschaftlichen Fakultät
der
Rheinischen Friedrich-Wilhelms-Universität Bonn
vorgelegt von
Pavel Dublin
aus Moskau
Bonn 2012

Angefertigt mit Genehmigung der Mathematisch-Naturwissenschaftlichen
Fakulät der Rheinischen Friedrich-Wilhelms-Universität Bonn

1. Gutachter: Prof. Dr. Christian Steinhäuser
2. Gutachter: Prof. Dr. Klaus Willecke
Tag der Promotion: 04.07.2012
Erscheinungsjahr: 2012

Acknowledgments

I am sincerely and heartily grateful to Prof. Dr. Martin Theis for the supervision and guidance of my scientific work, and for his support. I am very grateful to my first supervisor Prof. Dr. Christian Steinhäuser for overall organization of my project and for revision of this thesis. I would like to thank Prof. Dr. Klaus Willecke for being the second supervisor of my thesis. I thank all members of the IZN, especially Dr. Peter Bedner and Dr. Kerstin Hüttman for perfect collaboration and for sharing of their experience. Special thanks to Ina Fiedler, Anja Matijevic and Joana Fischer for excellent technical assistance.

Contents

Glossary

ACSF- Artificial Cerebrospinal Fluid
AHS- Ammon Horn Sclerosis
BAC-Bacterial Artificial Chromosome
BrdU Bromodeoxyuridine
BSA-Bovine Serum Albumin
CA -Cornu Ammonis
CNS-Central Nervous System
Cx -Connexin
DG-Dentate Gyrus
DKO-Double Knock Out
ECFP- Enhanced Cyan Fluorescent Protein
EGFP- Enhanced Green Fluorescent Protein
EYFP- Enhanced Yellow Fluorescent Protein
EEG- Electroencephalogram
floxed-flanked by loxP sites
GFAP-Glial fibrillary acidic protein
GCD -Granule Cell Dispersion
GluT-Glutamate Transporter
GluR-Glutamate Receptor
KI-Knock In
KO-Knock Out
M-Molar
mg-milligram
ml-millilitre
NGS-Normal Goat Serum

PBS-Phosphate buffered saline
PCR-Polymerase chain reaction
PFA-Paraformaldehide
RT-Room Temperature
SGZ-subgranular zone
SE-Status Epilepticus
SVZ-subventricular zone
VPL-ventral posterolateral thalamic nucleus
VPM-ventral posteromedial thalamic nucleus
WT-wild type

Chapter 1

Introduction

1.1 Glial Cells in the Central Nervous System

Glial cells are non neuronal cells in the Central Nervous System (CNS). The term glia (from Greek glue), was a translation of the term "Nervenkitt" introduced by Virchow in 1858. By his opinion, glia is connective tissue completely devoid of any cellular elements (Verkhratsky & Butt, 2007). Later on it was shown, by different anatomists, that glia consists of different types of cells – astrocytes, oligodendrocytes, microglia, and recently, a different cell type was described, the so-called polydendrocytes (Nishiyama et al., 2009), or NG2 glia (Peters, 2004). The proportion of glial cells in the cerebral cortex increases with increasing complexity of the brain (Bass et al., 1971). The lineage relationship between different macroglial cell types was studied by Liu et al. 2002 and reviewed by Nishiyama et al. 2009; a summary is shown in Fig1.1. Until the eighties of the twentieth century, only a function in mechanical stability was attributed to glia, but since then, this view has changed. In fact, it was recognized that glia plays a crucial role in brain functioning. A great variety of ion channels (Verkhratsky & Steinhäuser, 2000) are expressed in glial cells including glutamatergic and non-glutamatergic receptors (de Jesus Domingues et al., 2010; Verkhratsky & Kirchhoff, 2007). NG2 glial cells form synapses with neurons (Bergles et al., 2000; Jabs et al., 2005). Astrocytes are involved in neurogenesis (Pinto & Götz, 2007), and they influence synaptic transmission (Volterra & Steinhäuser, 2004)

and neuronal excitability by spatial buffering of K^+ (Kofuji & Newman, 2004).

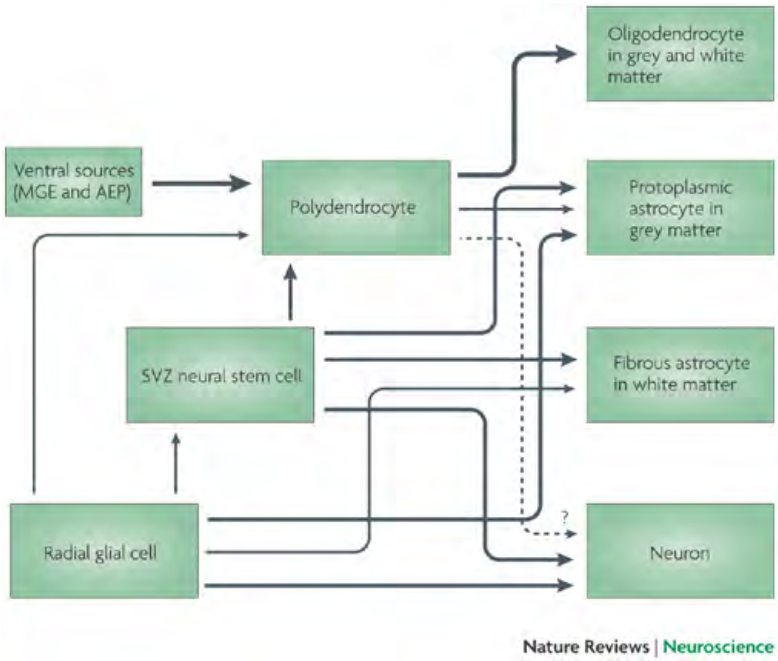

Fig. 1.1: Hypothetical lineage relationship between polydendrocytes (or NG2 cells) and other macroglial cells. The cellular source of each mature cell type is shown. The thickness of the arrows represents the relative contribution of the precursor population. Most polydendrocytes arise from the medial ganglionic eminence (MGE) and the anterior entopeduncular region (AEP), with a minor contribution from radial glia. Polydendrocytes give rise to oligodendrocytes and a subpopulation of protoplasmic astrocytes in the grey matter but do not give rise to white matter astrocytes. Other sources of astrocytes include cells in the subventricular zone (SVZ) and radial glia. The neuronal fate of polydendrocytes is still debated (as indicated by the dotted line). Although most neurons arise from neuroepithelial cells in the ventricular zone, radial glia and cells in the SVZ, a small number of neurons in the piriform cortex might be generated from NG2 positive cells in the adult brain (modified from Nishiyama et al. 2009).

1.1.1 Astrocytes

Astrocytes are the most abundant cell type in the CNS. The term"astrocyte" is an umbrella term which covers different cell types in the brain. According to Reichenbach and Wolburg (Reichenbach & Wolburg, 2005) eleven main types of astroglia exist (Fig 1.2): protoplasmic astrocytes, velate astrocytes, fibrous astrocytes, perivascular astrocytes, Bergmann glia, radial astrocytes, Müller

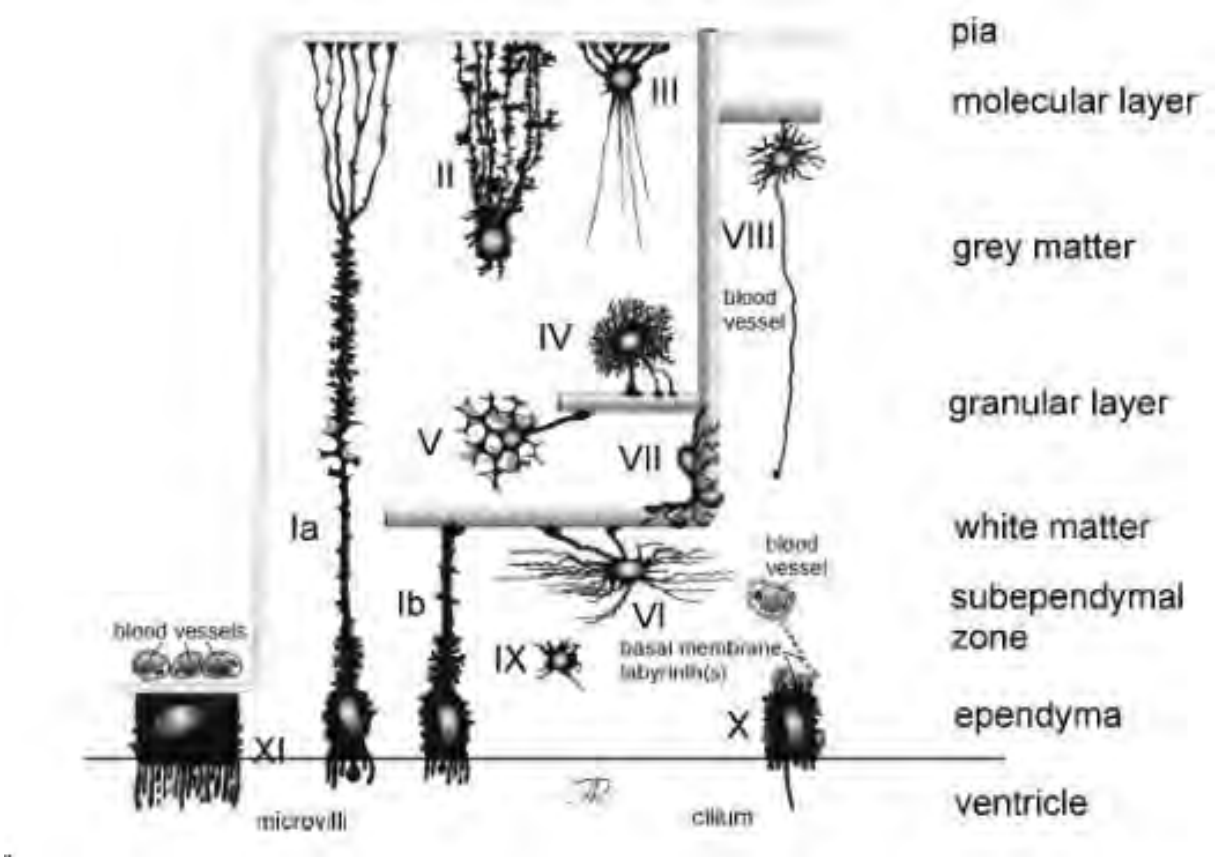

Fig. 1.2: Morphological types of astrocytes. Ia – pial tanycyte; Ib – vascular tanycyte; II– radial astrocyte (Bergmann glial cell); III – marginal astrocyte; IV – protoplasmic astrocyte; V – velate astrocyte; VI – fibrous astrocyte; VII – perivascular astrocyte; VIII – interlaminar astrocyte; IX – immature astrocyte; X – ependymocyte; XI – choroid plexus cell. (From:Reichenbach & Wolburg 2005)

glia, marginal glia and ependymal glia. All these cell types have different morphology - but have two common features - the first feature is the formation of specific processes – endfeet contacting the basal lamina of blood vessels and/or the *pia mater* or the vitreous body of the eye. The second feature is coupling by gap junctions. Astrocytes are involved in many brain functions, and influence neuronal activity in different ways: astrocytes guide neurites and are essential for synapse formation (Ullian et al., 2001; Slezak & Pfrieger, 2003). Astrocytes are implicated in the glutamate–glutamine cycle (glutamate is the main excitatory neurotransmitter in the CNS). Glutamate removal from

the synaptic cleft is critical for normal synaptic function. Astrocytes remove up to 80 % of glutamate from the synaptic cleft (Verkhratsky & Butt, 2007) mostly by the glutamate transporter GLT-1 (the human homologue is called EAAT2 Haugeto et al. 1996; Furness et al. 2008). After uptake of glutamate into astrocytes, it is converted to glutamine mainly by the astrocyte specific enzyme Glutamine Synthetase (GS; Liaw et al. 1995). Glutamine is transported into the extracellular space where it is taken up by neurons and again converted to glutamate (Bröer & Brookes, 2001). Glutamate could be, also, released from astrocytes using different mechanisms (Kimelberg et al., 1990; Szatkowski et al., 1990; Duan et al., 2003). Glutamate release from astrocytes may play a role in the astrocytic modulation of neuronal currents and synaptic transmission (Araque et al., 1998; Kang et al., 1998). Another important feature of astrocytes is the ability to regulate blood flow. Changes in neuronal activity cause an elevation of the calcium level in astrocytes which in turn change the diameter of the brain arterioles (reviewed by Iadecola & Nedergaard 2007; Jakovcevic & Harder 2007). Astrocytes are important for blood brain barrier (BBB) formation and maintenance. The BBB is constituted by endothelial cells which form tight junctions and are surrounded by astrocytic endfeet. Physical contact between astrocytes and endothelial cells is important for the formation of tight junctions. In the absence of astrocytes formation of tight junctions by endothelial cells is impaired (Isobe et al., 1996) . The Glial Fibrillary Acidic Protein (GFAP), an astrocytic intermediate filament seems to be required for this process, since a similar effect was observed in GFAP KO mice (Pekny et al., 1998). Some astrocytic functions are closely related to gap junctional coupling. These functions are reviewed in chapter 1.2.3.

Astrocytic markers

GFAP is an intermediate filament protein important for the cytoarchitectural stability of the cell (Liedtke et al., 1998), and its expression increases during reactive gliosis that occurs as a response to brain injury and disease (Eddleston & Mucke 1993, reviewed by Middeldorp & Hol 2011; Eng et al. 2000). GFAP is considered as a specific marker for astroglia (Ludwin et al.,

1976; Bignami et al., 1972) and cells from the astrocytic lineage. GFAP is expressed by mature astrocytes, starting from the stage of myelination (P5 in rats Dahl 1981) and by radial glia like cells (Alvarez-Buylla et al., 2002; Shapiro et al., 2005). Astrocytes in cortical layers III and IV do not express GFAP, except for cells clustering around blood vessels (Stichel et al., 1991).

S100β is a calcium binding protein involved in the regulation of astrocytic proliferation and activation (Brozzi et al., 2009). S100β is expressed mainly in astrocytes (Boyes et al., 1986; Ogata & Kosaka, 2002), results demonstrating expression of S100β in NG2 cells are controversial (see 1.1.1.1).

Glutamine Synthetase The main function of GS is ATP dependent conversion of glutamate to glutamine (Liaw et al., 1995). GS is expressed predominantly by astrocytes (Norenberg & Martinez-Hernandez, 1979), but its expression was also reported in a fraction of gray matter oligodendrocytes (Miyake & Kitamura, 1992).

1.1.1.1 NG2 Cells

NG2 cells are also called polydendrocytes (Nishiyama et al., 2002), synantocytes (Butt et al., 2005), NG2 positive cells (Nishiyama, 2001) or GluR cells (Wallraff et al., 2004) and are a newly identified type of glia. This type of glia is characterized by expression of platelet-derived growth factor receptor α (PDGFRα) and NG2 (an integral membrane chondroitin sulphate proteoglycan). In white matter the NG2 positive cells give rise to oligodendrocytes, whereas in the gray matter the NG2 positive cells are mostly mature postmitotic cells (Dimou et al., 2008).

Reports about S100β expression in NG2 cells are contradictory. From no overlap between S100β and NG2 (Nishiyama et al., 1996) to almost 100% overlap between S100β and NG2 (Deloulme et al., 2004) were reported. Utilizing mice expressing EYFP under control of all regulatory elements of the NG2 gene, Karram and colleagues observed 20 % of colocalization of EYFP with S100β in juvenile mice and 31% in adult mice (Karram et al., 2008). In cortex of PDGFRαCreERT2 mice 10 % YFP positive cells were also S100β positive

(Rivers et al., 2008). From all this data we can conclude that only a subset of NG2 glia is also S100β positive.

1.1.2 Microglia

Microglial cells are the resident macrophages of the CNS. They are derived from fetal macrophages which invade the brain during development (Perry et al., 1985). The proportion of microglia in the adult mouse brain varies between 5% in the *corpus callosum* and *cortex* and 12% in the *substantia nigra* (Lawson et al., 1990). The number of microglial cells increases with age (Vaughan & Peters, 1974). In adult brain, microglia exists in three different forms: 1) ramified microglia, 2) activated microglia and 3) reactive (phagocytotic) microglia. Ramified (resting) microglia is the most prominent type of this cell population in the adult brain. It is characterized by long thin processes and a small cell body. In the case of brain damage or inflammation, microglial cells change their morphology to swollen ramified microglia with thick processes and a bigger cell body. This state is called activated microglia. Stronger damage to the brain, for example stroke, causes transformation of activated or resting microglia to a round-shaped, reactive phagocytic form (reviewed by Streit et al. 1988; Davis et al. 1994; Hanisch & Kettenmann 2007).

Microglial markers

Iba-1 (ionized calcium-binding adapter molecule 1) is expressed in the monocytic lineage. In the brain Iba-1, is expressed predominantly by microglia (Imai et al., 1996; Hirasawa et al., 2005).

Lectins such as GSA, GS-1, RCA, WGA, and ConA, bind to specific sugar groups of the cell walls. Lectins stain both ramified and activated microglia. In addition, lectins stain endothelial cells (Streit, 1990; Colton et al., 1992).

CD11b/18 (CD11b in rat, CD18 in mouse) is a complement receptor 3 (CR3) and belongs to the family of β-2 integrins (Akiyama & McGeer, 1990).

CD11b/18 is expressed constitutively by macrophages and microglia (Akiyama & McGeer, 1990).

CD68 (macrosialin in mouse, ED-1 in rat) plays a role in phagocytosis and Low Density Lipoprotein (LDL) binding. CD68 is expressed at low level in resting microglia and at high level in activated microglia (Slepko & Levi, 1996; Kingham et al., 1999).

1.1.2.1 Oligodendrocytes

Oligodendrocytes are the cells that produce the myelin sheath surrounding axon in the central nervous system. Oligodendrocytes are classified into four different subtypes according to the size of their somata, the number and orientation of their processes and the diameter of associated axons (Butt, 2005). Commonly used oligodendrocytic markers are 2',3'-cyclic nucleotide 3'-phosphodiesterase (CNPase, McEwan 1996) and the oligodendrocyte specific transcriptional factor OLIG2 (Yokoo et al., 2004).

1.2 Astrocytic Connexins

1.2.1 Gap Junctions

Gap junctions are channels connecting the cytoplasm of two adjacent cells. These channels consist of two hemichannels or connexons (one for each cell). Each connexon is built of six connexins subunits (Makowski et al., 1977). The connexin protein structure was predicted by hydropathy plots and confirmed by immunohistochemistry and proteolytic cleavage (Zimmer et al., 1987; Milks et al., 1988; Goodenough et al., 1988; Yancey et al., 1989). Connexin proteins have four transmembrane domains, two extracellular domains, a cytoplasmic N and C terminus and one cytoplasmic loop (see Fig. 1.3). The internal diameter of the gap junction pore is 10 to 14 angstroms and permeable for molecules up to 1200 Dalton (Simpson et al., 1977). Small RNAs, glucose, cAMP, amino acids, calcium ions (Sáez et al., 1989) and many other molecules (reviewed in Harris 2001) can pass through gap junctions. A few thousand of single channels

group together to form a plaque (Caspar et al., 1977; Hoh et al., 1993). The connexin gene family includes 21 genes in the human genome and 20 in the mouse genome (reviewed in Söhl & Willecke 2003; Beyer & Berthoud 2009). Connexins are named according to their molecular weight, i.e. a connexin protein with the molecular weight of 43 kDa is called connexin 43 (Beyer et al., 1987).

1.2.2 Astrocytic gap junctions

Electrophysiological studies of glial cells showed that they are electrically coupled (Kuffler et al., 1966), and that the structures connecting the cells are gap junctions (Brightman & Reese, 1969). The first type of gap junction identified in astrocytes was Cx43 (Dermietzel et al., 1989; Yamamoto et al., 1990a,b). Later, the expression of two additional astrocytic connexins – Cx30 (Nagy et al., 1999; Rash et al., 2001) and Cx26 (Nagy et al., 2001, 2011) was shown. The expression of Cx40, Cx45 and Cx46 was observed in cultured astrocytes from newborn Cx43 knock out mice (Dermietzel et al., 2000), but their presence in astroglia of the intact brain and their possible physiological function remains unclear.

1.2.3 Cx43 and Cx30

Connexins 43 and 30 are the main astrocytic connexins in CNS. In Cx43 KO mice astrocytic gap junctional coupling measured by spread of tracer, was reduced by 50% (Theis et al., 2003). In Cx43 Cx30 DKO mice, interastrocytic gap junctional coupling was completely lacking (Wallraff et al., 2006).

1.2.4 Functions of the astrocytic gap junctions

1.2.4.1 Spatial buffering of K^+

As a result of neuronal activity, both normal and pathological, extracellular K^+ is elevated (Syková, 1981; Syková & Chvátal, 1993; Heinemann & Lux, 1977). High concentrations of K^+ impairs neuronal excitability. Thus, for normal neuronal function the excess of extracellular K^+ must be removed. The main

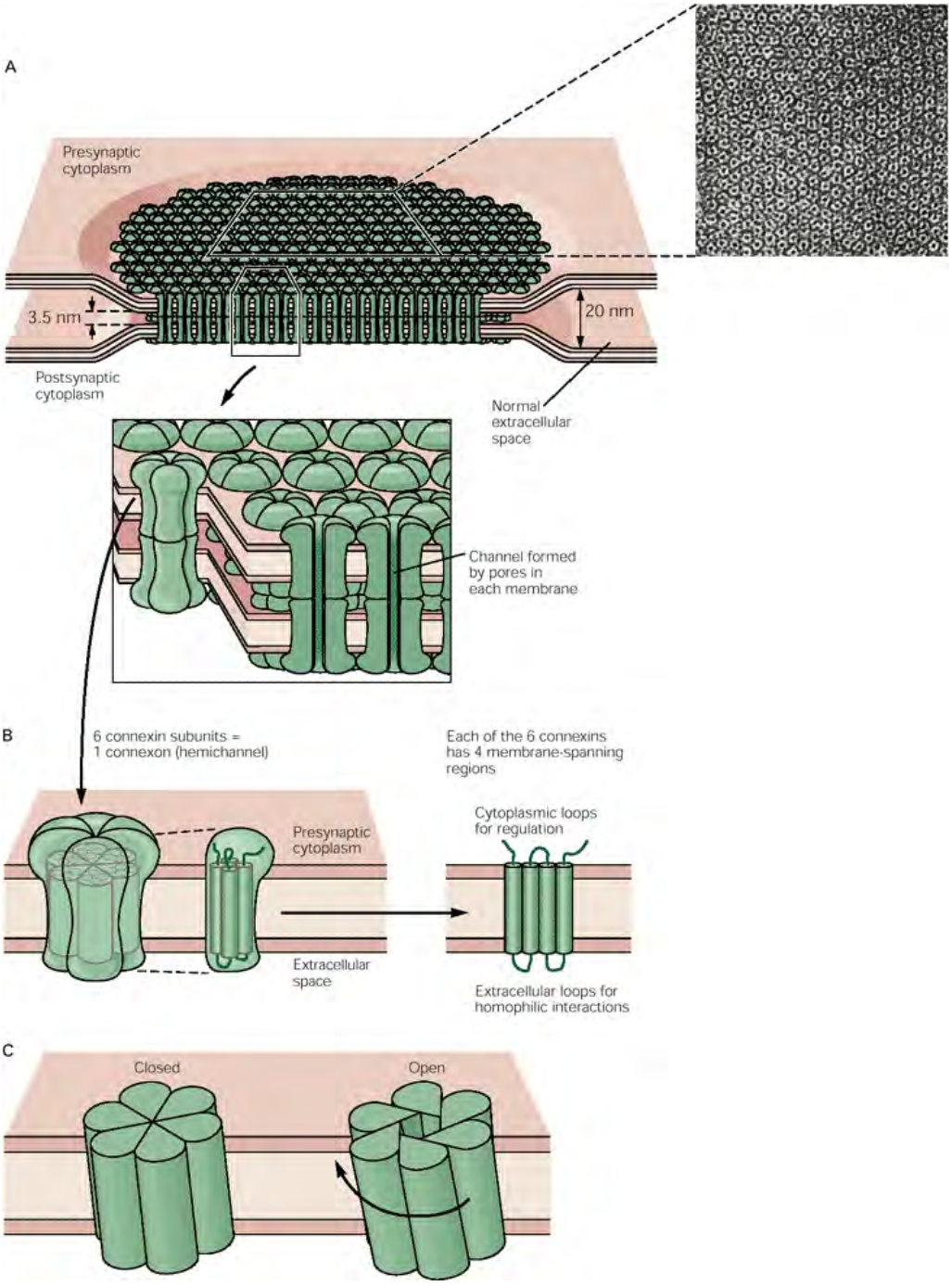

Fig. 1.3: Gap Junction Structure. A. A gap-junction channel is actually a pair of hemichannels, one in each opposite cell, that match up in the gap junction through homophilic interactions. The channel thus connects the cytoplasm of the two cells and provides a direct means of flow between the cells. This bridging of the cells is facilitated by a narrowing of the normal intercellular space (20 nm) to only 3.5 nm at the gap junction. Electron micrograph: Each channel appears hexagonal in outline. Magnification × 307,800. B. Each hemichannel, or connexon, is made up of six identical protein subunits called connexins. Each connexin is about 7.5 nm long and spans the cell membrane. A single connexin is thought to have four membrane-spanning regions. C. The connexins are arranged in such a way that a pore is formed in the center of the structure. The resulting connexon, with an overall diameter of approximately 1.5-2 nm, has a characteristic hexagonal outline. The pore is opened when the subunits rotate about 0.9 nm at the cytoplasmic base in a clockwise direction.(from Kandel et al. 2000)

mechanism of K^+ removal from the extracellular space is K^+ spatial buffering (Kofuji & Newman, 2004; Orkand et al., 1966). In the Müller cells of the retina, this mechanism is termed K^+ siphoning (Newman et al., 1984). In this mechanism K^+ is transferred from a place with high extracellular concentration to a place with low extracellular concentration through the astrocytic syncytium. The inwardly rectifying K^+ channels Kir4.1 are responsible for most of the K^+ uptake by astrocytes (Djukic et al., 2007). Kir4.1 K^+ localized predominantly on the astrocytic processes surrounding synapses, and astrocytic endfeet wrapping blood vessels (Higashi et al., 2001; Neusch et al., 2006), and due to its localization may serve as a main efflux of K^+ out of astrocytic syncytium (Butt & Kalsi, 2006). Kir4.1 is highly colocalized with the water transport protein aquaporin4 (Nagelhus et al., 1999). Efflux of K^+ from the astrocytes to the blood is followed by massive water efflux (reviewed in Rash 2010; Simard & Nedergaard 2004). For the mechanism of K^+ buffering astrocytic gap junctional coupling is necessary. Animals with genetic deletion of Cx30 and Cx43 show impaired spatial K^+ buffering and increased epileptiform activity (Wallraff et al., 2006).

1.2.4.2 Transport of glucose and metabolites

Astrocytes, due to their position between blood vessels and neurons, can transfer glucose and metabolites to the neurons from the blood. Currently, two models of the mechanism of glucose and metabolites transfer to the neurons are proposed (reviewed in Barros & Deitmer 2010). According to the first model, astrocytes transfer metabolites to neurons, neurons metabolize it and release lactate (i.e. neurons are involved only in the anaerobic stage of glycolysis), which is absorbed by astrocytes and partially metabolized, partially transfered to the blood flow. According to the second model (astrocyte-to-neuron-lactate shuttle hypothesis, ANLSH, Pellerin & Magistretti 1994), astrocytes take up the glucose and metabolize it to lactate, then the lactate is transferred to neurons and metabolized by them (i.e. neurons are involved only in the aerobic stage of glycolysis). To supply metabolites effectively, astrocytes have to form a syncytium coupled by gap junctions. Transfer of glucose from the blood flow

is completely absent in Cx30/Cx43 double KO mice (Rouach et al., 2008).

1.2.4.3 The role of Cx30 and Cx43 in neurogenesis

Neurogenesis is a process of the generation of neurons from stem cells. Until the eighties of the twentieth century, despite of some reports (Altman & Das, 1967, 1965), it was widely accepted, that neurogenesis occurs only during developmental stages of ontogenesis. However recent studies clearly showed that neurogenesis occurs likewise in the adult brain (Goldman & Nottebohm, 1983; Eriksson et al., 1998; Kempermann et al., 1997). Adult neurogenesis occurs mainly in two places in the brain: in the Subgranular Zone (SGZ) of the dentate gyrus and in the Subventricular Zone (SVZ) of the lateral ventricle (Ming & Song, 2005). The neuronal progenitors in the adult brain are called radial glia-like cells (other names: type I progenitor cells, radial astrocytes, vertical astrocytes; Ehninger & Kempermann, 2008; von Bohlen Und Halbach, 2007; Kempermann et al., 2004), which belong to the neuroepithelial $\rightarrow$ radial glia $\rightarrow$ astrocyte lineage. Radial glia-like cells express the astrocytic markers GFAP and nestin, but do not express S100β (von Bohlen Und Halbach, 2007; Ehninger & Kempermann, 2008). These cells give rise to both neurons and glia (Alvarez-Buylla et al., 2001). Type I progenitor cells divide asymmetrically and give rise to type IIa cells, which are negative for the immature neuronal marker doublecortin (DCX). They also generate type IIb cells which are DCX-positive and Prox-1 positive - progenitor cells (Kronenberg et al., 2003; Steiner et al., 2008; Ehninger & Kempermann, 2008). Both these cell types are GFAP negative and nestin positive, and they are proliferative. Type II progenitor cells give rise to nestin negative and DCX-positive, proliferating type III progenitor cells (Kronenberg et al., 2003). The next two stages of adult neurogenesis are: immature neurons which are expressing the Ca^{2+}-binding protein calretinin and DCX and mature granule neurons which are expressing the Ca^{2+}-binding protein calbindin (Brandt et al., 2003; Kempermann et al., 2004). Cx43 and Cx30 were shown to be crucial for adult neurogenesis. Mice lacking both Cx43 and Cx30 show a low proliferation rate in the SGZ and a reduction in the number of granule cells in the dentate gyrus (Kunze et al., 2009).

1.3 The Cre/LoxP system

The Cre/LoxP system is the main tool for mouse genome manipulation (Nagy, 2000). The Cre recombinase is a site specific recombinase from the E.Coli bacteriophage P1. It is used by the bacteriophage for incorporation of the phage genome into the E.Coli genome. No additional proteins are necessary for Cre recombinase action (Sauer & Henderson, 1988). The Cre recombinase binds to 34bp long recognition sites which are called LoxP sites. The DNA flanked by LoxP sequences is called "floxed" DNA. Depending on the orientation of LoxP sites a floxed part of DNA could be inverted or excised. Two monomers of Cre bind to a LoxP site (one to each strand of the DNA) and form a dimer. Two Cre dimers from two LoxP sites form a tetramer, and recombination occurs (Guo et al., 1997). As result of the recombination, the DNA between two directly oriented LoxP sites is irreversibly excised (Figure 1.4).

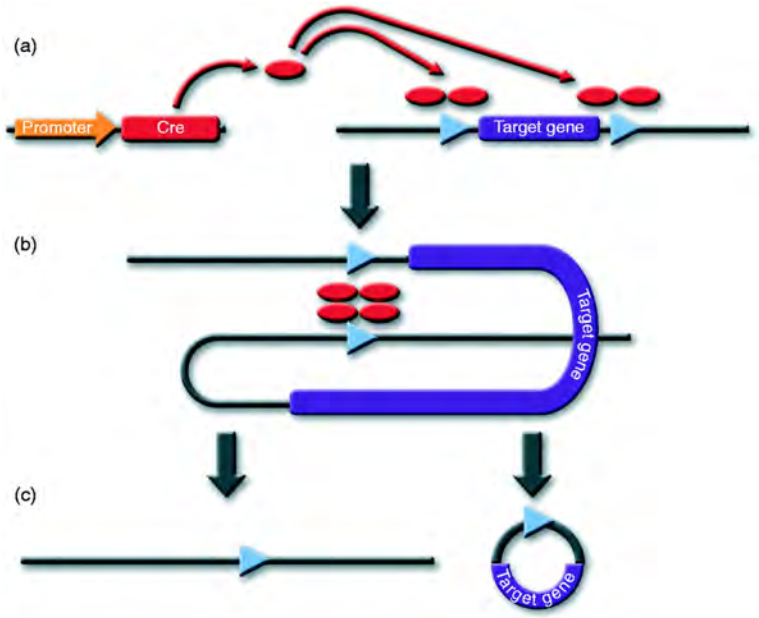

Fig. 1.4: Cre mediated DNA recombination. (a) Cre expression is driven by an exogenous promoter of choice, enters the cell nucleus and binds to LoxP sites flanking a target gene. (b) The DNA surrounding the target gene undergoes a conformational change to bring the two LoxP sites into close proximity where a synaptonemal complex is formed. DNA strand exchange occurs at the sites of homology leading to the excision of the target gene (c) and the presence of a single LoxP site (generated from two half-sites) at the original genomic location (modified from Smith, 2011)

.

By expression of Cre recombinase under a cell-type specific promoter, deletion of a gene can occur in a specific cell type (Gu et al., 1994). A floxed coding region could be followed by a reporter gene. As a result of the gene deletion, the reporter gene is expressed instead of the deleted gene (Theis et al., 2001b). For Cre activation at a specific time point, a fusion protein of the Cre recombinase and the ligand binding domain of a mutated estrogen receptor (CreERT) was generated (Metzger et al., 1995; Feil et al., 1996). The modified receptor is activated by tamoxifen and 4-hydroxytamoxifen (4-OHT), but not by estradiol itself. CreERT is located in the cytoplasm, where it is bound to heat shock proteins (Picard, 1994; Mattioni et al., 1994). After 4-OHT application, the CreERT- heat shock protein complex is dissociated, CreERT is translocated to the nucleus where it induces recombination (Hayashi & McMahon, 2002).

1.4 Anatomy and functions of the mouse brain regions investigated in this study

1.4.1 The Hippocampus

The hippocampal formation is a part of the limbic system responsible for explicit memories (declarative memory- the ability to recall facts and events), and for spatial memory (Martin, 2003). The hippocampal formation consists of the Ammon's horn (or Cornu Ammonis), the dentate gyrus, and the subiculum. Each structure consists of several regions(Fig. 1.5 A).

1.4.1.1 Anatomy of the hippocampus

Cornu Ammonis (CA) is differentiated into regions three regions: CA1, CA2, and CA3. CA is also structured to clearly separated layers. **Layers of CA**: *Stratum pyramidale*. The layer of the Cornu Ammonis contains the cell bodies of the pyramidal neurons. The *stratum oriens* contains the basal dendrites of the pyramidal cells, and a variety of interneurons. This layer is located just above pyramidal cell layer, and below the corpus callosum. A very thin layer below the *stratum pyramidale* in the CA3 region contain mossy fibers and is named *stratum lucidum*.The *stratum radiatum* is located below the *stratum pyramidale* in the CA1 and CA2 regions and below the *stratum lucidum* in the CA3 region. This layer contains the Schaffer collaterals (projections from CA3 to CA1) as well as other commisural projections, dendrites of the pyramidal cells and interneurons. The *stratum lacunosum-moleculare* contains the apical dendrites of the pyramidal cells. In this layer, projections from the entorhinal cortex, the nucleus reuniens and the thalamus terminate. The *hippocampal fissure* or *sulcus* serves as border between *dentate gyrus* and the Ammon's horn. Layers of *dentate gyrus*: Closest to the *hippocampal fissure* is the *stratum moleculare*. This layer mainly consists of dendritic trees of the granule cells. The *stratum granulosum* or granule cell layer is comprised of the principal neurons of the dentate gyrus. This layer is 6-8 cells thick, and together with the *stratum moleculare* forms a V shaped structure. The polymorphic layer (*hilus*) of the dentate gyrus consists of axons of granule cells (proximal part

of mossy fibers), and of interneurons (accordingly to Martin, 2003; Insanti & Amaral, 2004; Taupin, 2008; Amaral & Lavenex, 2006.)

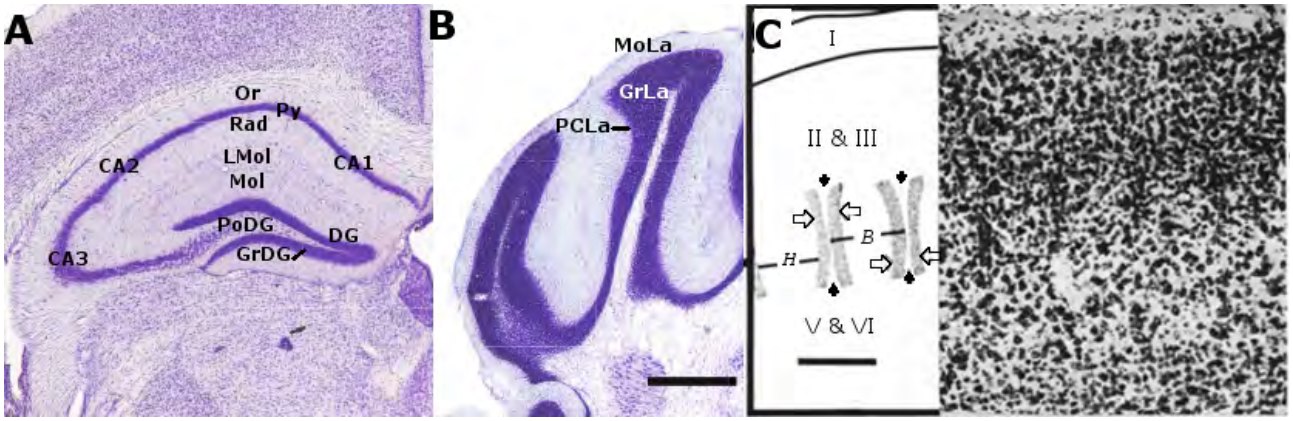

Fig. 1.5: Anatomy of the regions used in this work. **A.** Anatomy of the hippocampus. barrel field. S1Tr primary somatosensory cortex trunk region. Py- pyramidal cell layer, CA1, CA2, CA3 regions of the pyramidal cell layer. Or- stratum oriens of hippocampus, Rad-stratum radiatum, Lmol-stratum lacunosum-moleculare, Mol-stratum moleculare, DG-dentate gyrus GrDG-granular layer of dentate gyrus, PoDG-polymorph layer of dentate gyrus (hilus, modified from Paxinos & Franklin 2001). **B.** Anatomy of the cerebellum. GrLa-Granular layer, MoLa-Molecular layer, PCLa-Purkinje cell layer. Bar=400 μm, for A and B (modified from Paxinos & Franklin 2001). **C**. Barrel field in somatosensory cortex. Barrel components: each barrel (B) is made up of a ring of high cell density, the side (stippling), which surrounds a less cellular area, the hollow (H). A wall (between hollow arrows) consists of the sides of two adjoining barrels and the intervening septum (marked by black arrow). Roman numerals indicate cortical layers. Bar=100 μm. (modified from Woolsey & der Loos, 1970).

1.4.1.2 Functions of the hippocampus

In rodents the hippocampus is most important for spatial memory and space representation . The hippocampus contains so called place cells whose firing is dependent on the mouse place in the space (O'Keefe & Nadel, 1978). Place cells, together with head direction cells in the presubiculum (Taube et al., 1990) and grid cells (Hafting et al., 2005) in the entorhinal cortex form the system of spatial orientation in rodents. **In human** hippocampus, in addition to the role in the spatial memory (people with bilateral hippocampal lesion can recall old spatial memories but cannot achieve new memories; Teng & Squire, 1999; Rosenbaum et al., 2000), plays a role in explicit memory (memory with

possibility of conscious recollection). Explicit memory is divided into episodic (the ability to recollect previous experiences) and into semantic (the ability to recollect general facts; Tulving, 1972). In patients with hippocampal lesions, episodic memory is damaged more severe than the semantic memory. The hippocampus is not involved in implicit memory (the type of memory that is involved in the tasks which is not required the conscious recollection i.e the type of memory which is used in professional activities, or for performing everyday tasks, etc. Squire & Zola, 1997).

1.4.1.3 Pathology of the hippocampus

Diseases such as schizophrenia, epilepsy, Alzheimer's disease and many others cause pathological changes in the hippocampus. Most prevalent of them are epilepsy and Alzheimer's disease. Alzheimer's disease has a higher prevalence than epilepsy in developed countries because of high proportion of aged people. For example in 2000, in USA 1.6% of population suffered from Alzheimer's disease (Hebert et al., 2003) and 0.9% of population suffered from epilepsy (Begley et al., 2000), but in the whole world, epilepsy has a higher prevalence: about 0.36% of the world population is suffering from Alzheimer's disease (Ferri et al., 2005), whereas about 0.4-1% of the world population is suffering from epilepsy, and 40-70 new cases per 100000 people per year occur (Squire & Zola, 1997; Sander, 2003). Most of all epilepsy cases are Temporal Lobe Epilepsy (TLE) - a type of epilepsy that in 65 % of all cases is associated with pathological changes in the hippocampus - Ammon's Horn Sclerosis (AHS; Engel, 1998). The main pathological changes in AHS are massive neuronal cell loss and gliosis in the CA1 region, granule cell dispersion in the dentate gyrus, and only minor cell loss in the CA3 region (Armstrong, 1993; Margerison & Corsellis, 1966).

1.4.2 Primary somatosensory cortex

In rodents, the primary somatosensory cortex (S1) is a brain region, which contains the body surface representation with a clear domination of the face and whisker areas (Tracey, 2004). The S1 area in rodents is corresponding to

the 3b area of the primate somatosensory cortex (Kaas, 2004). The primary somatosensory cortex is a typical koniocortex (or granular cortex; Nieuwenhuys et al., 2007) consist of six layers with layer IV rich in granular cells and poorly distinguishable layers II and III (Wise & Jones, 1978). In addition to the granular cells ,large body pyramidal cells were observed predominantly in the layers III, V, VI (Simons & Woolsey, 1984). In layer IV of the part of S1 which represents the head, barrel structures are clearly visible (Fig.1.5 C). On coronal sections, barrels are rectangular shaped and on tangential sections elliptically shaped structures. Each barrel has a ring with high cell density on the periphery named *side*. In the middle of the barrel, an area with lower granule cells density is located named the *hollow*. Each barrel is separated from adjacent cells by a nearly acellular structure -the *septum* (Woolsey & der Loos, 1970). The number of barrels is corresponding to the number of whiskers (vibrissae), and each barrel represents one whisker (Welker & Woolsey, 1974; Woolsey et al., 1975).

1.4.3 Cerebellum

The cerebellum is part of the brain which plays a crucial role in motor coordination. The cerebellum is comprised of three main parts - cortex, white matter and cerebellar nuclei (Martin, 2003) The cerebellar cortex (Fig.1.5 B) consists of three layers. The superficial layer of cerebellar cortex is molecular layer which contains processes of neurons and scattered cell bodies of small neurons. The profound layer of cerebellar cortex is called granule cell layer. This layer consist of densely packed small neurons. Between these two layers a single layer is located - the Purkinje cell layer. In this layer, the cell bodies of big Purkinje neurons are located (Mescher, 2009). In the same layer, Bergman glia cells are located, which are a special type of cerebellar astrocytes (Grosche et al., 2002). Even thought the main function of the cerebellum is motor coordination, it also plays a role in implicit memory (Molinari et al., 1997; Doyon et al., 1997) and in emotional control (reviewed by Schutter & van Honk, 2005).

Chapter 2

Aim of this work

Despite of the growing knowledge about astrocytic connexins, their expression pattern and function is not yet fully elucidated. The main goal of this study was, by using novel transgenic tools, to clarify the expression pattern of the astrocyic connexins Cx30 and Cx43 under normal conditions and in an epilepsy model.

Specific aims of this work were:

1. Characterization of a novel Cx43 conditional knockout mouse, expressing ECFP after Cre-mediated recombination,

2. Thorough analysis of the Cx30 and Cx43 expression patterns utilizing reporter and fate mapping approaches.

3. Establishing an astrocytic fate mapping method to study the fate of astrocytes in a mouse model of temporal lobe epilepsy .

Chapter 3

Materials and Methods

3.1 Animals

Mice were kept under standard housing conditions (12 h/12 h dark–light cycle, food and water ad libitum). All experiments were carried out in accordance with local and state regulations for research with animals. All transgenic lines were backcrossed at least 10 times to C57BL/6.

3.1.1 Cx30 KO animals

The Cx30 coding sequence of these mice has been replaced with a lacZ reporter sequence under control of Cx30 gene regulatory elements (Teubner et al., 2003). The lacZ-encoded βgalactosidase contains a nuclear localization signal.

3.1.2 Cx43fl(lacZ) and Cx43del animals

In Cx43fl(lacZ) animals, the Cx43 coding region is floxed. The floxed region is followed by a lacZ gene which encodes βgalactosidase reporter with a nuclear localization signal. As a result of Cx43 excision, the expression of βgalactosidase is turned on under the control of the Cx43 gene regulation element (Theis et al., 2001a). The Cx43del mouse is a result of breeding of Cx43fl animals with the Deleter mouse (Schwenk et al., 1995). In Cx43del mice Cx43 is heterozygously deleted in all cells of the body.

3.1.3 Cx43 Cx30 double KO animals

Cx43 Cx30 double KO (DKO) animals are a result of the breeding of Cx30KO animals with Cx43fl(LacZ) animals and hGFAPCre (Zhuo et al., 2001) animals. DKO mice lack Cx30 in all cells of the body, and Cx43 in astrocytes. Homozygous deletion of Cx43 in all cells of the body is lethal (Reaume et al., 1995; Theis et al., 2001b).

3.1.4 R26R and R26R-EYFP reporters

R26R(Rosa) and R26R-EYFP(Rosy) are reporter mice for fate mapping and monitoring of Cre expression. In R26R reporter mice, a splice acceptor sequence, a neo expression cassette, flanked by loxP sites, a lacZ gene and a triple polyadenylation (bpA) sequence were inserted in the ROSA26 locus (Soriano, 1999). R26R-EYFP contains as a reporter Enhanced Yellow Fluorescent Protein (EYFP) instead of lacZ (Srinivas et al., 2001). As a result of breeding of these reporter mice with mice expressing the Cre recombinase, the neo cassette is excised and reporter gene expression is turned on in the cells expressing Cre recombinase and in their descendants.

3.1.5 Cx30CreERT2:R26R-EYFP and Cx43CreERT: R26R-EYFP

Cx43KI-CreERT mice express a tamoxifen-inducible Cre recombinase under control of the Cx43 gene regulatory elements (Eckardt et al., 2004). In the Cx30CreERT2 mice the construct, which contains CreERT that is expressed under the control of the Cx30 regulatory elements, is inserted into large genomic fragment of the Cx30 gene using the Bacterial Artificial Chromosome (BAC) technology (Slezak et al., 2007). As a reporter R26R-EYFP was used.

3.1.6 Cx30CreERT2:Cx43fl(lacZ)

In this mouse, CreERT2 is expressed in the cells expressing Cx30. As a reporter Cx43fl(lacZ) is used. In this mouse expression of βgalactosidase occurs in cells

that express both Cx43 and Cx30.

3.1.7 NG2KI-EYFP:Cx43del mouse

This mouse was produced by breeding of NG2KI-EYFP mouse and Cx43del (see 3.1.2) mouse. NG2KI-EYFP mice express the EYFP under control of the NG2 gene-regulatory elements (Karram et al., 2008). In this mouse βgalactosidase is expressed in the cells expressing Cx43 and EYFP is expressed in NG2 glia (see 1.1.1.1). This double transgenic mouse is suitable for monitoring of Cx43 expression in NG2 glia.

3.1.8 Cx43fl(ECFP) and Cx43KI-ECFP mice

Cx43fl(ECFP) is a novel conditional KO mouse line expressing ECFP (Enhanced Cyan Fluorescent Protein) instead for Cx43 after Cre mediated recombination (Degen et. al unpublished results). The Cx43KI-ECFP mouse line was generated by breeding Cx43fl(ECFP) mice, with PGK-Cre mice (Lallemand et al., 1998). In Cx43KI-ECFP mouse one allele of Cx43 is deleted in all cells of the body, and ECFP is expressed instead.

3.1.9 GFAPCreERT2:R26R

In GFAPCreERT2 mice the tamoxifen-inducible Cre is expressed in an astrocyte-specific manner under control of a human GFAP promoter fragment (Hirrlinger et al., 2006). R26R was used as a reporter. In GFAPCreERT:R26R mice, expression of βgalactosidase in astrocytes is expected after tamoxifen injection.

3.1.10 GLASTCreERT:R26R

In the GLASTCreERT mice the construct, which contains CreERT that is expressed under the control of the astrocyte-specific glutamate transporter (GLAST) regulatory elements, is inserted into genome using BAC (Slezak et al., 2007). As a reporter R26R was used. In GLASTCreERT:R26R mice expression of βgalactosidase in GLAST-positive subpopulation of astrocytes is expected after tamoxifen injection.

3.2 Tamoxifen injection

Tamoxifen (Sigma, Munich, Germany) was dissolved in a 1:9 mixture of ethanol and sunflower oil (Fluka, Ulm, Germany, Slezak et al. 2007). A stock solution of 20 mg/ml was used. The solution was prepared daily. Mice were injected intaperitoneally with 1 mg of this mixture twice a day, for 5 days.

3.2.1 Intrathecal injection

To avoid influence of the blood brain barrier on tamoxifen access to the brain, animals were injected intrathecally (i.t.). Injections were performed according to Wu et al. (2004). A catheter was made from 10.5 cm long polyethylene tubes (PE10 Reiss Laborbedarf, Mainz-Mombach, Germany). The tubes were warmed upon a hot plate until softening and were pressed and pulled to form an elongated part and two buds as shown on the figure 3.1. A tungsten wire with a diameter of 0.127 mm (MsWil, Wil, Switzerland) was inserted into the tube as a guide. The catheter was inserted between vertebrae L4 and L5 of the deeply anesthetized mouse, and left in place for one week. The correct place of insertion was confirmed by 0.001 ml of Lidocaine (AstraZeneca, Wedel, Germany) injection, which caused temporal paralysis of the hind paws, and by a yellowish color of cerebrospinal fluid (which appears as a result of the oil injection) during mouse dissection. Mice were injected with 0.001 ml of ethanol/sunflower oil mixture twice a day.

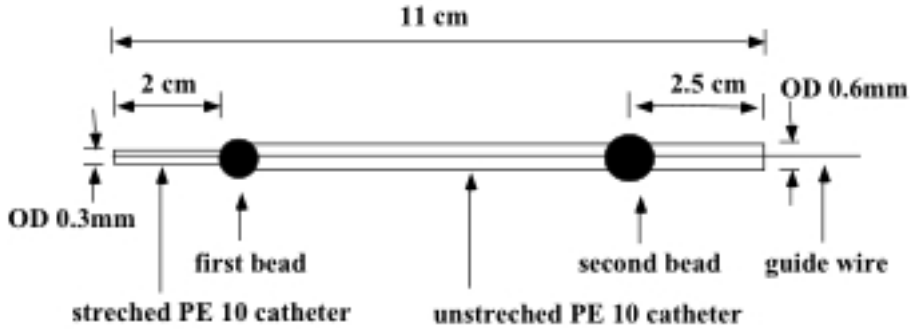

Fig. 3.1: Construction of the catheter for intrathecal injection. (Wu et al., 2004).

3.3 Chemicals and solutions

Chemicals and Reagents	
Chemicals, Reagents	**Manufacturer**
Ethanol	Roth, Karlsruhe Germany
Methanol	Roth, Karlsruhe Germany
Sterile Water	B.Braun, Melsungen, Germany
Parafarmaldehide	Roth, Karlsruhe Germany
Hoechst 33258	Invitrogen, Carlsbad, CA, USA
TritonX-100	Sigma, Munich, Germany
Ketamine (ketaminehydrochloride)	Pharmanovo, Hannover, Germany
Cepetor® KH (medetomidinehydrochloride)	CP Pharma, Burgdorf, Germany
Lidocaine	AstraZeneca,Wedel,Germany
Sunflower oil	Fluka, Ulm, Germany
Tamoxifen	Sigma, Munich, Germany
Ringer Solution	Fresenius Kabi, Bad Homburg, Germany
Antisedan (atipamezolhydrochlorid)	Orion Pharma, Espor, Finland
Draq5	Biostatus, UK, Shepshed
Biocytin	Sigma, Taufkirchen, Germany
Kainate	Tocris Bioscience, Bristol, UK
Normal Goat Serum (NGS)	Millipore, Schwalbach, Germany
Streptavidine-CY3	Dianova, Hamburg, Germany
Tissue-Tek	Sakura,Zoeterwoude, NL
VectaShield mounting medium	Vector Laboratories, Burlingame, USA
PermaFluor mounting medium	Thermo Fisher Scientific, Fremont USA

Tab. 3.1: Chemicals

Solutions	
Solution type	**Content**
Phosphate Buffered Saline (PBS)	150 mM NaCl, 8.3 mM Na_2HPO_4, 1.7 mM NaH_2PO_4
Fixation solution (4% Paraformaldehyd (PFA))	4% PFA in PBS
Cryoprotection solutions	1 x PBS with 30 % (w/v) sucrose
Artificial Cerebrospinal Fluid (ACSF)	126mM NaCl, 3mM KCl, 2mM $MgSO_4$, 2mM $CaCl_2$, 10mM glucose, 1.25mM NaH_2PO_4, 26mM $NaHCO_3$, pH 7.4 (equilibrated with 95% O_2/5% CO_2).
Laird buffer	100 mM Tris, 5 mM EDTA, 0.2% SDS, 200 mM NaCl, pH adjusted with HCl to 8.5

Tab. 3.2: Solutions

Equipment	
Equipment	**Manufacturer**
Cryostat	Microm, Walldorf, Germany
Stereotactic frame	TSE Systems GmbH, Bad Homburg, Germany
Wide-field fluorescence microscope	Axiophot, Zeiss, Oberkochem, German
Confocal microscope	Leica TCS, Pulheim, Germany
Digital SPOT camera	Diagnostic Instruments, Sterling Heights, MI,USA
Microsyringe	Hamilton, Bonaduz, Switzerland
PCR cycler	Biorad, München, Germany

Tab. 3.3: Equipment

3.4 Anaesthesia

Mice were deeply anesthetized by i.p. injection of 2:3 Ketamine/Cepetor 3.3µl/g body weight. After surgery, Ketamine was neutralized by application of 100μL 1:5 Antisedan/Ringer solution per mouse. Later on animals were placed under an infra-red lamp to avoid hypothermia.

3.5 Immunohistochemistry

Mice were deeply anesthetized and were perfused transcardially with 30 ml PBS followed by 20 ml 4% PFA. Brains were removed and stored overnight at 4% PFA, in 4 $^\circ$C, then the brains were transfered to 30% sucrose solution in PBS for 2-4 days. Subsequently brains were embedded in Tissue-Tek, frozen, and cut on a cryostat. Free floating sections were incubated in blocking solution including 10% NGS and 0.4% TritonX100 in PBS for two hours. Sections were incubated with primary antibody dissolved in blocking solution overnight in 4 $^\circ$C. Sections were washed in PBS and incubated with secondary antibodies for two hours. As secondary antibodies, we used goat anti-rabbit, goat anti-mouse or goat anti-chicken conjugated to Alexa fluor 488, Alexa fluor 568 or Alexa fluor 647 (1:500 Invitrogen, Karlsruhe, Germany). Sections were washed and incubated with Hoechst (1:100) or alternatively with Draq5 (1:1000) for nuclear staining and washed in PBS again. Section were mounted on the glass slides using mounting medium and covered by cover slip.

Antibodies and Reactives			
Antigen	**Origin**	**Dilution**	**Manufacturer**
GFP(FITC coupled)	Goat	1:500	Abcam
GFP	Chicken	1:500	Abcam
GFP	Mouse	1:500	Invitrogen
S100β	Rabbit	1:1000	Abcam
S100β	Rabbit	1:500	Swant
Iba1	Rabbit	1:500	Wako
Glutamine synthetase	Mouse	1:250	Millipore

Antigen	Origin	Dilution	Manufacturer
βgalactosidase	Mouse	1:500	Abcam
βgalactosidase	Chicken	1:500	Abcam
βgalactosidase	Rabbit	1:500	Invitrogen
NeuN neuronal marker	Mouse	1:100	Millipore
NG2	Rabbit	1:100	Chemicon
GFAP(CY3 coupled)	Mouse	1:500	Sigma
GFAP	Rabbit	1:500	Dako
BLBP	Rabbit	1:250	abcam

Tab. 3.4: Antibodies

Images were taken with a Zeiss Axiophot equipped with fluorescence optics, a digital SPOT camera and MetaView software (Universal Imaging, West Chester, PA,USA). Alternatively, fluorescent images were obtained with confocal laser scanning microscopy (Leica TCS, Pulheim, Germany). Images were analyzed using ImageJ software (NIH, Bethesda, Maryland, USA). For cell counting image stacks were used. The step between two focal planes was 1μm. The size of the individual image in the stack (one visual field) was 0.56 mm^2.To quantify β-galactosidase and ECFP reporter expression, cells were counted in the stratum radiatum of the CA1 region fitting to one visual field. To measure the efficacy of hGFAP at the allelic level, cells were quantified in strata radiatum, oriens, and lacunosum-moleculare in the CA1 region. For quantification of Cx30 upregulation, cells were counted in the cortex (all layers), the CA1 region (strata radiatum, oriens, lacunosum-moleculare) and the dentate gyrus of the hippocampus (hilus and granule cell layer). For comparison of Cx30 and Cx43 expression utilizing inducible R26R-EYFP expression, 200μm X 200μm counting boxes were used.

3.5.1 Measurement of the relative area occupied by the signal

For measurement of the upregulation of GFAP and Iba1 in the hippocampus of the animals in the TLE model (see 3.8), changes in the area of the hippocampus occupied by the specific immunofluorescent signal were measured. The image of the whole hippocampus was obtained and the size of the area occupied by the immunofluorescent signal was measured. The area was measured using ImageJ, after adjusting a threshold using the ImageJ threshold plugin. The part of the hippocampus occupied by the immunofluorescent signal was measured using the following formula:

$$\textbf{area fraction} = \frac{\textbf{area occupied by immunofluorescent signal}}{\textbf{area of the hippocampus}}$$

The increase in the level of the immunofluorescent signal is a quotient of area fractions occupied by the immunofluorescent sygnal in the contralateral and ipsilateral side to kainate injection.

3.5.2 Measurement of granule cell dispersion

To quantify granule cell dispersion (see 4.2), we measured the width of the granule cell layer of the medial (upper) blade of the dentate gyrus 50μm from the edge.

3.6 Measurement of dye coupling

The measurements of dye coupled cells were performed as described (Wallraff et al., 2004; Theis et al., 2003). Mice were anesthetized by Isofluran, decapitated, the brains were quickly removed and 200 µm-thick coronal slices were cut on a vibratome (VT1000S, Leica, Nussloch, Germany). During cutting, brains were submerged in ice-cold oxygenated solution containing (in mM): 150 NaCl, 5 KCl, 2 $MgSO_4$, 1 Na-pyruvate, 10 glucose, 10 HEPES, pH 7.4. Then, slices were transferred into ACSF. For electrophysiological analysis, a slice was placed into a recording chamber and continuously perfused with carbogenated ACSF at room temperature. Cells were visualized using an upright microscope (Eclipse FN-1,

Nikon, Düsseldorf, Germany) with infrared differential interference contrast optics. Whole-cell voltage-clamp recordings were obtained from cells located in the stratum radiatum of the CA1 subfield. Patch pipettes (3-6 MΩ) were filled with (in mM): 130 K-gluconate, 1 $MgCl_2$, 3 Na_2-ATP, 20 HEPES, and 10 EGTA, pH 7.2. Currents were recorded using an EPC8 amplifier (HEKA Elektronik, Lambrecht, Germany). Data were sampled at 30 kHz, filtered at 10-30 kHz, and monitored with TIDA software (HEKA). For tracer coupling analysis, N-biotinyl-L-lysine (biocytin; Sigma, Taufkirchen, Germany) was added to the internal solution (0.5%), and cells were loaded during 20 min recording in the voltage-clamp mode. Only one astrocyte was filled with biocytin in any individual slice. Immediately after recordings, slices were fixed in 4% PFA in 100 mM PBS, pH 7.4, at 4 ° C. The slices were then incubated for two hours with blocking solution consisting of 2% NGS in 0.1 M PBS with 0.1% Triton X-100. Then, streptavidin-Cy3 (Dianova; 1:100) was applied overnight. The reaction was stopped by washing with PBS. The slices were co-stained with anti-GFP and anti-βgal antibodies. Slices were embedded in mounting medium (VectaShield, Vector Laboratories, Burlingame, USA) and images were taken as described above.

3.7 Genotyping

Animals were genotyped at the age of 4 weeks. Tail tips were cut and incubated in Laird lysis buffer containing 0.2mg/ml proteinase K at 55 ° C overnight. The tail lysates were precipitated in isopropanol, centrifuged for 10 min at 14000 rpm, the supernatant was discarded, the pellet washed in 70% ethanol and centrifuged again. The supernatant was discarded and the pellet was dried for two hours. Extracted DNA was dissolved in 50μl of double distilled water. Extracted DNA was analyzed by PCR using the GoTaq PCR kit and primers mentioned in table 3.5.

Primers and PCR program			
Detects	**Program**	**Primer sequence from 5' to 3'**	**Product size**
Cre and CreERT	94°C -1´, (94°C-1´, 60°C-1´, 72°C-1´) X 30, 72°C-10´	Intcre-UP-TTT GCC TGC ATT ACC GGT CGA TGC Intcre-REV-TCC ATG AGT GAA CGA ACC TGG TCG	400bp
GFAP-Cre	94°C -min´, (94°C-1´, 60°C-1´, 72°C-1´) X 30, 72°C-10´	GFAP-LZ1-ACT CCT TCA TAA AGC CCT CG Cre-LZ4-ATC ACT CGT TGC ATC GAC CG	200bp
GLAST-Cre	95°C-2', (95°C-30", 65°C-30", 72°C-70") X 35 72°C-5'	GLASTCreERT2f-AAA TGT GGG TGC TTG GTC TC GLASTCreERT2r-AGG CAA ATT TT GGT GTA CGG	1150bp
Cx43wt and Cx43fl	94°C-4´, (94°C-2´, 65°C-1´, 72°C-1´30") X 25 72°C-10´	43del-foward-GGC ATA CAG ACC CTT GGA CTC C UMPR-TCA CCC CAA GCT GAC TCA ACC G	Cx43fl:650bp WT:500bp

Detects	**Program**	**Primer sequence from 5' to 3'**	**Product size**
Cx43KO(lacZ)	95°C-5´, (94°C-30", 62°C-45" 72°C-1´30") X 40, 72°C-10´	43del-foward-GGC ATA CAG ACC CTT GGA CTC C 43del-rev-TGC GGG CCT CTT CGC TAT TAC G	670bp
Cx43CreERT	95°C-5´, (94°C-30", 62°C-45" 72°C-1´30") X 40, 72°C-10´	43-del-foward-GGC ATA CAG ACC CTT GGA CTC C Cx30CreERT2r-CAG GTT CTT GCG AAC CTC AT	500bp
Floxed Cx43/CFP, Floxed Cx43/Lacz, Cx43KO/CFP	95°C-5´, (95°C-30", 65°C-30", 72°C-1') X 30, 72°C-10'	in-kod-reg-Cx43-GCT TCC CCA AGG CGC TCC AGT CAC CC fw-loxP-GCAC TTG GTA GGT AGA GCC TGT CAG GTC DSP-CFP-AAG AAG TCG TGC TGC TTC ATG TGG	WT:340bp floxedCFP:395bp floxed-LacZ: 450bp Cx43KO/CFP: 700bp
Cx30CreERT2	95°C-2', (95°C-30", 65°C-30", 72°C-70") X 35 72°C-5	Cx30CreERT2f-ATC ATG GGC ATT CCT TCT CA Cx30CreERT2r-CAG GTT CTT GCG AAC CTC AT	1050bp

Detects	**Program**	**Primer sequence from 5' to 3'**	**Product size**
R26R and R26R-EYFP	94°C-1´, (94°C-45“, 67°C-30”, 72°C-40”) X 35, 72°C-5´	Rosa-WT-Xba-sense-TTT TGG AGG CAG GAA GCA CTT G Rosa-WT-Xba asense-GAA GGA GCG GGA GAA ATG GAT A SA-1as-GAC ATC ATC AAG GAA ACC CTG GAC	WT:650bp R26R:290bp
R26R recombined	94°C-1',(94°C-45”, 67°C-30”, 72°C-40”) X 25, 72°C-10'	Sas-GGT TGA GGA CAA ACT CTT CGC PGKas-CTA CCC GCT TCC ATT GCT CAG YFPas-CTC GTT GGG GTC TTT GCT CAG	Recombined R26R:829bp Non-recombined R26R:440bp
Cx30KO and Cx30 WT	94°C-5´ (92°C-45”, 60°C-45”, 72°C-45”) X 35, 72°C-10´	Cx30wt5-GGT ACC TTC TAC TAA TTA GCT TGG Cx30wt3-AGG TGG TAC CCA TTG TAG AGG AAG Cx30lacZ3-AGC GAG TAA CAA CCC GTC GGA TTC	WT:544bp KO:460bp

Tab. 3.5: Primers and PCR programs

3.8 Temporal lobe epilepsy model

Dr. P. Bedner and Dr. K. Hüttmann, Institute for Cellular Neurosciences established a new model for TLE. In this model kainate is injected into the cortex above the hippocampus, avoiding mechanical damage to hippocampus. It is a big advantage over the TLE model with intrahipocamapal injection (Heinrich et al., 2006). The mice subjected to TLE model with intrahipocampal injections do not show spontaneous generalized seizures, and in these mice impossible to investigate morphological change in CA1 region due to mechanical damage in this region. Animals were anaesthetised with a ketamine/cepetor mixture and injected stereotactically into the right parietal cortex (coordinates from bregma point: AP:-1.9 mm and ML:-1.5 mm, DV: 1.8 mm) with kainate using a Hamilton microsyringe. Animals were placed under an automatic video recording system. Electroencephalograms (EEGs) were recorded using a telemetric recording system (Data Sciences International (DSI), Minneapolis, USA)

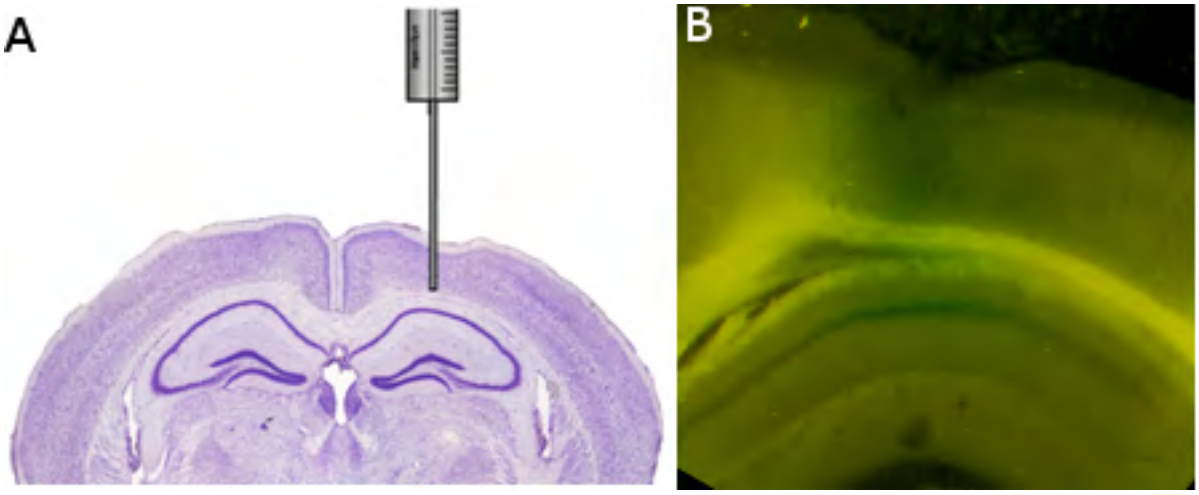

Fig. 3.2: Intracortical kainate injection. **A.** Schema of injection of kainate in the parietal cortex. Note the placement of the Hamilton syringe (modified from MBL, courtesy of Dr. Bedner). **B.** Injection of the blue dye into the cortex to simulate the kainate injection. The dye diffused from the cortex to the hippocampus.

3.9 Statistical Analysis

For data analysis R (R Development Core Team, 2010) and SPSS (PASW statistics version 18) were used. Data are presented as mean ±Standard Error of the Mean (SEM). Differences were considered significant at $p<0.05$. T-test, Mann–Whitney U test, ANOVA, Kruskal-Wallis rank sum test were used as appropriate.

Chapter 4

Results

4.1 Characterization of novel conditional Cx43 KO mice

We characterized novel Cx43 conditional KO mice, expressing ECFP instead of Cx43, in the mouse brain. The mice were generated by Dr. Joachim Degen in the laboratory of Prof. Dr. Klaus Willecke

4.1.1 Comparison of Cx43del and Cx43KI-ECFP mice

We compared the expression of cytoplasmic ECFP in the hippocampus of Cx43KI-ECFP mice with the well-characterized expression of nuclear β-galactosidase in Cx43del mice previously described (Theis et al., 2003, 2001b). We found that the immunolocalization of ECFP and β-galactosidase in the hippocampus was essentially the same (Fig. 4.1, Tab. 4.1). We observed a high degree of colocalization of the astrocytic marker GFAP with both of the Cx43-driven reporters (Fig. 4.1): 96.9% of all β-galactosidase positive cells and 96.1% of all ECFP-positive cells expressed GFAP. By contrast, neither β-galactosidase nor ECFP colocalized with the markers NeuN (Fig. 4.1 A3, B3), NG2 (Fig. 4.1 A4, B4), or Iba1 (Fig. 4.1 A5, B5). For total numbers of cells and animals counted, see Tab. 4.1.

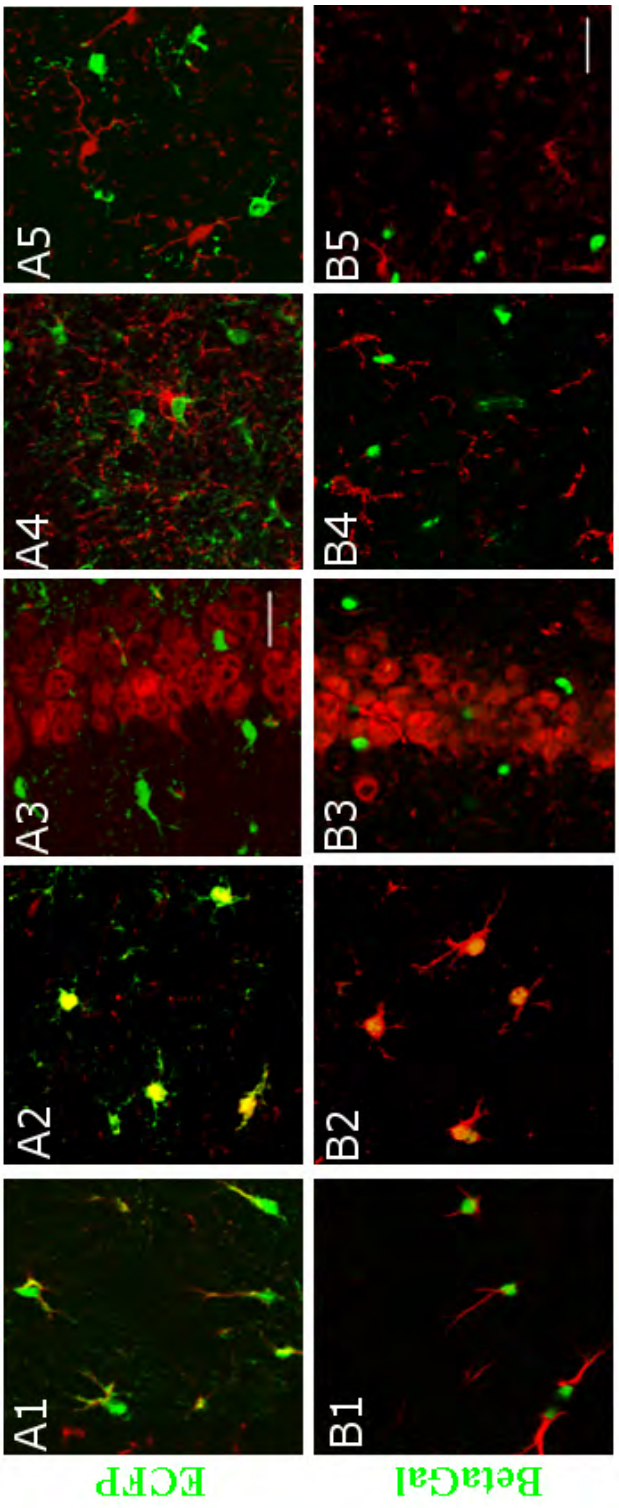

Fig. 4.1: Comparison of Cx43del and Cx43KI-ECFP mice. Double staining for ECFP (A1-A5) or β-galactosidase (B1-B5) and the cell-type-specific markers GFAP (A1, B1), S100β(A2, B2), NeuN (A3, B3), NG2 (A4, B4), and Iba1 (A5, B5) in the stratum radiatum of the hippocampal CA1 region from Cx43KI-ECFP mice (A) and Cx43del mice (B). The β-galactosidase contains an engineered nuclear localization signal, whereas the ECFP fills the cell body and the fine astrocytic processes. Bar: 25 μm.

Comparison of Cx43KI-ECFP and Cx43del mice						
Cell Type Marker	**ECFP/Marker Colocalization**	**Marker only**	**ECFP only**	**βgal/Marker Colocalization**	**Marker only**	**βgal only**
NeuN	0/0%(6)	1953	711	0/0%(6)	1930	602
GFAP	1200/97.3%(12)	9	33	1194/96.7%(12)	37	40
S100β	1364/99%(12)	58	14	1241/99.1%(12)	79	11
NG2	0/0%(6)	186	667	0/0%(6)	152	486
Iba1	0/0%(6)	263	587	0/0%(6)	281	652

Tab. 4.1: Comparison of Cx43KI-ECFP and Cx43del mice. Number of counted cells followed by percentage value of colocalization with the respective marker. Number of sections counted in parentheses. 3 animals were screened per marker.

4.1.2 Mutual exclusion of NG2 and Cx43 expression shown with Cx43del/NG2KI-EYFP mouse.

To confirm the fact that NG2 cells do not express Cx43, we used Cx43del/NG2KI-EYFP mice, expressing β-galactosidase in Cx43 positive cells and EYFP in NG2 positive cells. No colocalization of these two signals was observed (225 EYFP and 1253 β-galactosidase positive cells from 3 different animals were quantified). Thus, Cx43 is not expressed in NG2 cells.

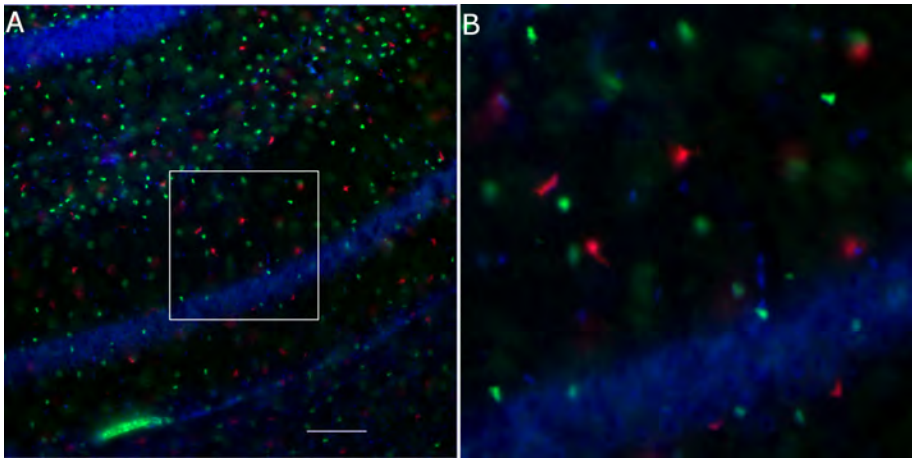

Fig. 4.2: Mutual exclusion of NG2 and Cx43 expression shown with Cx43del/NG2KI-EYFP mouse. B shows detailed images of the box in A. EYFP(green) is expressed in NG2 cells, β-galactosidase (red) is expressed in Cx43 positive cells. No colocalization of β-galactosidase and EYFP was observed. Scale bar 100μm.

4.1.3 Distinguishing Cx43 and Cx30 expression

The identical pattern of β-galactosidase and ECFP reporter expression allowed us to use ECFP as a second reporter in new DKO mice (Cx30lacZ/lacZ; Cx43fl[ECFP]/fl[ECFP]:hGFAP-Cre mice) which lacked both Cx30 (reporter: lacZ) and Cx43 (reporter: ECFP). We analyzed double-deficient mice expressing lacZ instead of Cx30 and ECFP after hGFAP-Cre-mediated ablation of Cx43. We compared immunohistochemical stainings with those from conventional DKO mice in which both Cx30 and Cx43 expression are represented by lacZ expression. In the latter, β-galactosidase immunoreactivity of individual cells

in Cx30lacZ/lacZ;Cx43fl[lacZ]/fl[lacZ]:hGFAP-Cre mice could indicate replacement of i) Cx30, ii) Cx43 or iii) replacement of both genes. This precluded the unambiguous allocation of reporter expression to a specific connexin gene (Fig. 4.3A). By contrast, in Cx30+/lacZ;Cx43fl[ECFP]/+:hGFAP-Cre mice, Cx30-driven lacZ expression (indicating lack of Cx30) and Cx43 driven ECFP expression (indicating loss of Cx43) could be easily differentiated (Fig. 4.3B).

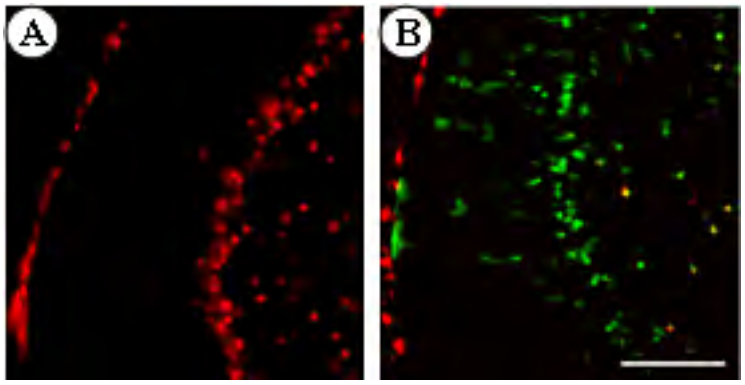

Fig. 4.3: Dual reporter-gene approach to distinguish Cx30 and Cx43 expression. A: Cerebellum of a Cx30lacZ/lacZ;Cx43fl[lacZ]/fl[lacZ]:hGFAP-Cre mouse. As β-galactosidase (β-galactosidase) expression (red) indicates both Cx30- and Cx43-deletion, we cannot distinguish their respective distribution. Leptomeningeal cells, cells in the Purkinje and granular cell layers were stained, consistent with expression of Cx30 and/or Cx43 in leptomeninges, Bergmann glia and astrocytes (Theis et al., 2003). B: Double staining of distinct reporters for Cx43 (ECFP, green) and Cx30 (β-galctosidase, red) in the cerebellum of a Cx30+/lacZ; Cx43fl[ECFP]/+:hGFAP-Cre mouse. After Cre-mediated deletion of Cx43, ECFP is expressed instead of Cx43. Cx30 is preferentially expressed in leptomeningeal cells and moderately expressed in some astrocytes of the granular cell layer, whereas Cx43 predominates in Bergmann glia but is also expressed in some astrocytes of the granule cell layer. Some colocalization of Cx30 and Cx43 is observed in yellow. Scale bar: 100μ for A-B.

4.1.4 Compensatory upregulation of Cx30 after Cx43 deletion

Immunoblot analyses suggested upregulation of Cx30 upon deletion of Cx43 (Theis et al., 2003, Nakase et al., 2004). We tested whether Cx30 is upregulated in the hippocampus after ablation of Cx43. We did so, *in situ*, with double immunofluorescence stainings for β-galactosidase (due to Cx30 replacement),

and for ECFP (indicating Cx43 replacement), in Cx30lacZ/lacZ;Cx43fl[ECFP]/fl[ECFP]:hGFAP-Cre mice. We found both in hippocampus and cortex a strong upregulation of β-galactosidase immunoreactivity compared to Cre-negative control mice (Fig. 4.4 A-D). The upregulation was pronounced in the vicinity of the CA1 pyramidal cell layer in the strata radiatum and oriens of the hippocampus (Fig. 4.4 A, C). It occurred throughout the cortex but was less pronounced in layer I, which lacks pyramidal cell somata (Fig. 4.4 E, F). Such restriction of Cx30 upregulation to the vicinity of neuronal cell bodies has also been observed in primary astrocytes co-cultured with neurons (Koulakoff et al., 2008). We quantified the density of cells which express Cx30 in different brain areas (2 animals/genotype; 6 sections/animal; differences between genotypes were significant ($p < 0.05$), Fig 4.4): The Cx30-driven β-galactosidase signal in the hippocampal CA1 region showed an 8-fold increase (from 32.4 $\pm$5.5 cells/mm^2 in Cx30lacZ/lacZ;Cx43fl[ECFP]/fl[ECFP] mice to 273.1 $\pm$17.7 cells/mm^2 in Cx30lacZ/lacZ;Cx43fl[ECFP]/fl[ECFP]:hGFAP-Cre mice). In the hilus of the dentate gyrus, the number increased 22-fold (from 13.2 $\pm$2 to 294.4 $\pm$14 cells/mm^2). In the cortex, we observed a 2.2-fold increase (from 261.5 $\pm$14.1 to 570.7 $\pm$15.2 cells/mm^2). A similar increase was observed in heterozygous Cx30+/lacZ mice: we found an increase of β-galactosidase positive cell numbers from Cx30+/lacZ;Cx43fl[ECFP]/fl[ECFP] mice to Cx30+/lacZ;Cx43fl[ECFP]/fl[ECFP]:hGFAP-Cre mice which was 7.6-fold in the CA1 region (10.6$\pm$1.6mm^2 to 80$\pm$10.2mm^2), 14.1 fold in the hilus (8.1$\pm$1.8mm^2 to 113.4$\pm$12.9mm^2), and 1.4-fold in cortex (311.5$\pm$32.9mm^2 to 443.8$\pm$19.9mm^2, 2 animals/genotype; 6 sections/animal; differences between genotypes were significant). We conclude that hippocampal and cortical Cx30 gene activity is upregulated upon ablation of Cx43.

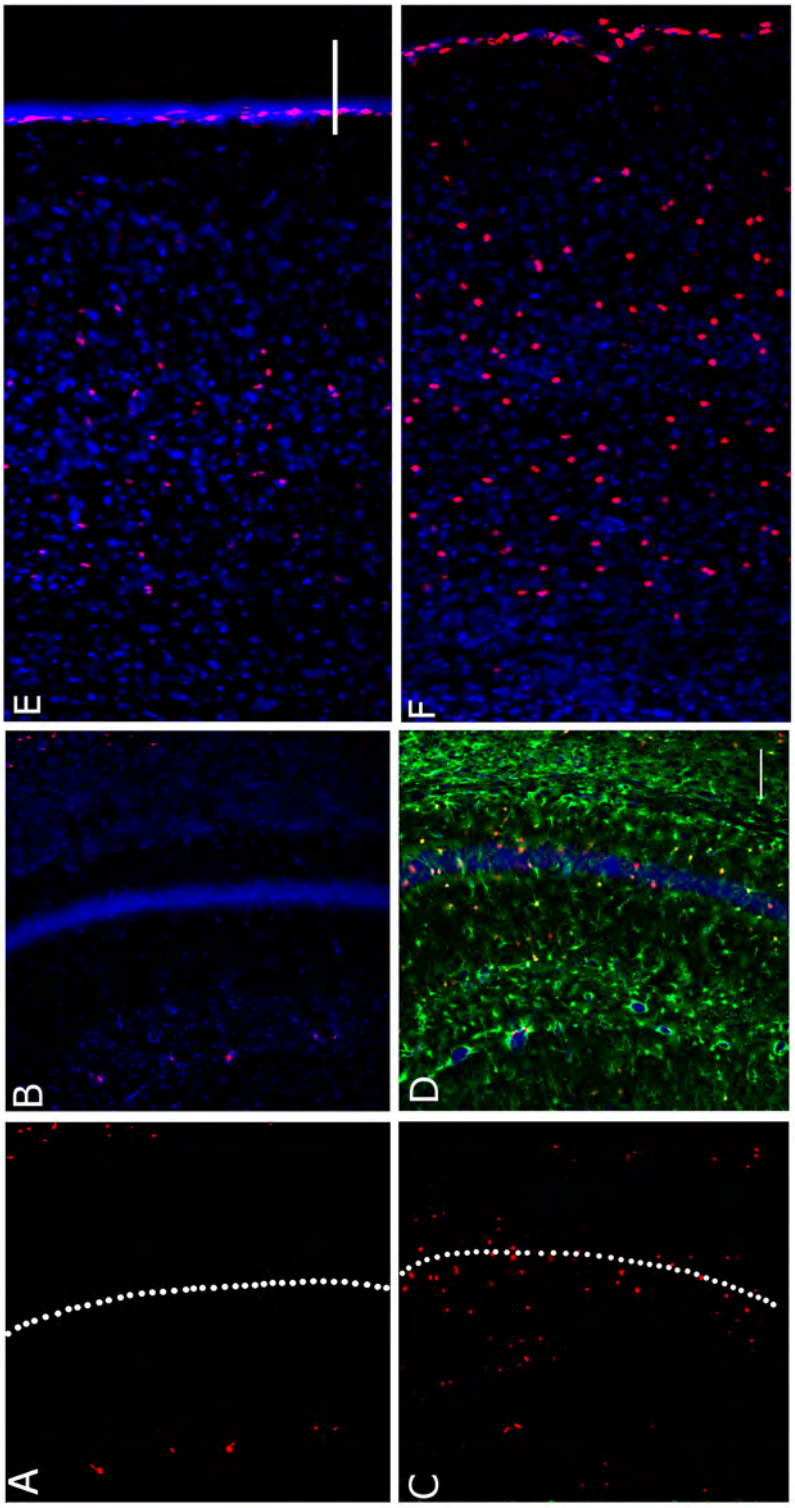

Fig. 4.4: Compensatory upregulation of Cx30 after Cx43 deletion.A-F: Compensatory upregulation of Cx30 after deletion of Cx43, monitored by the reporter-gene approach. Cx30lacZ/lacZ;Cx43fl[ECFP]/fl[ECFP] mice (A, B, E) and Cx30lacZ/lacZ;Cx43fl[ECFP]/fl[ECFP]:hGFAP-Cre mice (C, D, F), the latter expressing ECFP instead of Cx43. A-D: Hippocampal CA1 region. A, C: Beta-galactosidase expression after Cx30 deletion (red); B, D: Triple staining for Hoechst (blue), β-galactosidase (red) and ECFP (green). E, F: Cortex: Beta-galactosidase (red), Hoechst (blue). Loss of Cx43 led to CFP immunoreactivity (D) and to upregulation of Cx30-driven β -galactosidase expression (C, D, F). Bars: 100 μm for A-D (bar in D), and 100 μm for E-F (bar in E).

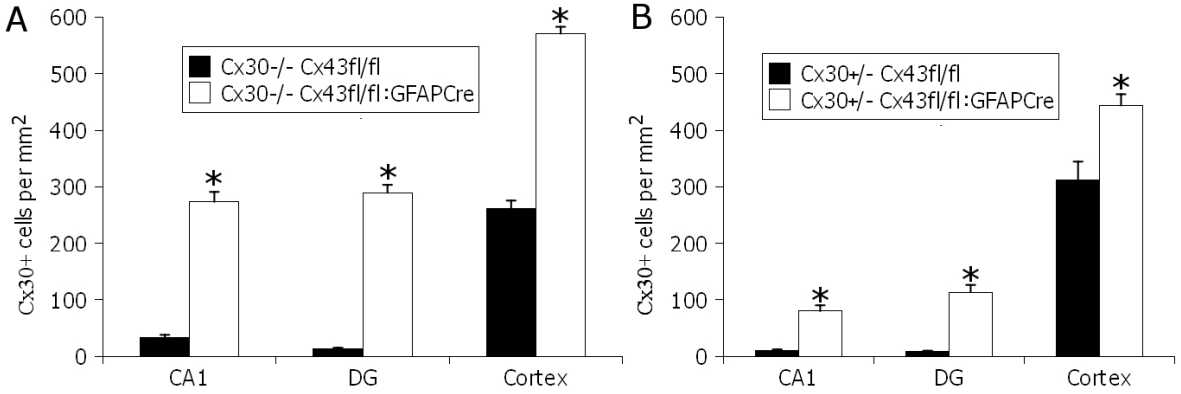

Fig. 4.5: Quantification of compensatory upregulation of Cx30 after Cx43 deletion. **A.** The Cx30-driven β-galactosidase signal in the hippocampal CA1 increased 8-fold in Cx30lacZ /lacZ;Cx43fl[ECFP]/fl[ECFP]:hGFAP-Cre compared to Cx30lacZ/lacZ;Cx43fl[ECFP]/fl[ECFP] mice. In the hilus of the dentate gyrus, the number increased 22-fold. In the cortex, we observed a 2.2-fold increase. **B.** A similar increase was observed in heterozygous Cx30+/lacZ mice. In the CA1 region we observed 7.6 fold upregulation, in the hilus an 14.1 fold upregulation, in cortex an 1.4 upregulation (2 animals/genotype; 6 sections/animal;) Cx30+/lacZ;Cx43fl[ECFP]/fl[ECFP]:hGFAP-Cre mice compared to Cx30+/lacZ;Cx43fl[ECFP] /fl[ECFP] mice .

4.1.5 A dual reporter-gene approach to quantify the efficacy of Cre-mediated deletion.

Cre-mediated replacement of Cx43 by lacZ or by ECFP creates a dominant signal. The reporter protein is expressed both after recombination of two floxed alleles and after deletion of only a single allele; this cannot be distinguished. In order to assess to which extent hGFAP-Cre deletes both floxed alleles, we raised mice with different reporter-genes (lacZ and ECFP, respectively) on the two floxed alleles of Cx43 (Cx43fl[ECFP]/fl[lacZ]:hGFAP-Cre mice). We measured the content of β-galactosidase and ECFP coexpression in the hippocampal CA1 region (Fig. 4.6). We found that 90.9 $\pm$4.3% of cells were double positive, while 4.1 $\pm$3.2% expressed β-galactosidase only, and 5 $\pm$2.8% of the cells expressed ECFP only (3 animals; 4 sections/animal; 1135 cells counted). Thus in the vast majority of cells, hGFAP-Cre deletes both alleles.

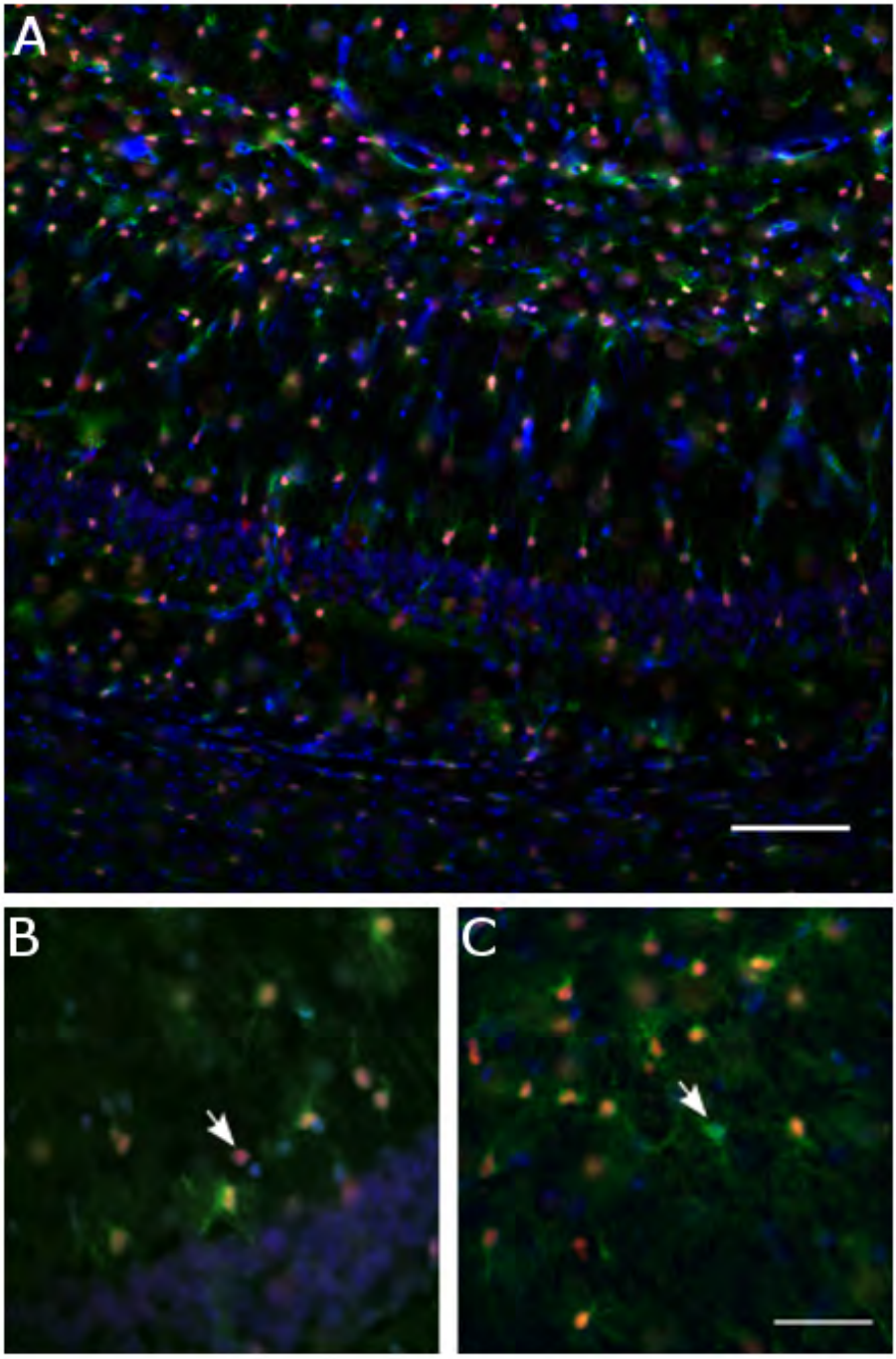

Fig. 4.6: Efficacy of Cre-mediated deletion. A-C: Efficacy of Cre-mediated recombination at the allelic level. Hippocampal section of a Cx43fl[ECFP]/ fl[lacZ]:hGFAP-Cre mouse, counterstained with Hoechst. GFP-antibody monitors Cre-mediated activation of ECFP reporter from one floxed allele, and β-galactosidase antibody monitors activation of lacZ reporter from the second floxed allele. Overlay of the three channels (A) demonstrates abundant colocalization of both reporters. B,C - Blow-ups: Arrows indicate few cells expressing β-galactosidase (B) or ECFP (C) only. Bar in A: 200 μm. Bar in C: 25 μm for B,C.

4.1.6 Biocytin injection of ECFP positive cells in Cx43KI-ECFP mice

Following electrophysiological investigation of current pattern with whole cell patch clamp (performed by Dr. Peter Bedner, Dr. Kerstin Hüttman and Simon Höft), ECFP positive cells were filled with biocytin in the hippocampus (CA1 region, 18 cells), the somatosensory cortex (7 cells), and the thalamus (ventral posterolateral thalamic nucleus -VPL, ventral posteromedial thalamic nucleus-VPM, 10 cells). In the hippocampus 97%±0.6%, in the cortex 77%±1.8% and in the thalamus 44%±4.6% of the biocytin positive cells were ECFP positive (the difference between proportions of biocytin positive cells in different regions were statistically significant). This indicates astrocytic heterogeneity of connexin expression across brain areas.

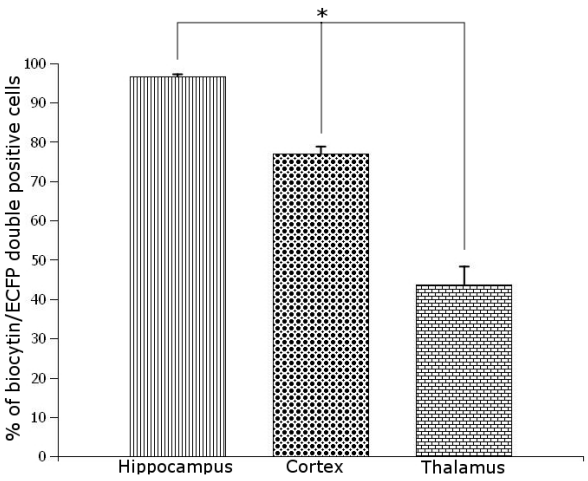

Fig. 4.7: Biocytin injection of the ECFP positive cells. ECFP positive cells were injected in hippocampus cortex and thalamus of Cx43KI-ECFP mouse. We compared the percentage of Cx43-driven ECFP positive cells among the biocytin-coupled cells and found that it was significantly different across brain regions.

4.2 Cx43 Cx30 double KO mice in a TLE model

To study the role of glial connexins in epilepsy, Cx43/Cx30 double KO mice (DKO) were subjected to our TLE model. As a control, litter mates lacking hGFAP-Cre and therefore expressing Cx43 were used. Animals were analysed

3 months after kainate injection. Three animals for each genotype were tested (four sections per animal).

The control animals showed loss of neurons in the pyramidal cell layer of the CA1 subregion in the hippocampus (neuronal loss was observed with both NeuN staining and with Hoechst staining), while the CA3 region looked largely intact (Fig. 4.8 A). Granule cell dispersion (GCD; Houser, 1990) was measured by the width of the granule cell layer. On the ipsilateral (injected) side, the granule cell layer was 3.57±0.12 times wider compared to the contralateral (noninjected) side. Granule cells of the dentate gyrus lost their NeuN immunoreactivity, and were visible only by Hoechst nuclear staining (Fig. 4.8 C). On the ipsilateral (injected) side the area occupied by astrocytes (GFAP) was increased 2.16±0.311 times in comparison to the contralateral side. The area occupied by Iba1 (microglia marker) was increased 3.37±0.53 times at the injected side. All these findings correspond to typical changes in Ammons Horn sclerosis (Armstrong, 1993).

DKO animals showed pyramidal cell loss in the CA1 region. Granule cells still had NeuN immunoreactivity (Fig. 4.8 B,D). The GCD was significantly less pronounced compared to control animals. The granule cell layer on the ipsilateral side was only 1.33±0.13 times wider compared to the ipsilateral side. The increase of the area occupied by Iba1 immunoreactivity was 1.87±0.22, significantly lower compared to control mice. The increase in GFAP expression was 1.8±0.13, which was not different from the control mice.

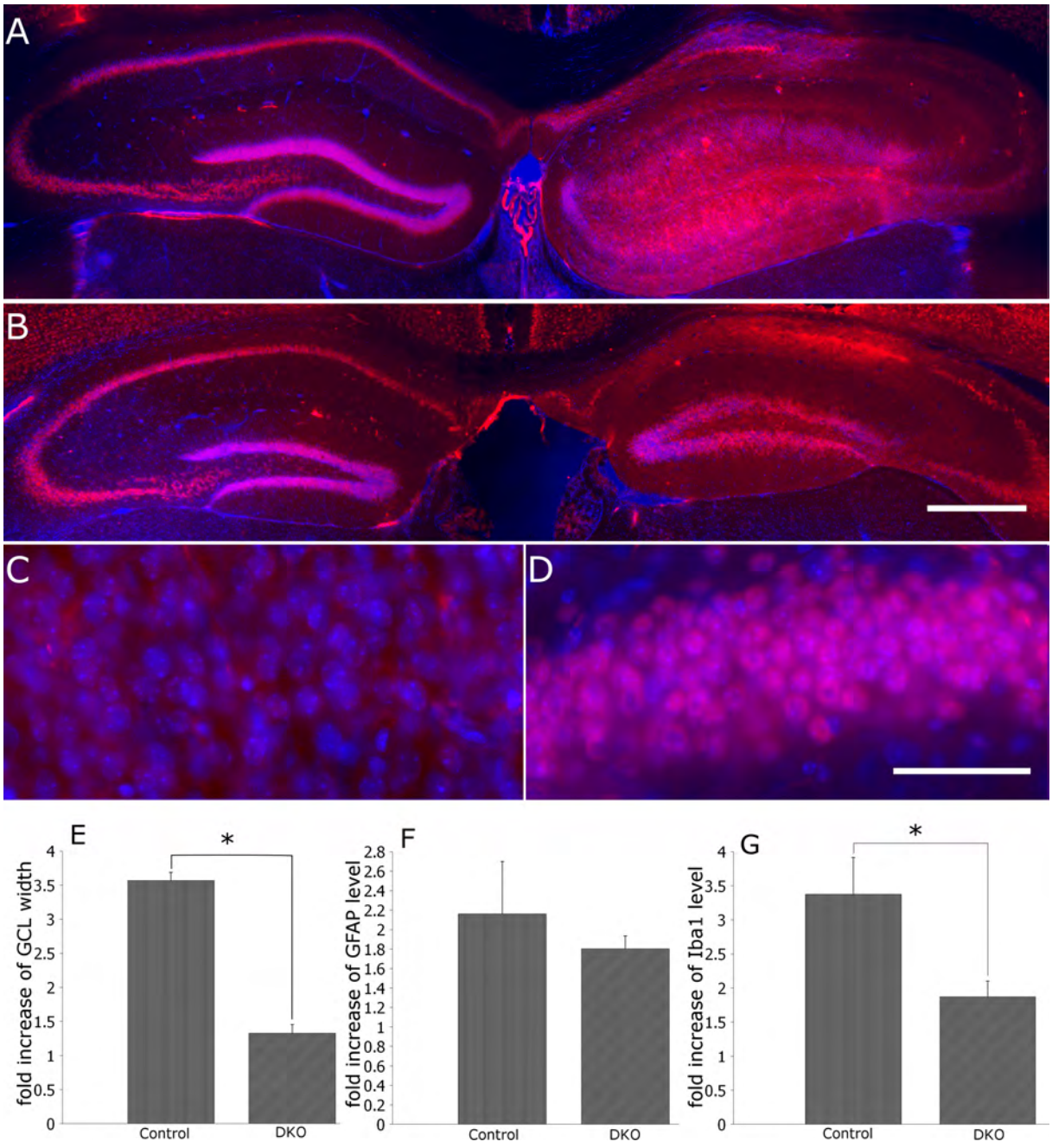

Fig. 4.8: Morphological changes of DKO and control mice in the TLE model. A-B: NeuN (red) and Hoechst (blue) stainings 6 weeks after kainate injection in control (A) and DKO (B) mice.GCD was less pronounced in DKO mice compared to controls. Bar in B is 250μm for A-B. C,D. Blow-up of granule cell layer of dentate gyrus of control and DKO animals respectively. C. in granule cell layer of control animals observed loss of immunoreactivity to NeuN (C), no such reduction in immunoreactivity observed in DKO animal (D) Bar in D is 50μm for C-D. E. GCD. The relative GCD was significantly higher in the control animals. F. No significant difference in increase of GFAP levels. G. The increase of Iba1 level was significantly higher in control animal.

4.3 Quality control of Cx30/Cx43 double KO mice.

During experiments on Cx43fl(lacZ)Cx30-/-: hGFAP-Cre (conditional DKO of Cx30 and Cx43 in astrocytes expressing LacZ instead of Cx43 and Cx30), we observed a reduction of function or no function of the hGFAP-Cre recombinase (Pseudo DKO). The extent of reporter positive astrocytes in the dentate gyrus was determined by double immunofluorescence analysis for GFAP and β-galactosidase: Cx30-/-;Cx43fl/fl mice were essentially devoid of β-galactosidase immunoreactivity in the hilar region (Fig. 4.9A). By contrast, DKO mice with efficient deletion showed numerous reporter gene expressing astrocytes (Fig.4.9 B). In pseudo DKO mice (Fig. 4.9C), the number of β-galactosidase positive cells was strongly decreased. In regions other than the hippocampus, the reduction of β-galactosidase expression due to Cx43 deletion could be masked by β-galactosidase expression due to Cx30 deletion. We correlated Cre expression with Cx43 ablation *in situ* by immunofluorescence detection of Cre recombinase in cerebellar cryosections. In DKO mice, Cre immunoreactivity within the Purkinje cell layer showed a distribution typical of the Bergmann glia nuclei (Fig. 4.9 E), whereas Cx30-/-;Cx43fl/fl control mice merely showed nonspecific background staining in blood vessels (Fig. 4.9 D) essentially identical to full pseudo-DKO mice (Fig. 4.9 F).

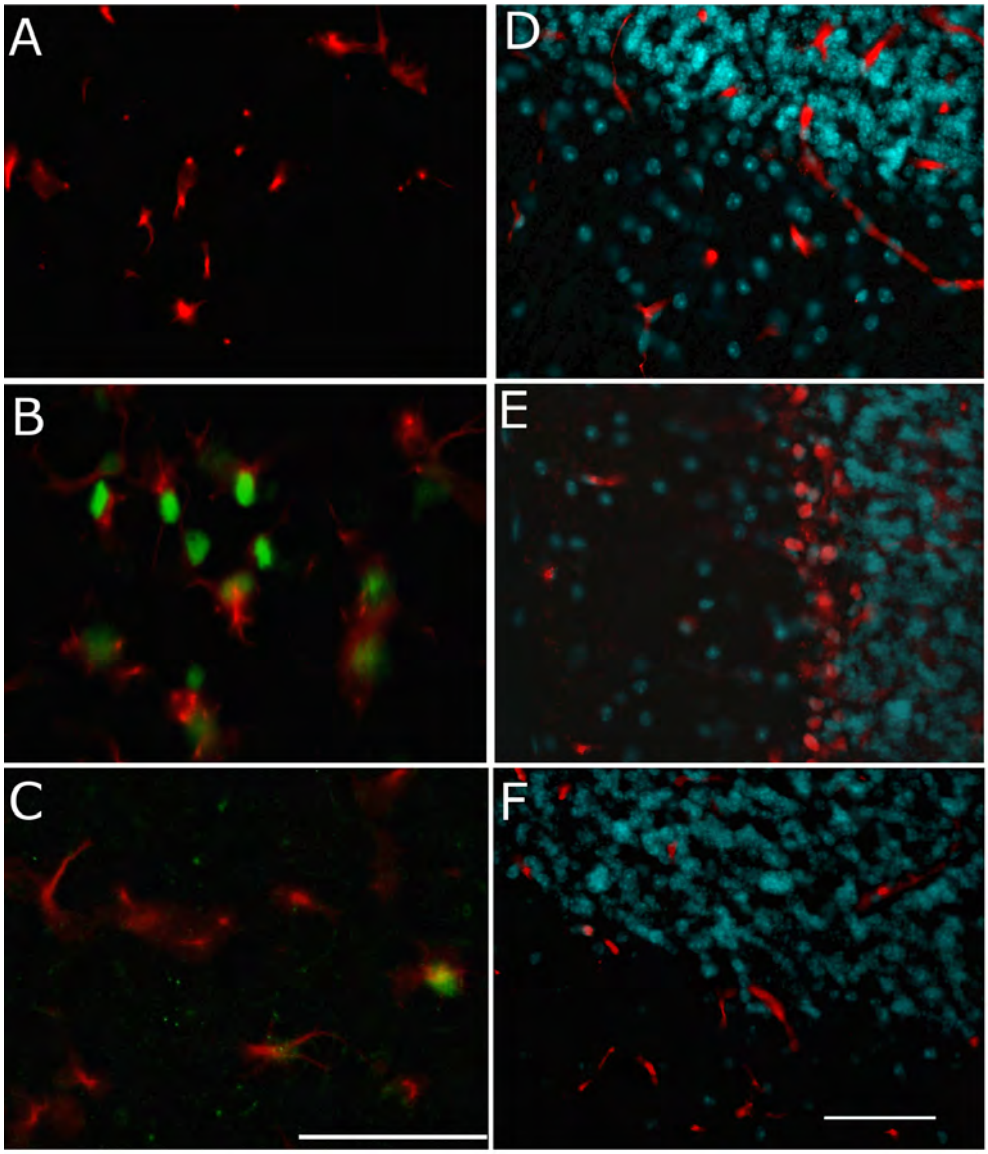

Fig. 4.9: Expression of β-galactosidase and Cre recombinase in DKO and pseudo-DKO animals.(A-C) Double immunofluorescence staining for GFAP and β-galactosidase in the hilar region of the dentate gyrus. (A) A Cx30-/-;Cx43fl/fl animal shows absence of β-galactosidase expression in the hippocampus consistent with virtual absence of Cx30 driven β-galactosidase expression in the hippocampus of Cx30 KO animals. (B) DKO mouse expressing β-galactosidase at a high level (C) Pseudo DKO animals shows only scattered expression of β-galactosidase. Scale bar: 50μm. D–F Immunohistochemical evaluation of Cre expression in DKO mice versus Cx30-/-;Cx43fl/fl controls in the cerebellum. Immunofluorescence analysis for Cre expression (red) from DKO mice, pseudo DKOs, and control mice. Hoechst counterstain (blue) was used to demarcate the border between molecular layer and granular layer (the cell density is higher in granular layer). (D) Cx30-/-;Cx43fl/fl mice are negative for Cre antibody staining (red). Some vessel-associated background staining is observed. (E) DKO mice with efficient Cx43 ablation show immunoreactivity for Cre in the Bergmann glia nuclei. (F) Full pseudo DKO mice lack immunoreactivity in Bergmann glia and are indistinguishable from Cre negative control mice. Bar in F is 50 μm for D-F.

4.4 Comparison of Cx30 expression monitored by different constitutively expressed and inducible reporter genes.

4.4.1 Cx30KO mouse: reporter gene experiments

The Cx30lacZ/lacZ mouse expresses an NLS-lacZ gene (a lacZ gene containing a nuclear localization signal) instead of Cx30 (Teubner et al., 2003). Therefore, LacZ expression represented transcriptional activity of the Cx30 gene. In the cerebellum β-galactosidase immunoreactivity was frequently observed in the granular cell layer and in leptomeninges (Fig.4.10 A1). No β-galactosidase signal was detected in the molecular layer. In the cerebral cortex, β-galactosidase positive cells were found mostly in medial cortical layers (Fig.4.10 B1). Expression was prominent in leptomeningeal cells (Fig.4.10 B1). Very low immunoreactivity was observed for β-galactosidase in the hippocampus (Fig. 4.10 C1). We quantified the number of lacZ expressing cells in cerebral cortex and hippocampus: 420.2 $\pm$10.9 cells/mm^2 showed lacZ expression in the cerebral cortex, while 52.5 $\pm$4.9 cells/mm^2 expressed the reporter in the hippocampal CA1 region of Cx30lacZ/lacZ mice (3 animals, 6 sections per animal). In the same sections, widespread β-galactosidase immunoreactivity was observed in the thalamus (not shown). Since considerable Cx30 expression in hippocampal astrocytes has been reported previously (Nagy et al., 1999; Theis et al., 2005), but we observed very low hippocampal β-galactosidase signal in the hippocampus of Cx30lacZ/lacZ mice (Fig 4.10C), we deemed further investigation of hippocampal Cx30 expression necessary (see 4.4.2).

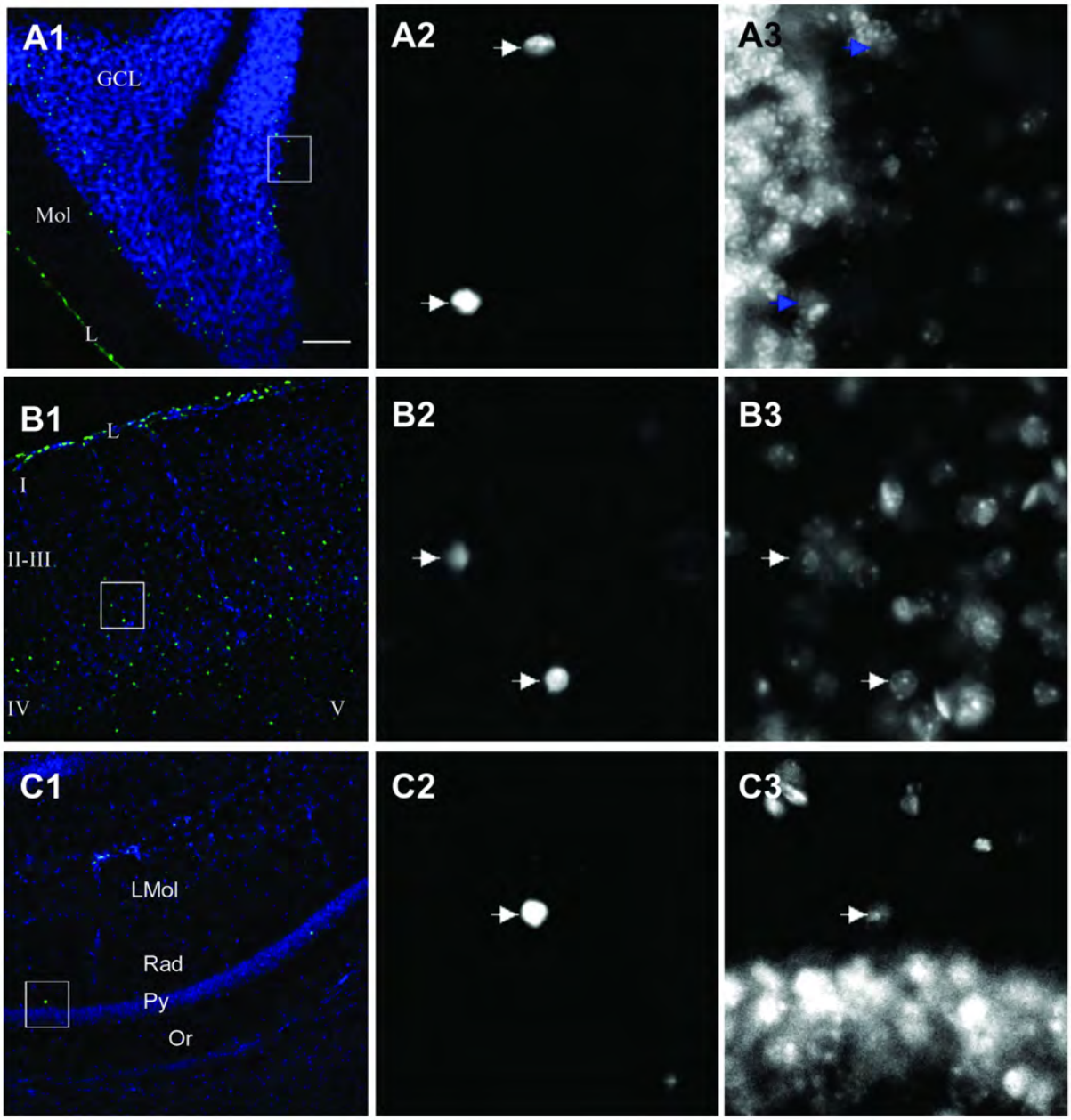

Fig. 4.10: Cx30 expression visualized by a reporter gene approach. Immunofluorescent staining for β-galactosidase of sections from a Cx30lacZ/lacZ mouse. The β-galactosidase staining (green) was observed in nuclei (stained with Hoechst dye, blue) in the cerebellum (A1) and the cerebral cortex (B1), but was very infrequent in the hippocampus (C1). A2, B2, C2: Insets from corresponding merged pictures, showing the β-galactosidase signal. A3, B3, C3: Hoechst nuclear stain. Arrows indicate colocalization of β-galactosidase and nuclear stain. GCL: Granule cell layer. Mol: Molecular layer. L: Leptomeningeal cell layer. I-V: Layers of the cerebral cortex. LMol: Stratum lacunosum moleculare. Rad: Stratum radiatum. Py: Pyramidal cell layer. Or: Stratum oriens. Scale Bar: 100μm.

4.4.2 Reporter activation mediated by Cx30CreERT2 transgenic mice in astrocytes

Utilizing a reporter gene, we scored Cx30CreERT2-mediated activation of a lacZ reporter gene driven by gene regulatory elements of the Cx43 gene (Theis et al., 2001b) in Cx30CreERT2:Cx43fl/+ mice. In this case lacZ expression indicated that the Cx30 gene and the Cx43 gene were active in the same cells. In double staining for S100β and β-galactosidase indicating Cx30CreERT2-driven recombination in Cx43 expressing astroglial cells (Fig. 4.11), we found similar numbers of double positive cells in the hippocampal CA1 region (25.7 $\pm$4.4 cells/mm^2) and cerebral cortex (27.0$\pm$3.5 cells/mm^2) of Cx30CreERT2:Cx43fl/+ mice (3 animals, 6 sections per animal). This served as evidence that Cx30 expression is similarly abundant in cerebral cortex and hippocampus, other than indicated by the Cx30 driven lacZ reporter embedded in the Cx30 KO allele.

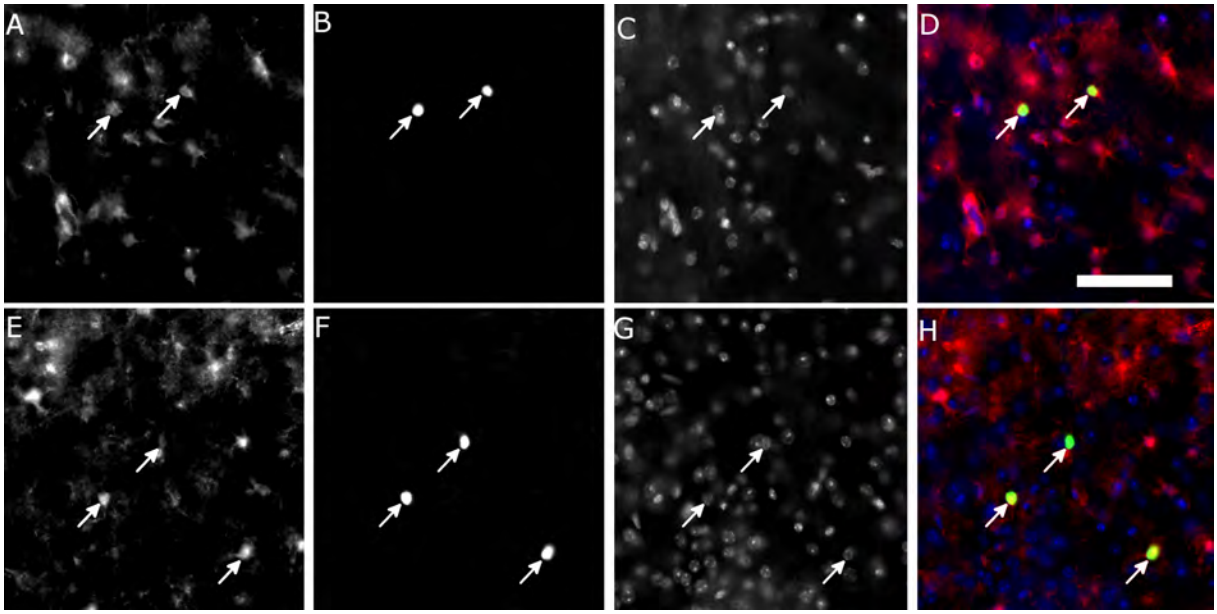

Fig. 4.11: A cre-based reporter approach indicates similar co-expression frequency of Cx30 with Cx43 in hippocampus and cortex. Hippocampus (A–D) and cerebral cortex (E–H) of Cx30CreERT2:Cx43fl/+ mice were stained with antibodies directed to S100β (A, E) and β-galactosidase (B,F), and Hoechst nuclear stain (C,G). Overlay (D,H) shows colocalization (arrows) of S100β (red), β-galactosidase (green) and nuclear stain (blue). Bar=50μm.

4.4.3 Expression levels of Cx43 and Cx30 in the hippocampus, primary somatosensory cortex, cerebellum, and thalamus assessed by R26R-EYFP reporter mice.

To compare the expression of Cx43 with Cx30 in hippocampus, cortex, thalamus, and cerebellum the co-expression of S100β and EYFP was investigated in Cx43CreERT:R26R-EYFP and in Cx30CreERT2:R26R-EYFP mice (3 animals, 6 sections for each genotype). This not only allowed us to compare expression of Cx43 with Cx30 in varios brain regions, but also to compare the efficacy of the inducible Cre transgene in different areas. In the CA1 region of the hippocampus, we calculated the proportion of EYFP positive astrocytes coexpressing S100β (see Fig. 4.12 A1-A4). In Cx43CreERT:R26R-EYFP mice, 57.8 $\pm$3.6% of S100β positive cells colocalized with EYFP and in the hippocampus of Cx30CreERT2:R26R-EYFP mice, 43.6$\pm$1.7% of S100β positive cells colocalized with EYFP (Fig 4.12 B1-B4). This difference in the proportions of S100β/EYFP double positive cells was significant.

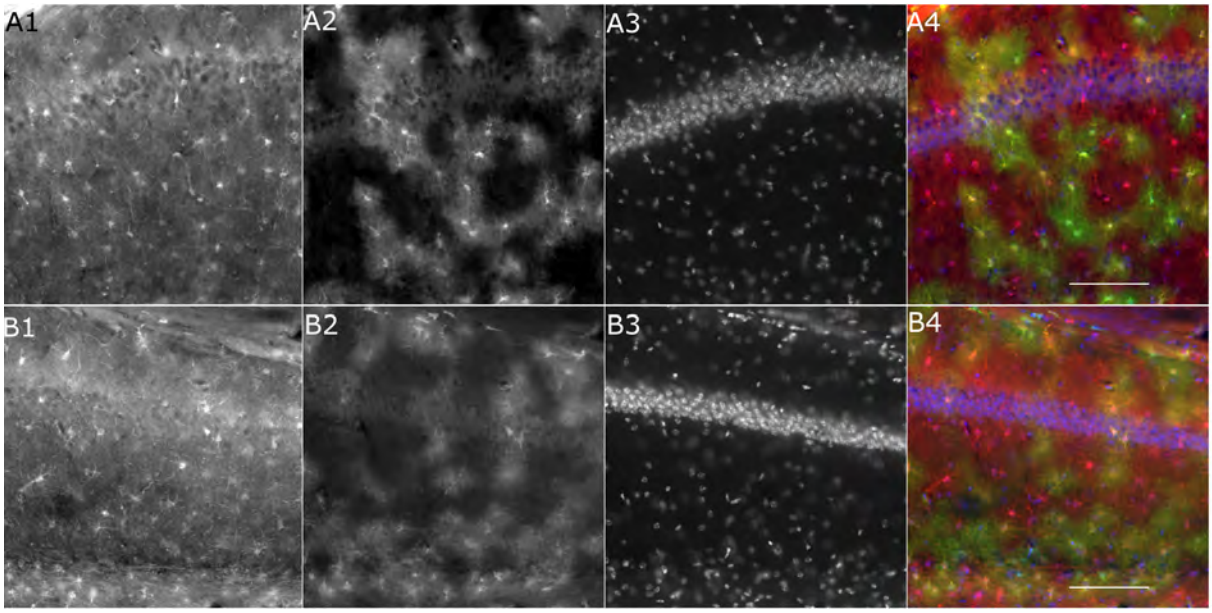

Fig. 4.12: Expression levels of Cx30 and Cx43 in the hippocampus assessed by R26R-EYFP reporter mice. A, B: Colocalization of S100β and EYFP. A: Hippocampus of a Cx43CreERT:R26R-EYFP mouse. B: Hippocampus of a Cx30CreERT2:R26R-EYFP mouse. A1, B1: S100β. A2, B2: EYFP. A3,B3: Hoechst. A4,B4: overlay of S100β (red), EYFP- (green) and nuclear stain (blue). Cells in which S100β and EYFP colocalized are yellow. Bar=100μm.

In the primary somatosensory cortex, we analyzed the so-called barrel field and the regions receiving input from shoulder, hind limb and trunk regions (Fig. 4.13 A,B). In of Cx43CreERT:R26R-EYFP mice, 38±3% of S100β positive cells coexpressed EYFP, while a higher percentage, namely 58±2% of S100β positive cells coexpressed EYFP in Cx30CreERT2:R26R-EYFP mice. This difference in the proportions of S100β/EYFP double positive cells was significant. In non-barrel regions of the primary somatosensory cortex of Cx43CreERT:R26R-EYFP mice, 52±4% of S100β positive cells colocalized with EYFP, while in Cx30CreERT2:R26R-EYFP mice, 50±3% of S100β positive cells colocalized with EYFP. This difference in the proportions of S100β/EYFP double positive cells was not significant. The proportions of S100β/EYFP double positive cells in barrel compared to non-barrel regions in Cx43CreERT:R26R-EYFP mice was significantly different , while no significant differences were observed in

Cx30CreERT2:R26R-EYFP mice.

We analyzed EYFP expression in the barrels and in the septa between the barrels in the primary somatosensory cortex. We observed a similar level of expression in the barrels and in the septa between the barrels. In Cx43CreERT:R26R-EYFP mice, in the barrels, 39.3±3.7% and in the septa 33±4% of S100β positive cells were also EYFP positive. In Cx30CreERT2:R26R-EYFP mice, in the barrels, 54.5±4% of S100β positive cells were also EYFP positive, while in the septa the number of S100β/EYFP positive cells was very similar- 53.3±6.5% These differences were not statistically significant for both mice type.

In the thalamus, EYFP expression in the ventral posterolateral thalamic nucleus (VPL) and the ventral posteromedial thalamic nucleus (VPM) was analyzed (Fig.4.13 C,D). In Cx43CreERT:R26R-EYFP mice, 40±3% of S100β positive cells colocalized with EYFP and in Cx30CreERT2:R26R-EYFP mice, 43±2% of S100β positive cells colocalized with EYFP. This difference was not statistically significant.

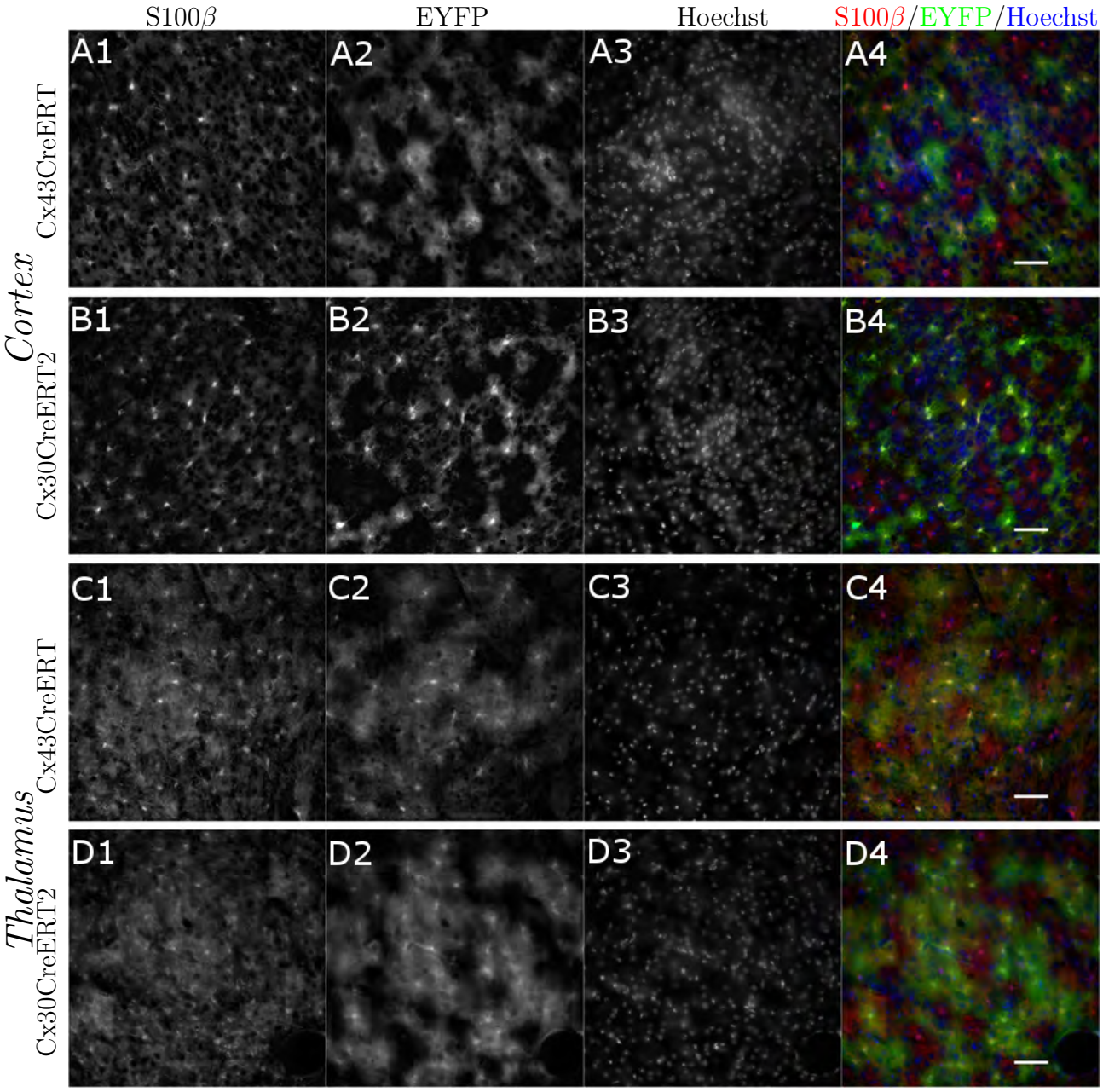

Fig. 4.13: Expression levels of Cx43 and Cx30 in the primary somatosensory cortex and thalamus assessed by R26R-EYFP reporter mice. A-D: Colocalization of S100β and EYFP A: Cortex of Cx43CreERT:R26R-EYFP mouse. B: Cortex of Cx30CreERT2:R26R-EYFP mouse C: Thalamus of Cx43CreERT:R26R-EYFP mouse. D: Thalamus of Cx30CreERT2:R26R-EYFP mouse. A4,B4,C4,E4- overlay of S100β (red), EYFP- (green) and nuclear stain (blue). Cells in which S100β and EYFP colocalized are yellow. Bar=50μm.

In the cerebellum, the proportion of the EYFP positive Bergmann glia expressing S100β (see Fig. 4.14) was calculated. In the Cx43CreERT:R26R-EYFP mice, 64.4±2.8 % of S100β positive cells expressed EYFP and in Cx30CreERT2:R26R-EYFP mice, 64.3±2.3% of S100β positive cells colocalized. This difference was not statistically significant.

S100β/EYFP/Hoechst

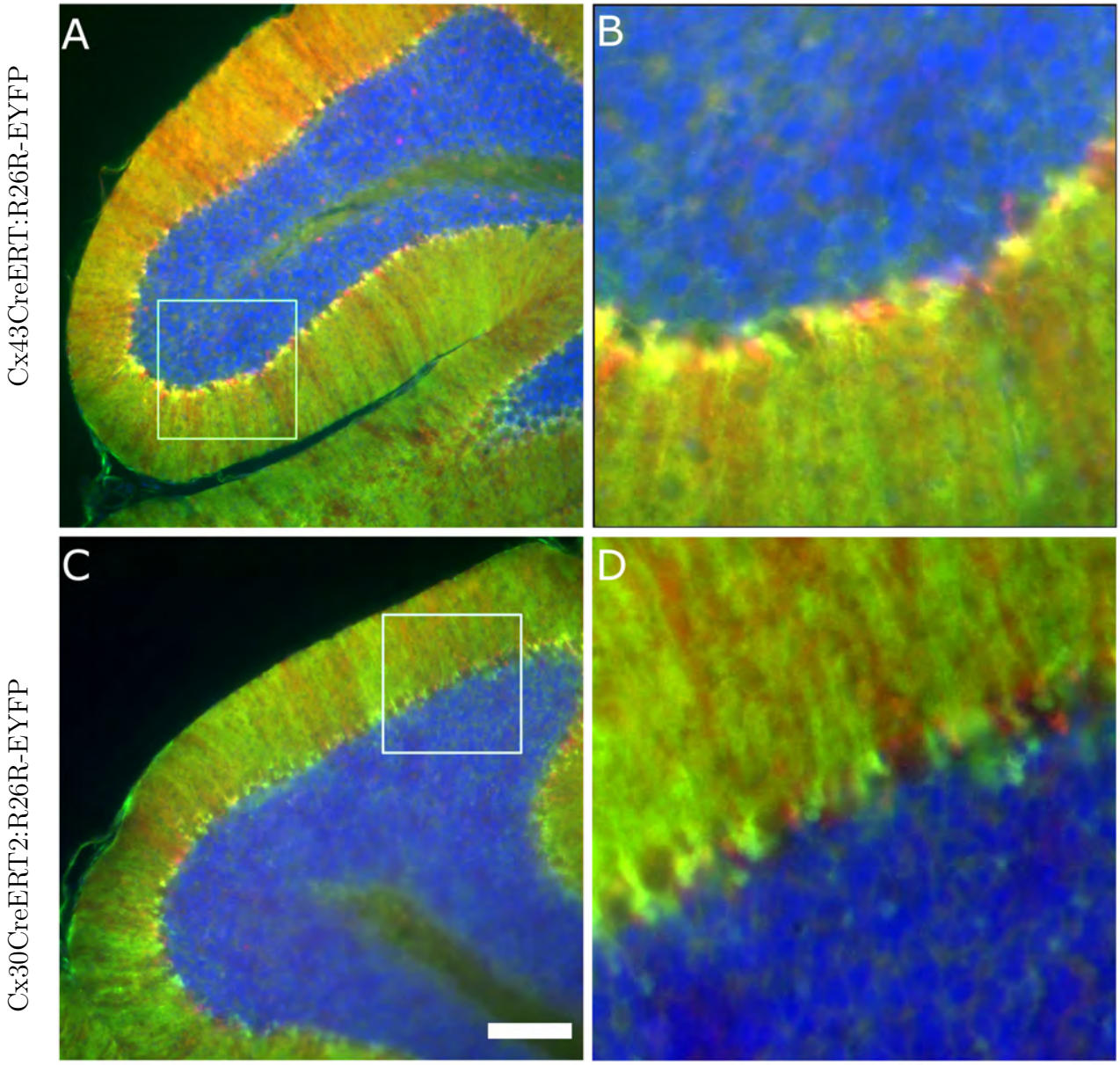

Fig. 4.14: Expression levels of Cx30 and Cx43 in cerebellum assessed by R26R-EYFP reporter mice. A: Cerebellum of a Cx43CreERT:R26R-EYFP mouse. C: Cerebellum of a Cx30CreERT2:R26R-EYFP mouse. B,D show detailed images of the boxes in A,C. S100β: red, EYFP: green, Hoechst nuclear stain: blue. Cells in which S100β and EYFP colocalized are yellow. Bar=100μm.

Figure 4.15 summarizes the results obtained using Cx43CreERT:R26R-EYFP and Cx30CreERT2:R26R-EYFP transgenic mice: In the hippocampus Cx43CreERT led to higher recombination efficacy, reproducing our previous findings (Gosejacob et al., 2011). In the barrel cortex, Cx30CreERT2 has higher recombination efficacy, while in non barrel regions of the cortex, in thalamus and in cerebellum the efficacies of both inducible Cre lines were similar.

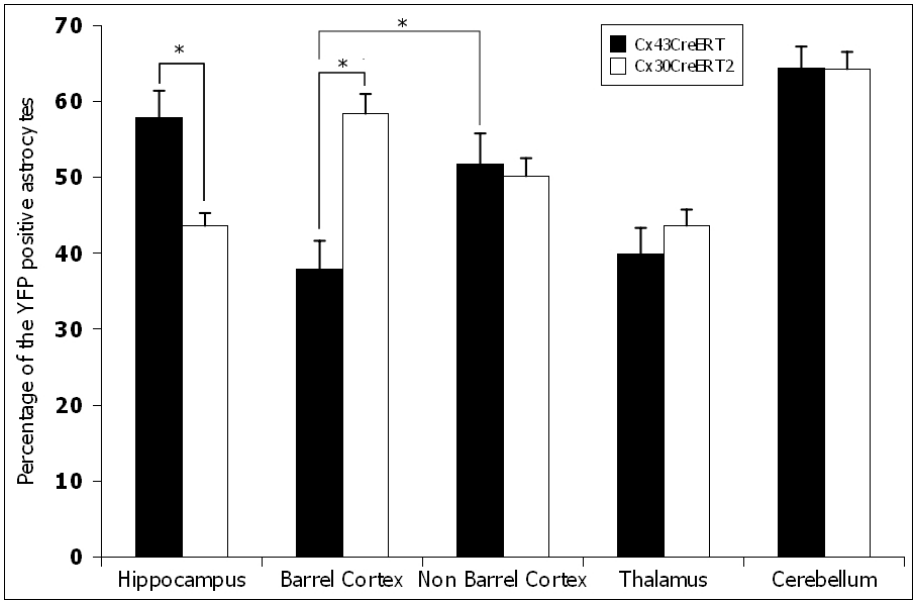

Fig. 4.15: Ratio of EYFP/ S100β double positive cells to all S100β positive cells in hippocampus, somatosensory cortex (somatosensory cortex barrel field and non-barrel field), thalamus and cerebellum of Cx43CreERT:R26R-EYFP and Cx30CreERT2:R26R-EYFP mice. The proportion of double positive cells in the hippocampus of Cx43CreERT:R26R-EYFP was significantly higher than in Cx30CreERT2:R26R-EYFP mice. In the barrel cortex, the proportion of double positive cells was significantly higher in Cx30CreERT2:R26R-EYFP mice. The proportion of the double positive cells in non barrel cortex, thalamus and cerebellum was similar in both transgenic mice. The proportion of double positive cells in the non-barrel cortex was significantly higher than in barrel cortex of Cx43CreERT:R26R-EYFP mice.

4.5 Comparing the role of Cx43 and Cx30 positive stem cells in neurogenesis

In the adult brain exist two main neurogenic niches -SGZ and SVZ. We compared the role of Cx30 and Cx43 in adult neurogenesis in the SGZ. For this purpose we analyzed the number of neurons generated from Cx43 and Cx30 positive RG-like cells.

4.5.1 Number of the generated neurones

Cx43CreERT: R26R-EYFP and Cx30CreERT2:R26R-EYFP mice were stained for NeuN and EYFP (3 animals per genotype, 6 sections each) (see Fig4.16). Cells in SGZ, and in the granule cell layer of the dentate gyrus were scored for double positive cells (3 animals per genotype, 6 sections each). In SGZ of Cx43CreERT:R26R-EYFP mice, 9.4±1.6 % of EYFP positive cells were NeuN positive (or 3.1±0.5 cells per section), and in the SGZ of Cx30CreERT2:R26R-EYFP mice, 1.7±0.8% of EYFP positive cells were NeuN positive (or 0.5±0.2 cells per section). The difference in expression levels was statistically significant. In the granule cell layer, these values were 8.7±3 % (or 1±0.3 cells per section) and 0.95±1.7% (or 0.17±0.09 cells per section) respectively. The difference in expression levels was statistically significant.

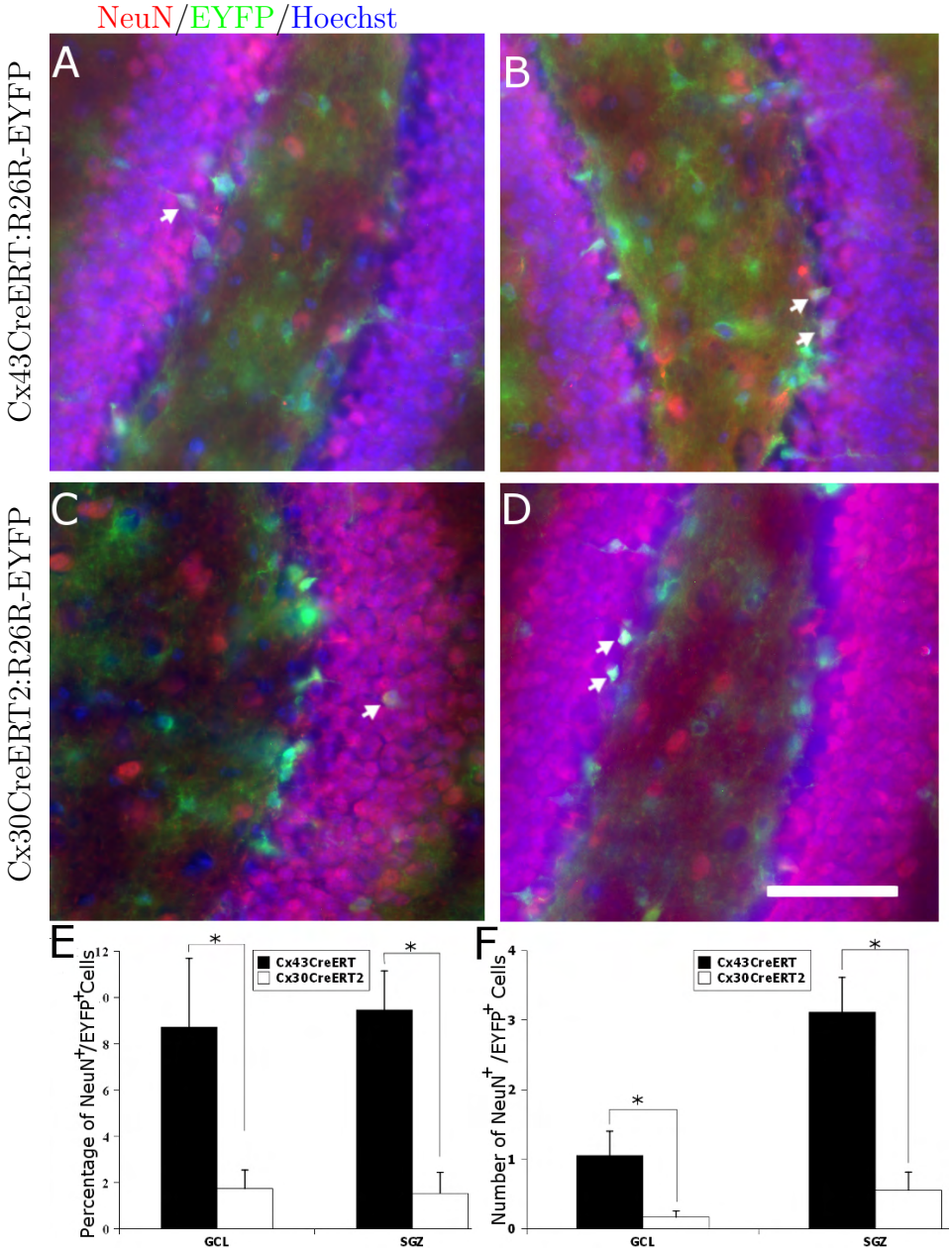

Fig. 4.16: Double labelling for NeuN and EYFP R26R-EYFP reporter mice. A,B: Dentate gyrus of Cx43CreERT:R26R-EYFP mouse stained for EYFP (green), NeuN (red) and Hoechst (blue). C, D: Cx30CreERT2: R26R-EYFP mouse stained for EYFP (green), and NeuN (red) and Hoechst (blue). Arrows point to double positive cells in the granule cell layer A,C, and in the SGZ B,D. E: Proportion of NeuN/EYFP double positive cells of all EYFP positive cells in the granule cell layer and SGZ of Cx43CreERT:R26R-EYFP and Cx30CreERT2:R26R-EYFP mice. F: Absolute number of NeuN/EYFP double positive cells per section in the granule cell layer (GCL) and SGZ of Cx43CreERT:R26R-EYFP mice and Cx30CreERT2:R26R-EYFP mice. Bar=50μm.

4.5.2 Number of Cx43 and Cx30 positive RG-like cells

To assess the number of Cx43 and Cx30 positive RG-like cells we used double staining for the RG-like cells marker Brain Lipid Binding Protein (BLBP; Feng et al., 1994) and EYFP in Cx43CreERT:R26R-EYFP and Cx30CreERT2:R26R-EYFP mice (Fig. 4.17). In Cx43CreERT:R26R-EYFP mice 40.1±3.4% of BLBP positive cells were also EYFP positive, vs. 10.7±1.2% in Cx30CreERT2:R26R-EYFP mice. The difference was statistically significant.

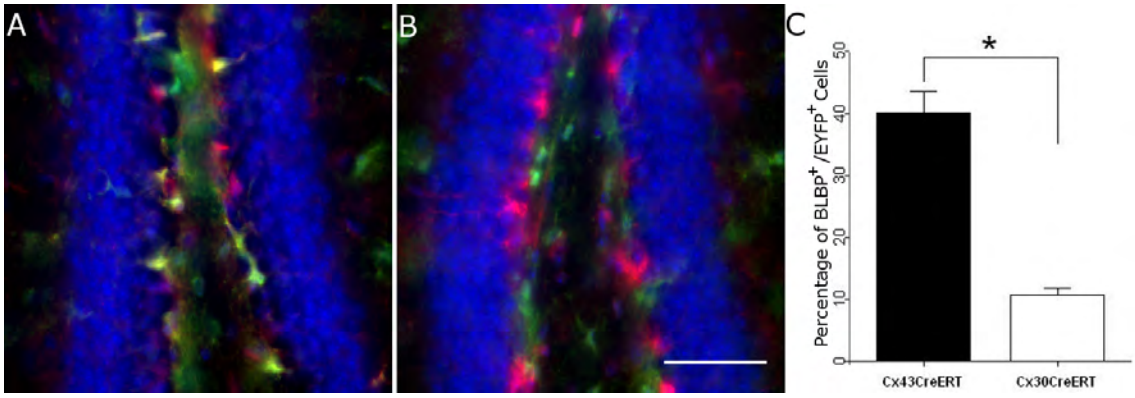

Fig. 4.17: Double labelling for BLBP and EYFP in R26R-EYFP reporter mice recombined by Cx43CreERT or Cx30CreERT2. A: The dentate gyrus of a Cx43CreERT:R26R-EYFP mouse was stained for EYFP (green) BLBP (red) and Hoechst (blue). B: A Cx43CreERT: R26R-EYFP mouse was stained for EYFP (green), BLBP (red) and Hoechst (blue). C: Proportion of BLBP/YFP double positive cells of all BLBP positive cells in the SGZ of Cx43CreERT:R26R-EYFP mice and Cx30CreERT2:R26R-EYFP mice. We analyzed 3 animals per genotype, 6 sections for each animal. Bar=50μm.

4.6 Fate mapping of astrocytes in TLE

In the hippocampus of TLE patients, astrocytes disappeared, and most of the glial cells remaining in the hippocampus were NG2 positive cells (Hüttmann and Bedner, unpublished results). The aim of this project was to study the

fate of astrocytes in a TLE model, to answer the question -if they just died or acquired another phenotype.

4.6.1 Establishing a method for fate mapping of astrocyte in a model for temporal lobe epilepsy

Several transgenic mice with inducible Cre recombinase were tested for suitability to the study the fate of astrocytes in the hippocampus in our TLE model. We used GLASTCreERT mice with Cx43fl(LacZ) as a reporter, GFAPCreERT mice with R26R as a reporter, and Cx43CreERT and Cx30CreERT2 mice with R26R-EYFP as a reporter. By application to wild type mice the maximal non-letal dose of tamoxifen was determined, which was 1 mg i.p. twice a day. Application of tamoxifen for 5 consecutive days to GFAPCreERT mice, as well as intrathecal injection of tamoxifen did not cause any expression of reporter in the hippocampus (Fig. 4.18 A). Only weak expression of β-galactosidase in the cerebellum was observed. Intraperitoneal injection of tamoxifen into GLASTCreERT mice caused a very low level of recombination in the hippocampus (Fig. 4.18 B). However application of tamoxifen to Cx43CreERTR26R-EYFP and Cx30CreERT2:R26R-EYFP mice resulted in strong recombination in the CA1 region of the hippocampus (see section 4.4.3 and Fig. 4.12)

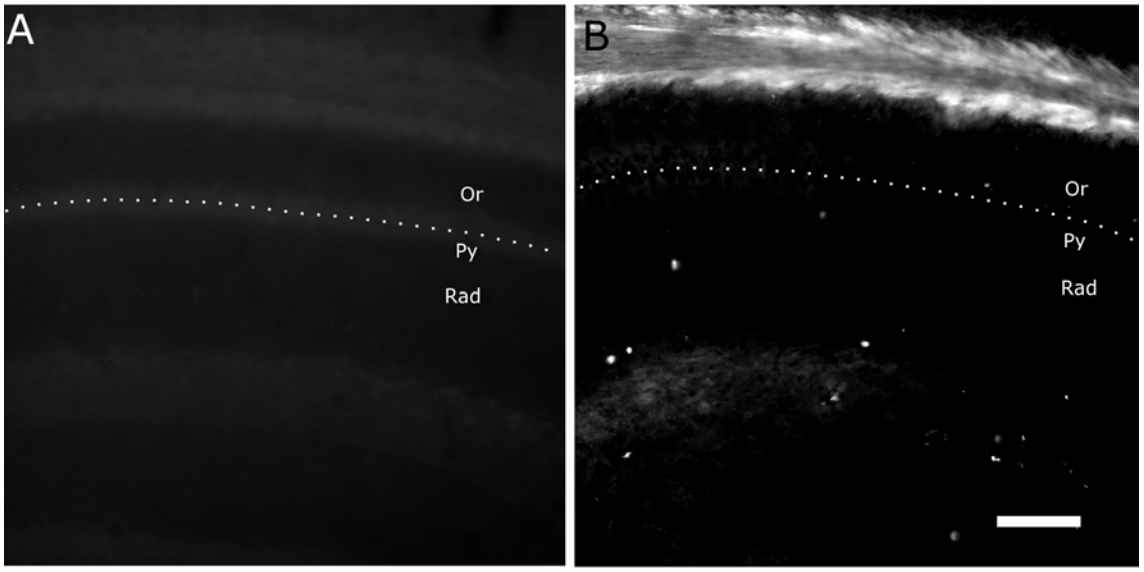

Fig. 4.18: Induction of the Cre mediated recombination in two different mouse models A. Using GFAPCreERT:R26R no β-galactosidase expression in hippocampus was observed. B. Using GLASTCreERT:Cx43fl(LacZ) only low level of β-galactosidase expression in hippocampus was observed. Or - stratum orience, Rad - stratum radiatum, Py and dotted line - stratum pyramidale, Bar=100μm

4.6.2 Cx43CreERT:R26R-EYFP mice subjected to our TLE model induced by intracortical injection of kainate.

We chose to use Cx43CreERT:R26R-EYFP mice in our TLE model because of the high recombination efficacy in the hippocampus (see 4.4.3 and Fig. 4.15). An important prerequisite to use of fate mapping approach is lack of Cx43CreERT induced recombination in NG2 cells in the normal brain. We tested this, and found that Cx43CreERT:R26R-EYFP animals after tamoxifen induction do not show colocalization of the EYFP signal with the NG2 signal in the CA1 region of the hippocampus (3 mice, 3 sections per mouse were tested). Cx43CreERT:R26R-EYFP animals subjected to our TLE model of intracortical kainate injection , showed GCD, pyramidal cell loss and reactive gliosis 6 months after kainate injection (similar changes are observed in human

TLE (Armstrong, 1993)). To evaluate the fate of astrocytes, we screened the sections stained for EYFP and NG2 for double positive cells. No colocalization of EYFP with the NG2 signal was observed (Fig.4.19A), and most of the EYFP positive were also GFAP positive (Fig.4.19B). A small fraction of EYFP positive cell was neither NG2 nor GFAP positive (Fig.4.19 C,D; 3 mice, 3 sections per mouse were tested). This indicated that astrocytes in TLE do not transdifferentiate into NG2 cells. The finding of recombined, GFAP negative cells indicates that astrocytes may acquire an atypical phenotype.

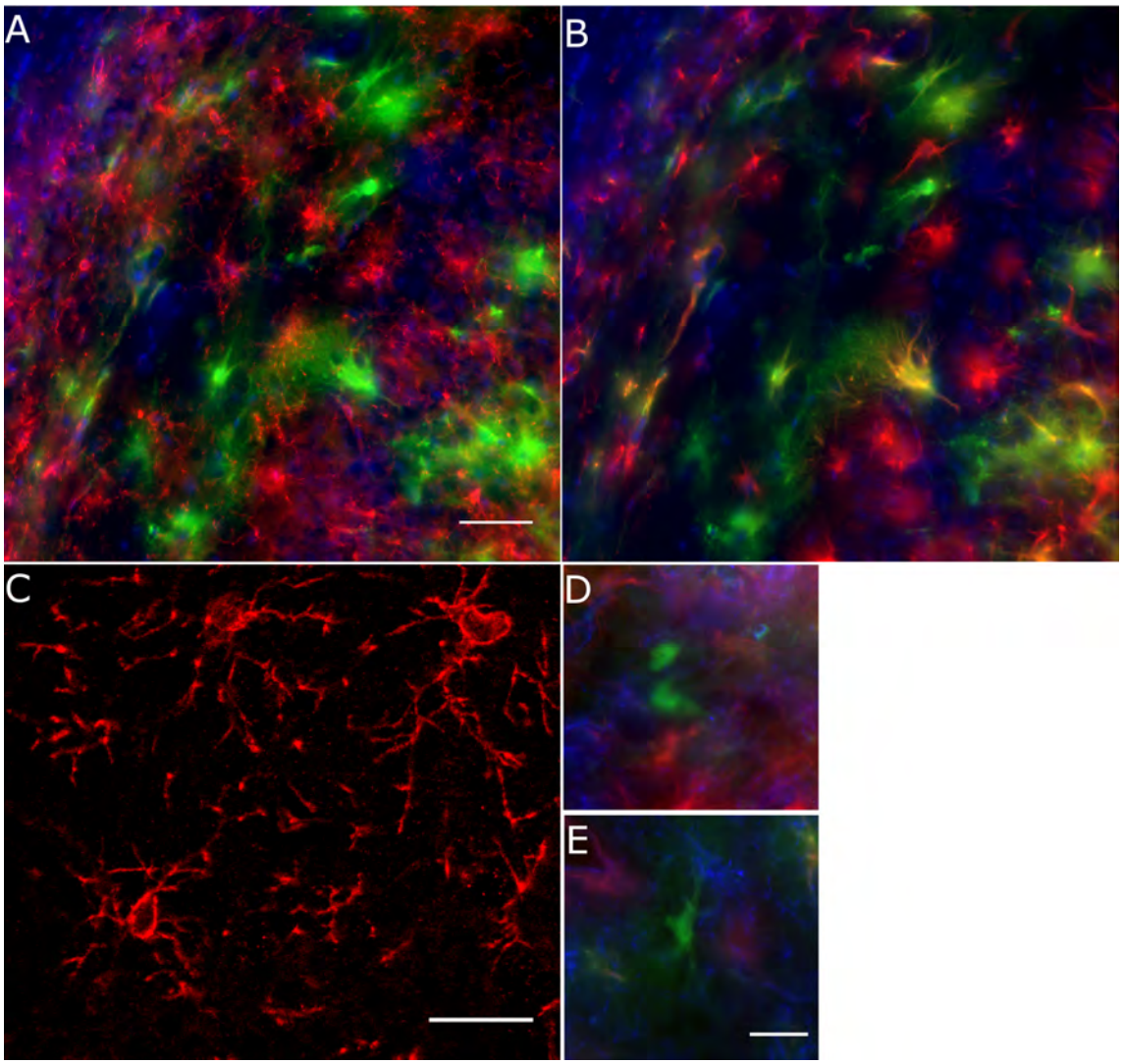

Fig. 4.19: Cx43CreERT:R26R-EYFP mice subjected to a model of TLE induced by intracortical injection of kainate. Staining of the CA1 region. A: EYFP (green), NG2 (red) and Hoechst (blue). No colocalization of NG2 with EYFP was observed. B. EYFP (green), GFAP (red) and Hoechst (blue). Most of EYFP positive cells are GFAP positive. C: Normal morphology of the NG2 cells from the contralateral to kainate injection side. D,E: Some EGFP positive cells showed no immunorectivity for GFAP or NG2. EYFP (green), GFAP (red) and Hoechst (blue). Bar in A: 50 μm, for A,B. Bar in C:25 μm, Bar in E: 25 μm for D,E.

4.7 Quality control of Cx43CreERT:R26R-EYFP

We observed spontaneous (uninduced) recombination of Cx43CreERT:R26R-EYFP by PCR analysis of tail tip DNA (not shown). These mice possessed the R26R-EYFP recombined allele, without tamoxifen injection, as revealed by PCR analysis. On immunofluorescent stainings from brain sections of these mice, we observed a high number of neurons expressing EYFP (Fig. 4.20 A) and a low number of EYFP expressing astrocytes (Fig. 4.20 C), in comparison to the Cx43CreERT:R26R-EYFP animals with proper recombination induced by tamoxifen injection. The frequency of the spontaneous recombination was 7.5% (3 of 40 mice). No such phenomenon was observed in Cx30CreERT2:R26R-EYFP (40 mice were analysed).

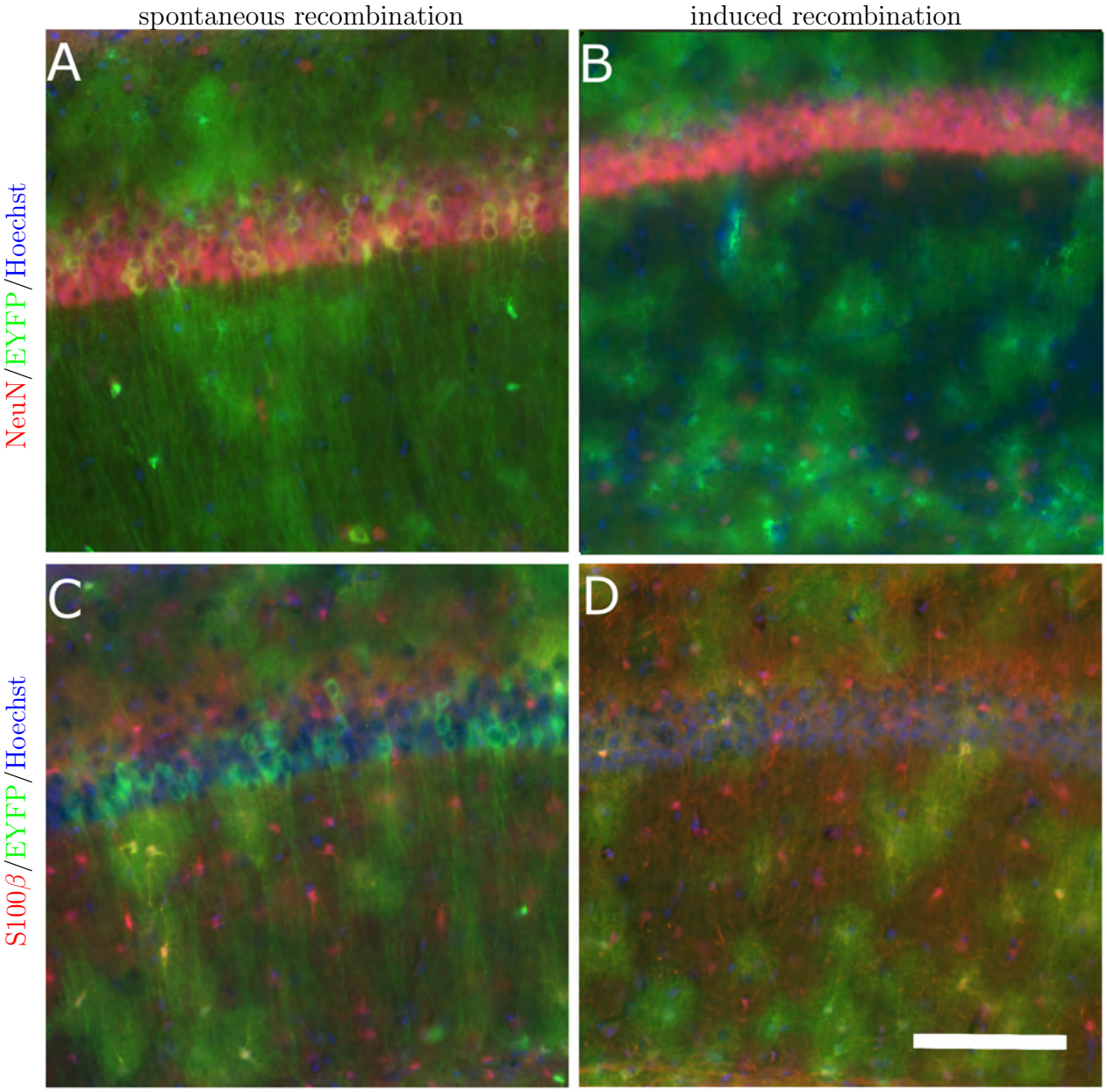

Fig. 4.20: Spontaneous recombination in Cx43reERT:R26R-EYFP mice in the CA1 region of the hippocampus. A, C: Sections from a mouse with spontaneous recombination (without induction by tamoxifen). Note the high level of colocalization of NeuN with EYFP in the pyramidal cell layer in A. B, D: Sections from a Cx43CreERT:R26R-EYFP mouse with proper recombination induced by tamoxifen injection. A,B: NeuN-(red), EYFP-(green) and nuclear stain Hoechst -(blue). C,D: S100β -(red) EYFP-(green) and nuclear stain Hoechst -(blue). Bar=100μm.

Chapter 5

Discussion

5.1 Characterization of a novel conditional KO mouse

Gene inactivation reporters show loss of gene expression in each individual mouse, but in double knockout mice which use identical reporters, it is impossible to differentiate loss of one or the other gene, or both of the genes. This is the situation in Cx43/Cx30 DKO mice we and others already described (Wallraff et al., 2006; Rouach et al., 2008) . With a novel conditional transgenic mouse line recently generated by J. Degen, expressing the enhanced cyan fluorescent protein (ECFP) instead of Cx43 after Cre-mediated recombination, we present a new concept - a dual reporter approach - to differentiate loss of Cx30 expression (lacZ) from loss of Cx43 expression (ECFP). In contrast to hGFAP/EGFP mice with labeling of both astrocytes and GluR/NG2 cells (Matthias et al., 2003), fluorescence in Cx43kiECFP mice is invariably confined to astrocytes. Furthermore, we analyzed a new conditional KO construct for Cx43: In cells with Cx43 gene-activity, ECFP was expressed after Cre-mediated Cx43 ablation. By this approach with different reporter-genes, we could differentiate Cx30 from Cx43 expression. It gives us a opportunity to study expression of each connexin. Upon Cx43 ablation, Cx30 was upregulated, preferentially in the vicinity of pyramidal cells, i.e. in stratum radiatum adjacent to the hippocampal pyramidal cell layer and in stratum oriens, as well as in all layers

of the cortex except for layer I. Both Cx43 and Cx30 constitute astrocytic gap junctions and allow interastrocytic coupling in the hippocampus. This was inferred from three observations: (1) Mice lacking Cx43 show residual interastrocytic coupling amounting to 50% of control conditions (Theis et al., 2003). (2) DKO mice lacking both connexins exhibit complete loss of interastrocytic tracer spread in the hippocampus (Rouach et al., 2008; Wallraff et al., 2006). (3) Tracer spread in Cx30-deficient mice showed 22% decrease of interastrocytic coupling (Gosejacob et al., 2011). Thus, coupling of astrocytes in the hippocampus predominantly depends on Cx43. Obviously, Cx43 and Cx30 do not have a simple additive role in mediating gap junction communication. This discrepancy could be explained by observed upregulation of the Cx30 in Cx43 KO mice. The exact mechanism by which Cx30 is upregulated upon loss of Cx43 requires further investigation.

In a second approach, we used two different reporters of gene-inactivation at the same genetic locus. We assessed the efficacy of Cre-mediated recombination at the level of individual cells and individual alleles. In this way we can estimate the efficacy of conditional KO, i.e. weather after recombination both alleles of Cx43 are deleted, or one of them remains intact. Indeed, hGFAP-Cre deleted both floxed Cx43 alleles in the majority of cells expressing Cx43 in the hippocampus. Few cells lost only one allele and might have expressed residual Cx43 protein. Such an assessment of complete deletion within a cell is even more important for inducible Cre-recombinase transgenes, which are expected to be less active compared to their constitutive versions (Zhuo et al., 2001; Hirrlinger et al., 2006). In conclusion, we here present conceptual advances of gene inactivation reporters – dual reporter approaches – which allow identifying compensatory regulation of genes and which allow quantifying the efficacy of Cre-mediated gene inactivation - both with single cell resolution *in situ*.

5.2 Evaluation of Cx30 expression in the brain

Contradictory findings about Cx30 expression assessed by a reporter gene in Cx30lacZ/lacZ mice (Requardt et al., 2009; Theis et al., 2005) and from previous immunohistochemical studies (Nagy et al., 1999) prompted us to

reinvestigate hippocampal Cx30 expression. Expression of Cx30 in hippocampal astrocytes has been reported previously (Nagy et al., 1999; Rouach et al., 2008). Immunoblotting and immunoflourescence experiments indicated similar abundance of Cx30 in cerebral cortex and hippocampus (Gosejacob et al., 2011). In all areas gap junction plaques composed of Cx30 were found at blood vessels (Rouach et al., 2008; Gosejacob et al., 2011). Because of the dotted staining pattern of connexins, which makes assignment to specific cells or cell types difficult or even impossible, reporter genes were useful to study connexin expression (Requardt et al., 2009; Theis et al., 2005). With double labeling against the expressed product of a reporter gene and cell-type specific marker proteins the identity of connexin expressing cells can be clearly identified. An important prerequisite for the usefulness of reporter genes is their authenticity. We therefore performed a detailed comparative analysis of hippocampal Cx30 expression using two approaches: (1) Antibodies directed to β-galactosidase were used for lacZ expression studies of Cx30 gene transcriptional activity (section 4.4.1 of this thesis); (2) A Cre/loxP-based approach was applied to monitor transcriptional activity of the Cx30 gene (sections 4.4.2 and 4.4.3 of this thesis).

The Cx30lacZ allele (Teubner et al., 2003) was used to study Cx30 expression in the hippocampus with immunohistochemical analysis. The lacZ reporter gene approach using Cx30lacZ/lacZ mice showed prominent β-galactosidase expression in the cerebral cortex. Only scattered β-galactosidase immunoreactivity could be detected in the hippocampus of Cx30lacZ/lacZ animals. We wondered whether Cx30 gene activity was properly reflected by the lacZ reporter. As an independent approach to confirm or disconfirm authenticity of the Cx30lacZ reporter allele, Cx30CreERT2:R26R-EYFP mice were used as reporter for Cx30 expression. To monitor transcriptional activity of the Cx30 gene, the Cx30CreERT2 BAC transgenic mouse line was used. As readout, recombination-activation of an EYFP reporter embedded in the ROSA26 locus was used. The EYFP expression pattern matched the Cx30 expression pattern determined by Cx30 antibody stainings in the hippocampus. Most importantly the EYFP expressing cells showed also expression of the astrocytic marker S100β. Similar results were obtained using astrocytic marker GFAP (Gosejacob

et al., 2011). Thus, using EYFP expression in the Cx30CreERT2;R26R-EYFP mice as Cx30 reporter, Cx30 expression was observed predominantly in astrocytes.

Our results indicate that the lacZ expression in the Cx30lacZ/lacZ is not reflect properly Cx30 expression in the hippocampus, even though the Cx30lacZ allele was generated by homologous recombination and the lacZ reporter gene is inserted into the Cx30 locus. Disturbance of authentic expression may be related to the presence of a neomycin resistance cassette in the Cx30lacZ allele (Teubner et al., 2003). For the hippocampus the Cx30CreERT2 BAC allele seems to be better suited to study the expression pattern of Cx30. Altogether Cx30 expression was demonstrated in the hippocampus by immunofluorescence and immunoblot analysis (Gosejacob et al., 2011) as well as recombination activation of a reporter gene.

We wanted to assess the relative role of Cx43 an Cx30 in different brain regions and to quantify the recombination efficacy of the inducible transgenes at the same time. We observed similar levels of Cx30 and Cx43 expression utilizing the R26R-EYFP reporter in the cortex and cerebellum. In the barrel cortex, expression of Cx43 reported by EYFP expression was significantly lower than in other regions of the somatosensory cortex. No difference in the proportion of EYFP positive cells was observed in barrels and the septa between the barrels. Previously, a lower level of connexin expression was reported in the septa in comparison with the barrels, and reduced astrocytic coupling in the septa was detected by tracer injection (Houades et al., 2008). The difference to our results might link at a lower level of Cx43 expression in each cell in the septa, but a similar proportion of astrocytes expressing Cx43 in barrels and septa.

5.2.1 The role of C43 and 30 in adult neurogenesis

Previously Kunze and colleagues (Kunze et al., 2009) showed the importance of Cx43 and Cx30 for adult neurogenesis. Mice lacking both connexins (Cx30/Cx43 DKO) showed a significant reduction in the rate of proliferation in the dentate gyrus. A reduction in the number of Ki67 (a marker for proliferation) expressing cells, in the number of Prox1 positive cells (a marker for granule

cells), and in the number of BrDU labeled cells was observed. From the results obtained from DKO mice, it is impossible to differentiate effects of Cx30 and Cx43 on neurogenesis. We therefore used Cx43CreERT:R26R-EYFP and Cx30CreERT2:R26R-EYFP mice for fate mapping studies of Cx43 and Cx30 positive neuronal precursor cells. We analyzed the number of neurons generated during a one month period, following tamoxifen injection. The number of the generated neurons, both mature (in the granule cell layer) and immature (in the subgranular zone) was significantly higher in Cx43CreERT:R26R-EYFP mice. We also analyzed the number of RG-like cells expressing Cx43 an Cx30 utilizing Cx43CreERT:R26R-EYFP and Cx30CreERT2:R26R-EYFP mice, by double labeling with BLBP. We observed a significantly higher number of Cx43 positive RG-like cells than Cx30 positive cells. Our results indicate that most of neuronal precursor cells are Cx43 positive but not Cx30 positive. Similar results was obtained by Kunze and colleagues (Kunze et al., 2009), by single cell RT-PCR analysis they revealed that 50% of the RG-like cells express Cx43 and 30 % express Cx30. These findings are in nice correlation with observations of J. Zhang, who showed a 83% reduction in the number of Ki67-positive cells, and a 22% reduction in the number of Prox1 positive cells in Cx43 KO mice, but no such reduction in Cx30 KO mice (J. Zhang unpublished results) From all these findings, we can conclude that Cx43 is more important for adult neurogenesis in SGZ than Cx30.

5.3 Quality control of double KO mice

We have observed heterogeneity of hGFAP-Cre mediated recombination, but the underlying mechanism is still not revealed. Possible influences on the fidelity of hGFAP-Cre may stem from (i) methylation status (Barresi et al.,1999), (ii) genetic background, (iii) spontaneous transgene rearrangements (Schulz et al., 2007), or (iv) other epigenetic mechanisms such as chromatin remodeling (Lee et al., 2006). Subsequently, possible reproductive deficits in DKO parents may lead to evolutionary selection against Cre activity. We have presented strategies assessment of astrocyte-directed DKO mice by immunodetection. Mice could be analyzed immunostaining for Cre in cerebellum or for β-galactosidase in

hippocampus. The same mice could be analyzed utilizing immunobloting or PCR technique (Requardt et al., 2009). The deletion status of DKO mice was consistent within breedings. Thus, the procedures described here allow pre-experimental assessment of siblings in order to estimate the activity status of Cre within a litter. Although we found a strong consistency of Cre deletion status among siblings, we nevertheless recommend postexperimental evaluation of individual mice to correlate the gene inactivation status with phenotypical alterations.

5.4 Quality control of Cx43CreERT:R26R-EYFP

We observed spontaneous recombination (background recombination without induction by tamoxifen injection) in Cx43CreERT:R26R-EYFP mice. but not in Cx30CreERT2:R26R-EYFP mice. In these mice different types of inducible Cre are expressed: in Cx43CreERT:R26R-EYFP mice, CreERT1 (Feil et al., 1996) is expressed and in Cx30CreERT2:R26R-EYFP mice, CreERT2 (Feil et al., 1997) is expressed. For both types of CreERT background recombination was previously reported (Kemp et al., 2004; Hameyer et al., 2007; Matsuda & Cepko, 2007). The background recombination in Cx43CreERT mice is higher most probably because of higher levels of Cx43CreERT expression (higher level of expression results in higher level of background recombination; Joyner & Sudarov, 2011).

This background recombination could be detected easily by PCR analysis of tail tip DNA. Since Cx43CreERT:R26R-EYFP mice show background recombination and higher variability in expression levels in the different brain regions, and higher numbers of EYFP expressing neurons because of Cx43 expression in stem cells, Cx30CreERT2:R26R-EYFP mice are more suitable for fate mapping studies in astrocytes.

5.5 DKO mice in epilepsy

In control mice subjected to TLE model we observed neuronal cell loss in CA1 region, granule cell dispersion, similar morphological changes were observed in TLE patients (Armstrong, 1993). We also observed loss of NeuN related immunoreactivity in the dentate gyrus, while neurones were still visible on the Hoechst staining. Loss of NeuN immunoreactivity without neuronal loss was observed previously under different pathological conditions: transient reduction of NeuN after axototomy (McPhail et al., 2004) and permanent loss in cerebrall ischemia (Unal-Cevik et al., 2004). This loss of NeuN immunoreactivity was accompanied by a reduction in immunoreactivity of other neuron specific proteins as choline acetyl transferase (ChAT; McPhail et al., 2004) and microtubule-associated protein-2 (MAP-2; Chen et al., 2001), and may be associated with reduction of the protein synthesis or increase in protein degradation under pathological conditions (Unal-Cevik et al., 2004).

In DKO animals, morphological changes in the TLE model were less pronounced, i.e. AHS was less severe. At the same time, these animal showed a shorter status epilepticus after kainate injection (Peter Bedner, unpublished results). These findings could be a result of a reduction in glutamatergic synaptic transmission and neuronal activity due to decreased metabolite supply to neurones by the astrocytic network, due to loss of astrocytic gap junctional coupling (Rouach et al., 2008). Less pronounced morphological changes indicated a pro-epileptic function of astrocytic gap junctions. DKO mice however, showed a shorter latency period and higher number of spontaneous seizures indicating an anti-epileptic functions of astrocytic gap junctions, as well. This anti-epileptic function might be linked to reduction of neuronal excitability by a mechanism of the spatial buffering of K^+ (Wallraff et al., 2006). Another study recently showed that in DKO mice lacking Cx43 and Cx30 neuronal excitability is increased (Pannasch et al., 2011). This led us to the following working hypothesis: immediately after kainate injection, i.e. in status epilepticus metabolite supply may be the predominant function of astrocytic connexins supporting neuronal hyperexcitability. However, during the chronic phase, removal of the K^+ by a mechanism of spatial buffering may be the predominant

function of astrocytic connexins, which limits neuronal activity.

5.6 Fate mapping of astrocytes in TLE

In the hippocampi of patients suffering from TLE, almost complete loss of "bona fida" astrocytes showing passive currents and coupling by gap junctions was observed (Bedner et al., unpublished), while most of the remaining glial cells showed properties of NG2 glial cells. We decided to investigate the fate of the astrocytes, i.e. if they transdifferentiate into NG2 glial cells, or if they just die. First, we established a model for astrocytic fate mapping *in vivo*. We analyzed four different transgenic mouse models (GFAPCreERT:R26R, GLASTCreERT:Cx43fl(LacZ), Cx30CreERT2:R26R-EYFP, and Cx43CreERT:R26R-EYFP with different paradigms of tamoxifen and hydroxytamoxifen injection. Cx30CreER:R26R-EYFP and Cx43CreERT:R26R-EYFP mice showed highest levels of recombination in astrocytes, and they were found suitable for fate mapping of astrocytes in the TLE model. No EYFP expression was observed in NG2 glia (detected by immunofluorescence) in the hippocampus of Cx43CreERT:R26R-EYFP mice up to 6 month after kainate injection. At this time point, morphological changes in hippocampus were already very pronounced (see Fig. 4.8), and EYFP positive cells showed a current pattern untypical for astrocytes (Bedner et al., unpublished). Most of the EYFP positive cells were also GFAP positive. Some of the EYFP positive cells were neither NG2 nor GFAP positive. Part of these cells exhibited a non-astrocytic morphology, but a precise determination of these cells needs further investigation. Taking all findings together, we can conclude that astrocytes in TLE do not transdifferentiate into NG2 cells.

Summary

Despite of the growing number of studies, the expression pattern as well as the exact functions of astrocytic connexins are not yet fully elucidated. In this study I analyzed the expression pattern and functions of the two major astrocytic connexins, Cx30 and Cx43, under normal conditions and in a mouse model for temporal lobe epilepsy (TLE).

In the first part of my work I characterized novel conditional knock out mice, expressing ECFP instead of Cx43 after Cre-mediated recombination. Utilizing this mouse, I demonstrated dual reporter approaches to i) simultaneously examine astrocyte subpopulations expressing different connexins, ii) identify compensatory upregulation within gene families and iii) quantify Cre-mediated deletion at the allelic level.

In the second part of my work, I re-evaluated the expression of Cx30 in different brain regions. I analyzed the reporter gene expression of Cx30 knockout mice. Utilizing a fate mapping approach, I showed that the reporter gene expression does not reflect properly the Cx30 expression in the hippocampus. Using a fate mapping approach, I also demonstrated that Cx30 is expressed at similar levels compared to Cx43 in most brain regions. In addition, utilizing the same fate mapping approach, I showed that radial glia like cells express mostly Cx43, indicating that Cx43 is the most important connexin for adult neurogenesis.

In the third part of my work, I analyzed the influence of Cx30 and Cx43 on morphological changes in brain of mice subjected to a novel mouse TLE model (intracortical kainate injection). In mice lacking both Cx43 and Cx30, I observed less pronounced morphological changes in the hippocampus. I also established methods for quality control of the trangenic mice used in this study. My study adds to a better understanding of expression pattern of astrocytic connexines in the brain, and its role in the epilepsy.

References

Akiyama, H. & McGeer, P. L. (1990). Brain microglia constitutively express beta-2 integrins. J Neuroimmunol, 30, 81–93.

Altman, J. & Das, G. D. (1965). Autoradiographic and histological evidence of postnatal hippocampal neurogenesis in rats. J Comp Neurol, 124, 319–335.

Altman, J. & Das, G. D. (1967). Postnatal neurogenesis in the guinea-pig. Nature, 214, 1098–1101.

Alvarez-Buylla, A., García-Verdugo, J. M., & Tramontin, A. D. (2001). A unified hypothesis on the lineage of neural stem cells. Nat Rev Neurosci, 2, 287–293.

Alvarez-Buylla, A., Seri, B., & Doetsch, F. (2002). Identification of neural stem cells in the adult vertebrate brain. Brain Res Bull, 57, 751–758.

Amaral, D. & Lavenex, P. (2006). The Hippocampus Book (Oxford Neuroscience Series), chap. Hippocampal Neuroanatomy, pp. 37–114. (Oxford University Press, USA).

Araque, A., Parpura, V., Sanzgiri, R. P., & Haydon, P. G. (1998). Glutamate-dependent astrocyte modulation of synaptic transmission between cultured hippocampal neurons. Eur J Neurosci, 10, 2129–2142.

Armstrong, D. D. (1993). The neuropathology of temporal lobe epilepsy. J Neuropathol Exp Neurol, 52, 433–443.

Barros, L. F. & Deitmer, J. W. (2010). Glucose and lactate supply to the synapse. Brain Res Rev, 63, 149–159.

Bass, N. H., Hess, H. H., Pope, A., & Thalheimer, C. (1971). Quantitative cytoarchitectonic distribution of neurons, glia, and DNA in rat cerebral cortex. The Journal of Comparative Neurology, 143, 481–490.

Begley, C. E., Famulari, M., Annegers, J. F., Lairson, D. R., Reynolds, T. F., Coan, S., Dubinsky, S., Newmark, M. E., Leibson, C., So, E. L., & Rocca, W. A. (2000). The cost of epilepsy in the United States: an estimate from population-based clinical and survey data. Epilepsia, 41, 342–351.

Bergles, D. E., Roberts, J. D., Somogyi, P., & Jahr, C. E. (2000). Glutamatergic synapses on oligodendrocyte precursor cells in the hippocampus. Nature, 405, 187–191.

Beyer, E. C. & Berthoud, V. M. (2009). Connexins: A Guide, chap. The Family of Connexin Genes., pp. 3–75. (Humana press).

Beyer, E. C., Paul, D. L., & Goodenough, D. A. (1987). Connexin43: a protein from rat heart homologous to a gap junction protein from liver. J Cell Biol, 105, 2621–2629.

Bignami, A., Eng, L., Dahl, D., & Uyeda, C. (1972). Localization of the glial fibrillary acidic protein in astrocytes by immunofluorescence. Brain Research, 43, 429 – 435.

Boyes, B., KiM, S., Lee, V., & Sung, S. (1986). Immunohistochemical co-localization of S-100b and the glial fibrillary acidic protein in rat brain. Neuroscience, 17, 857 – 865.

Brandt, M. D., Jessberger, S., Steiner, B., Kronenberg, G., Reuter, K., Bick-Sander, A., von der Behrens, W., & Kempermann, G. (2003). Transient calretinin expression defines early postmitotic step of neuronal differentiation in adult hippocampal neurogenesis of mice. Mol Cell Neurosci, 24, 603–613.

Bröer, S. & Brookes, N. (2001). Transfer of glutamine between astrocytes and neurons. J Neurochem, 77, 705–719.

Brightman, M. W. & Reese, T. S. (1969). Junctions between intimately apposed cell membranes in the vertebrate brain. J Cell Biol, 40, 648–677.

Brozzi, F., Arcuri, C., Giambanco, I., & Donato, R. (2009). S100B Protein Regulates Astrocyte Shape and Migration via Interaction with Src Kinase: Implications for astrocyte development, activation, and tumor grouwth. J Biol Chem, 284, 8797–8811.

Butt, A. (2005). Neuroglia, chap. Structure and functions of oligodendrocytes, pp. 37–47. (Oxford University Press).

Butt, A. M., Hamilton, N., Hubbard, P., Pugh, M., & Ibrahim, M. (2005). Synantocytes: the fifth element. J Anat, 207, 695–706.

Butt, A. M. & Kalsi, A. (2006). Inwardly rectifying potassium channels (Kir) in central nervous system glia: a special role for Kir4.1 in glial functions. J Cell Mol Med, 10, 33–44.

Caspar, D. L., Goodenough, D. A., Makowski, L., & Phillips, W. C. (1977). Gap junction structures. I. Correlated electron microscopy and x-ray diffraction. J Cell Biol, 74, 605–628.

Chen, C. J., Liao, S. L., Chen, W. Y., Hong, J. S., & Kuo, J. S. (2001). Cerebral ischemia/reperfusion injury in rat brain: effects of naloxone. Neuroreport, 12, 1245–1249.

Colton, C. A., Abel, C., Patchett, J., Keri, J., & Yao, J. (1992). Lectin staining of cultured CNS microglia. J Histochem Cytochem, 40, 505–512.

Dahl, D. (1981). The vimentin-GFA protein transition in rat neuroglia cytoskeleton occurs at the time of myelination. J Neurosci Res, 6, 741–748.

Davis, E. J., Foster, T. D., & Thomas, W. E. (1994). Cellular forms and functions of brain microglia. Brain Res Bull, 34, 73–78.

de Jesus Domingues, A. M., Taylor, M., & Fern, R. (2010). Glia as transmitter sources and sensors in health and disease. Neurochem Int, 57, 359–366.

Deloulme, J. C., Raponi, E., Gentil, B. J., Bertacchi, N., Marks, A., Labourdette, G., & Baudier, J. (2004). Nuclear expression of S100B in oligodendrocyte progenitor cells correlates with differentiation toward the oligodendroglial lineage and modulates oligodendrocytes maturation. Mol Cell Neurosci, 27, 453–465.

Dermietzel, R., Gao, Y., Scemes, E., Vieira, D., Urban, M., Kremer, M., Bennett, M. V., & Spray, D. C. (2000). Connexin43 null mice reveal that astrocytes express multiple connexins. Brain Res Brain Res Rev, 32, 45–56.

Dermietzel, R., Traub, O., Hwang, T. K., Beyer, E., Bennett, M. V., Spray, D. C., & Willecke, K. (1989). Differential expression of three gap junction proteins in developing and mature brain tissues. Proc Natl Acad Sci U S A, 86, 10148–10152.

Dimou, L., Simon, C., Kirchhoff, F., Takebayashi, H., & Götz, M. (2008). Progeny of Olig2-expressing progenitors in the gray and white matter of the adult mouse cerebral cortex. J Neurosci, 28, 10434–10442.

Djukic, B., Casper, K. B., Philpot, B. D., Chin, L.-S., & McCarthy, K. D. (2007). Conditional knock-out of Kir4.1 leads to glial membrane depolarization, inhibition of potassium and glutamate uptake, and enhanced short-term synaptic potentiation. J Neurosci, 27, 11354–11365.

Doyon, J., Gaudreau, D., Laforce, R., Castonguay, M., Bédard, P. J., Bédard, F., & Bouchard, J. P. (1997). Role of the striatum, cerebellum, and frontal lobes in the learning of a visuomotor sequence. Brain Cogn, 34, 218–245.

Duan, S., Anderson, C. M., Keung, E. C., Chen, Y., Chen, Y., & Swanson, R. A. (2003). P2x7 receptor-mediated release of excitatory amino acids from astrocytes. J Neurosci, 23, 1320–1328.

Eckardt, D., Theis, M., Degen, J., Ott, T., Rijen, H. V. M. v., Kirchhoff, S., Kim, J.-S., Bakker, J. M. T. d., & Willecke, K. (2004). Functional role of connexin43 gap junction channels in adult mouse heart assessed by inducible gene deletion. J Mol Cell Cardiol, 36, 101–110.

Eddleston, M. & Mucke, L. (1993). Molecular profile of reactive astrocytes–implications for their role in neurologic disease. Neuroscience, 54, 15–36.

Ehninger, D. & Kempermann, G. (2008). Neurogenesis in the adult hippocampus. Cell Tissue Res, 331, 243–250.

Eng, L. F., Ghirnikar, R. S., & Lee, Y. L. (2000). Glial fibrillary acidic protein: GFAP-thirty-one years (1969-2000). Neurochem Res, 25, 1439–1451.

Engel, J. (1998). Research on the human brain in an epilepsy surgery setting. Epilepsy Res, 32, 1–11.

Eriksson, P. S., Perfilieva, E., Björk-Eriksson, T., Alborn, A. M., Nordborg, C., Peterson, D. A., & Gage, F. H. (1998). Neurogenesis in the adult human hippocampus. Nat Med, 4, 1313–1317.

Feil, R., Brocard, J., Mascrez, B., LeMeur, M., Metzger, D., & Chambon, P. (1996). Ligand-activated site-specific recombination in mice. Proc Natl Acad Sci U S A, 93, 10887–10890.

Feil, R., Wagner, J., Metzger, D., & Chambon, P. (1997). Regulation of Cre recombinase activity by mutated estrogen receptor ligand-binding domains. Biochem Biophys Res Commun, 237, 752–757.

Feng, L., Hatten, M. E., & Heintz, N. (1994). Brain lipid-binding protein (BLBP): a novel signaling system in the developing mammalian CNS. Neuron, 12, 895–908.

Ferri, C. P., Prince, M., Brayne, C., Brodaty, H., Fratiglioni, L., Ganguli, M., Hall, K., Hasegawa, K., Hendrie, H., Huang, Y., Jorm, A., Mathers, C., Menezes, P. R., Rimmer, E., Scazufca, M., & International, A. D. (2005). Global prevalence of dementia: a Delphi consensus study. Lancet, 366, 2112–2117.

Furness, D. N., Dehnes, Y., Akhtar, A. Q., Rossi, D. J., Hamann, M., Grutle, N. J., Gundersen, V., Holmseth, S., Lehre, K. P., Ullensvang, K., Wojewodzic, M., Zhou, Y., Attwell, D., & Danbolt, N. C. (2008). A quantitative assessment of glutamate uptake into hippocampal synaptic terminals and astrocytes: new insights into a neuronal role for excitatory amino acid transporter 2 (EAAT2). Neuroscience, 157, 80–94.

Goldman, S. A. & Nottebohm, F. (1983). Neuronal production, migration, and differentiation in a vocal control nucleus of the adult female canary brain. Proc Natl Acad Sci U S A, 80, 2390–2394.

Goodenough, D. A., Paul, D. L., & Jesaitis, L. (1988). Topological distribution of two connexin32 antigenic sites in intact and split rodent hepatocyte gap junctions. J Cell Biol, 107, 1817–1824.

Gosejacob, D., Dublin, P., Bedner, P., Hüttmann, K., Zhang, J., Tress, O., Willecke, K., Pfrieger, F., Steinhäuser, C., & Theis, M. (2011). Role of astroglial connexin30 in hippocampal gap junction coupling. Glia, 59, 511–519.

Grosche, J., Kettenmann, H., & Reichenbach, A. (2002). Bergmann glial cells form distinct morphological structures to interact with cerebellar neurons. J Neurosci Res, 68, 138–149.

Gu, H., Marth, J. D., Orban, P. C., Mossmann, H., & Rajewsky, K. (1994). Deletion of a DNA polymerase beta gene segment in T cells using cell type-specific gene targeting. Science, 265, 103–106.

Guo, F., Gopaul, D. N., & van Duyne, G. D. (1997). Structure of Cre recombinase complexed with DNA in a site-specific recombination synapse. Nature, 389, 40–46.

Hafting, T., Fyhn, M., Molden, S., Moser, M.-B., & Moser, E. I. (2005). Microstructure of a spatial map in the entorhinal cortex. Nature, 436, 801–806.

Hameyer, D., Loonstra, A., Eshkind, L., Schmitt, S., Antunes, C., Groen, A., Bindels, E., Jonkers, J., Krimpenfort, P., Meuwissen, R., Rijswijk, L., Bex,

A., Berns, A., & Bockamp, E. (2007). Toxicity of ligand-dependent Cre recombinases and generation of a conditional Cre deleter mouse allowing mosaic recombination in peripheral tissues. Physiol Genomics, 31, 32–41.

Hanisch, U.-K. & Kettenmann, H. (2007). Microglia: active sensor and versatile effector cells in the normal and pathologic brain. Nat Neurosci, 10, 1387–1394.

Harris, A. L. (2001). Emerging issues of connexin channels: biophysics fills the gap. Q Rev Biophys, 34, 325–472.

Haugeto, O., Ullensvang, K., Levy, L. M., Chaudhry, F. A., Honoré, T., Nielsen, M., Lehre, K. P., & Danbolt, N. C. (1996). Brain glutamate transporter proteins form homomultimers. J Biol Chem, 271, 27715–27722.

Hayashi, S. & McMahon, A. P. (2002). Efficient recombination in diverse tissues by a tamoxifen-inducible form of Cre: a tool for temporally regulated gene activation/inactivation in the mouse. Dev Biol, 244, 305–318.

Hebert, L. E., Scherr, P. A., Bienias, J. L., Bennett, D. A., & Evans, D. A. (2003). Alzheimer disease in the US population: prevalence estimates using the 2000 census. Arch Neurol, 60, 1119–1122.

Heinemann, U. & Lux, H. D. (1977). Ceiling of stimulus induced rises in extracellular potassium concentration in the cerebral cortex of cat. Brain Res, 120, 231–249.

Heinrich, C., Nitta, N., Flubacher, A., Müller, M., Fahrner, A., Kirsch, M., Freiman, T., Suzuki, F., Depaulis, A., Frotscher, M., & Haas, C. A. (2006). Reelin deficiency and displacement of mature neurons, but not neurogenesis, underlie the formation of granule cell dispersion in the epileptic hippocampus. J Neurosci, 26, 4701–4713.

Higashi, K., Fujita, A., Inanobe, A., Tanemoto, M., Doi, K., Kubo, T., & Kurachi, Y. (2001). An inwardly rectifying K^+ channel, Kir4.1, expressed in astrocytes surrounds synapses and blood vessels in brain. Am J Physiol Cell Physiol, 281, C922–C931.

Hirasawa, T., Ohsawa, K., Imai, Y., Ondo, Y., Akazawa, C., Uchino, S., & Kohsaka, S. (2005). Visualization of microglia in living tissues using Iba1-EGFP transgenic mice. J Neurosci Res, 81, 357–362.

Hirrlinger, P. G., Scheller, A., Braun, C., Hirrlinger, J., & Kirchhoff, F. (2006). Temporal control of gene recombination in astrocytes by transgenic expression of the tamoxifen-inducible DNA recombinase variant CreERT2. Glia, 54, 11–20.

Hoh, J. H., Sosinsky, G. E., Revel, J. P., & Hansma, P. K. (1993). Structure of the extracellular surface of the gap junction by atomic force microscopy. Biophys J, 65, 149–163.

Houades, V., Koulakoff, A., Ezan, P., Seif, I., & Giaume, C. (2008). Gap junction-mediated astrocytic networks in the mouse barrel cortex. J Neurosci, 28, 5207–5217.

Houser, C. R. (1990). Granule cell dispersion in the dentate gyrus of humans with temporal lobe epilepsy. Brain Res, 535, 195–204.

Iadecola, C. & Nedergaard, M. (2007). Glial regulation of the cerebral microvasculature. Nat Neurosci, 10, 1369–1376.

Imai, Y., Ibata, I., Ito, D., Ohsawa, K., & Kohsaka, S. (1996). A novel gene iba1 in the major histocompatibility complex class III region encoding an EF hand protein expressed in a monocytic lineage. Biochem Biophys Res Commun, 224, 855–862.

Insanti, R. & Amaral, D. G. (2004). The Human Nervous System, Second Edition, chap. Hippocampal Formation, pp. 872–915. (Academic Press).

Isobe, I., Watanabe, T., Yotsuyanagi, T., Hazemoto, N., Yamagata, K., Ueki, T., Nakanishi, K., Asai, K., & Kato, T. (1996). Astrocytic contributions to blood-brain barrier (BBB) formation by endothelial cells: a possible use of aortic endothelial cell for in vitro BBB model. Neurochem Int, 28, 523–533.

Jabs, R., Pivneva, T., Hüttmann, K., Wyczynski, A., Nolte, C., Kettenmann, H., & Steinhäuser, C. (2005). Synaptic transmission onto hippocampal glial cells with hGFAP promoter activity. J Cell Sci, 118, 3791–3803.

Jakovcevic, D. & Harder, D. R. (2007). Role of astrocytes in matching blood flow to neuronal activity. Curr Top Dev Biol, 79, 75–97.

Joyner, A. L. & Sudarov, A. (2011). The Mouse Nervous System, chap. Genetic Neuroanatomy., pp. 36–50. (Academic Press).

Kaas, J. H. (2004). The Human Nervous System, Second Edition, chap. Somatosensory System, pp. 1059–1092. (Academic Press).

Kandel, E., Schwartz, J., & Jessell, T. (2000). Principles of Neural Science. (McGraw-Hill Medical).

Kang, J., Jiang, L., Goldman, S. A., & Nedergaard, M. (1998). Astrocyte-mediated potentiation of inhibitory synaptic transmission. Nat Neurosci, 1, 683–692.

Karram, K., Goebbels, S., Schwab, M., Jennissen, K., Seifert, G., Steinhäuser, C., Nave, K.-A., & Trotter, J. (2008). NG2-expressing cells in the nervous system revealed by the NG2-EYFP-knockin mouse. Genesis, 46, 743–757.

Kemp, R., Ireland, H., Clayton, E., Houghton, C., Howard, L., & Winton, D. J. (2004). Elimination of background recombination: somatic induction of cre by combined transcriptional regulation and hormone binding affinity. Nucleic Acids Res, 32, e92.

Kempermann, G., Jessberger, S., Steiner, B., & Kronenberg, G. (2004). Milestones of neuronal development in the adult hippocampus. Trends Neurosci, 27, 447–452.

Kempermann, G., Kuhn, H. G., & Gage, F. H. (1997). Genetic influence on neurogenesis in the dentate gyrus of adult mice. Proc Natl Acad Sci U S A, 94, 10409–10414.

Kimelberg, H. K., Goderie, S. K., Higman, S., Pang, S., & Waniewski, R. A. (1990). Swelling-induced release of glutamate, aspartate, and taurine from astrocyte cultures. J Neurosci, 10, 1583–1591.

Kingham, P. J., Cuzner, M. L., & Pocock, J. M. (1999). Apoptotic pathways mobilized in microglia and neurones as a consequence of chromogranin a-induced microglial activation. J Neurochem, 73, 538–547.

Kofuji, P. & Newman, E. A. (2004). Potassium buffering in the central nervous system. Neuroscience, 129, 1045–1056.

Koulakoff, A., Ezan, P., & Giaume, C. (2008). Neurons control the expression of connexin 30 and connexin 43 in mouse cortical astrocytes. Glia, 56, 1299–1311.

Kronenberg, G., Reuter, K., Steiner, B., Brandt, M. D., Jessberger, S., Yamaguchi, M., & Kempermann, G. (2003). Subpopulations of proliferating cells of the adult hippocampus respond differently to physiologic neurogenic stimuli. J Comp Neurol, 467, 455–463.

Kuffler, S. W., Nicholls, J. G., & Orkand, R. K. (1966). Physiological properties of glial cells in the central nervous system of amphibia. J Neurophysiol, 29, 768–787.

Kunze, A., Congreso, M. R., Hartmann, C., Wallraff-Beck, A., Hüttmann, K., Bedner, P., Requardt, R., Seifert, G., Redecker, C., Willecke, K., Hofmann, A., Pfeifer, A., Theis, M., & Steinhäuser, C. (2009). Connexin expression by radial glia-like cells is required for neurogenesis in the adult dentate gyrus. Proc Natl Acad Sci U S A, 106, 11336–11341.

Lallemand, Y., Luria, V., Haffner-Krausz, R., & Lonai, P. (1998). Maternally expressed PGK-Cre transgene as a tool for early and uniform activation of the Cre site-specific recombinase. Transgenic Res, 7, 105–112.

Lawson, L. J., Perry, V. H., Dri, P., & Gordon, S. (1990). Heterogeneity in the distribution and morphology of microglia in the normal adult mouse brain. Neuroscience, 39, 151–170.

Lee, Y., Su, M., Messing, A., & Brenner, M. (2006). Astrocyte heterogeneity revealed by expression of a GFAP-LacZ transgene. Glia, 53, 677–687.

Liaw, S. H., Kuo, I., & Eisenberg, D. (1995). Discovery of the ammonium substrate site on glutamine synthetase, a third cation binding site. Protein Sci, 4, 2358–2365.

Liedtke, W., Edelmann, W., Chiu, F. C., Kucherlapati, R., & Raine, C. S. (1998). Experimental autoimmune encephalomyelitis in mice lacking glial fibrillary acidic protein is characterized by a more severe clinical course and an infiltrative central nervous system lesion. Am J Pathol, 152, 251–259.

Liu, Y., Wu, Y., Lee, J. C., Xue, H., Pevny, L. H., Kaprielian, Z., & Rao, M. S. (2002). Oligodendrocyte and astrocyte development in rodents: an in situ and immunohistological analysis during embryonic development. Glia, 40, 25–43.

Ludwin, S. K., Kosek, J. C., & Eng, L. F. (1976). The topographical distribution of S-100 and GFA proteins in the adult rat brain: An immunohistochemical study using horseradish peroxidase-labelled antibodies. The Journal of Comparative Neurology, 165, 197–207. s100 and gfap ref.

Makowski, L., Caspar, D. L., Phillips, W. C., & Goodenough, D. A. (1977). Gap junction structures. II. Analysis of the x-ray diffraction data. J Cell Biol, 74, 629–645.

Margerison, J. H. & Corsellis, J. A. (1966). Epilepsy and the temporal lobes. a clinical, electroencephalographic and neuropathological study of the brain in epilepsy, with particular reference to the temporal lobes. Brain, 89, 499–530.

Martin, J. (2003). Neuroanatomy: Text and Atlas. (McGraw-Hill Medical).

Matsuda, T. & Cepko, C. L. (2007). Controlled expression of transgenes introduced by in vivo electroporation. Proc Natl Acad Sci U S A, 104, 1027–1032.

Matthias, K., Kirchhoff, F., Seifert, G., Hüttmann, K., Matyash, M., Kettenmann, H., & Steinhäuser, C. (2003). Segregated expression of AMPA-type glutamate receptors and glutamate transporters defines distinct astrocyte populations in the mouse hippocampus. J Neurosci, 23, 1750–1758.

Mattioni, T., Louvion, J. F., & Picard, D. (1994). Regulation of protein activities by fusion to steroid binding domains. Methods Cell Biol, 43 Pt A, 335–352.

McEwan, N. R. (1996). 2'3'-CNPase and actin distribution in oligodendrocytes, relative to their mRNAs. Biochem Mol Biol Int, 40, 975–979.

McPhail, L. T., McBride, C. B., McGraw, J., Steeves, J. D., & Tetzlaff, W. (2004). Axotomy abolishes NeuN expression in facial but not rubrospinal neurons. Exp Neurol, 185, 182–190.

Mescher, A. (2009). Junqueira's Basic Histology, 12th Edition: Text and Atlas. (McGraw-Hill Medical).

Metzger, D., Clifford, J., Chiba, H., & Chambon, P. (1995). Conditional site-specific recombination in mammalian cells using a ligand-dependent chimeric Cre recombinase. Proc Natl Acad Sci U S A, 92, 6991–6995.

Middeldorp, J. & Hol, E. (2011). GFAP in health and disease. Progress in Neurobiology, 93, 421 – 443.

Milks, L. C., Kumar, N. M., Houghten, R., Unwin, N., & Gilula, N. B. (1988). Topology of the 32-kd liver gap junction protein determined by site-directed antibody localizations. EMBO J, 7, 2967–2975.

Ming, G. & Song, H. (2005). Adult neurogenesis in the mammalian central nervous system. Annu Rev Neurosci, 28, 223–250.

Miyake, T. & Kitamura, T. (1992). Glutamine synthetase immunoreactivity in two types of mouse brain glial cells. Brain Res, 586, 53–60.

Molinari, M., Leggio, M. G., Solida, A., Ciorra, R., Misciagna, S., Silveri, M. C., & Petrosini, L. (1997). Cerebellum and procedural learning: evidence from focal cerebellar lesions. Brain, 120 (Pt 10), 1753–1762.

Nagelhus, E. A., Horio, Y., Inanobe, A., Fujita, A., Haug, F. M., Nielsen, S., Kurachi, Y., & Ottersen, O. P. (1999). Immunogold evidence suggests that coupling of K^+ siphoning and water transport in rat retinal Müller cells is mediated by a coenrichment of Kir4.1 and AQP4 in specific membrane domains. Glia, 26, 47–54.

Nagy, A. (2000). Cre recombinase: the universal reagent for genome tailoring. Genesis, 26, 99–109.

Nagy, J. I., Li, X., Rempel, J., Stelmack, G., Patel, D., Staines, W. A., Yasumura, T., & Rash, J. E. (2001). Connexin26 in adult rodent central nervous system: demonstration at astrocytic gap junctions and colocalization with connexin30 and connexin43. J Comp Neurol, 441, 302–323.

Nagy, J. I., Lynn, B. D., Tress, O., Willecke, K., & Rash, J. E. (2011). Connexin26 expression in brain parenchymal cells demonstrated by targeted connexin ablation in transgenic mice. Eur J Neurosci, 34, 263–271.

Nagy, J. I., Patel, D., Ochalski, P. A., & Stelmack, G. L. (1999). Connexin30 in rodent, cat and human brain: selective expression in gray matter astrocytes, co-localization with connexin43 at gap junctions and late developmental appearance. Neuroscience, 88, 447–468.

Neusch, C., Papadopoulos, N., Müller, M., Maletzki, I., Winter, S. M., Hirrlinger, J., Handschuh, M., Bähr, M., Richter, D. W., Kirchhoff, F., & Hülsmann, S. (2006). Lack of the Kir4.1 channel subunit abolishes K^+ buffering properties of astrocytes in the ventral respiratory group: impact on extracellular K^+ regulation. J Neurophysiol, 95, 1843–1852.

Newman, E. A., Frambach, D. A., & Odette, L. L. (1984). Control of extracellular potassium levels by retinal glial cell K^+ siphoning. Science, 225, 1174–1175.

Nieuwenhuys, R., Voogd, J., & van Huijzen, C. (2007). The Human Central Nervous System: A Synopsis and Atlas. (Steinkopff).

Nishiyama, A. (2001). Ng2 cells in the brain: a novel glial cell population. Hum Cell, 14, 77–82.

Nishiyama, A., Komitova, M., Suzuki, R., & Zhu, X. (2009). Polydendrocytes (NG2 cells): multifunctional cells with lineage plasticity. Nat Rev Neurosci, 10, 9–22.

Nishiyama, A., Lin, X. H., Giese, N., Heldin, C. H., & Stallcup, W. B. (1996). Co-localization of NG2 proteoglycan and PDGF alpha-receptor on O2A progenitor cells in the developing rat brain. J Neurosci Res, 43, 299–314.

Nishiyama, A., Watanabe, M., Yang, Z., & Bu, J. (2002). Identity, distribution, and development of polydendrocytes: NG2-expressing glial cells. J Neurocytol, 31, 437–455.

Norenberg, M. D. & Martinez-Hernandez, A. (1979). Fine structural localization of glutamine synthetase in astrocytes of rat brain. Brain Res, 161, 303–310.

Ogata, K. & Kosaka, T. (2002). Structural and quantitative analysis of astrocytes in the mouse hippocampus. Neuroscience, 113, 221–233.

O'Keefe, J. & Nadel, L. (1978). The Hippocampus as a Cognitive Map. (Oxford University Press, USA).

Orkand, R. K., Nicholls, J. G., & Kuffler, S. W. (1966). Effect of nerve impulses on the membrane potential of glial cells in the central nervous system of amphibia. J Neurophysiol, 29, 788–806.

Pannasch, U., Vargová, L., Reingruber, J., Ezan, P., Holcman, D., Giaume, C., Syková, E., & Rouach, N. (2011). Astroglial networks scale synaptic activity and plasticity. Proc Natl Acad Sci U S A, 108, 8467–8472.

Paxinos, G. & Franklin, K. B. (2001). The Mouse Brain in Stereotaxic Coordinates (Deluxe Edition), Second Edition. (Academic Press).

Pekny, M., Stanness, K. A., Eliasson, C., Betsholtz, C., & Janigro, D. (1998). Impaired induction of blood-brain barrier properties in aortic endothelial cells by astrocytes from GFAP-deficient mice. Glia, 22, 390–400.

Pellerin, L. & Magistretti, P. J. (1994). Glutamate uptake into astrocytes stimulates aerobic glycolysis: a mechanism coupling neuronal activity to glucose utilization. Proc Natl Acad Sci U S A, 91, 10625–10629.

Perry, V. H., Hume, D. A., & Gordon, S. (1985). Immunohistochemical localization of macrophages and microglia in the adult and developing mouse brain. Neuroscience, 15, 313–326.

Peters, A. (2004). A fourth type of neuroglial cell in the adult central nervous system. Journal of Neurocytology, 33, 345–357.

Picard, D. (1994). Regulation of protein function through expression of chimaeric proteins. Curr Opin Biotechnol, 5, 511–515.

Pinto, L. & Götz, M. (2007). Radial glial cell heterogeneity–the source of diverse progeny in the CNS. Prog Neurobiol, 83, 2–23.

R Development Core Team (2010). R: A Language and Environment for Statistical Computing. R Foundation for Statistical Computing, Vienna, Austria. ISBN 3-900051-07-0.

Rash, J. E. (2010). Molecular disruptions of the panglial syncytium block potassium siphoning and axonal saltatory conduction: pertinence to neuromyelitis optica and other demyelinating diseases of the central nervous system. Neuroscience, 168, 982–1008.

Rash, J. E., Yasumura, T., Davidson, K. G., Furman, C. S., Dudek, F. E., & Nagy, J. I. (2001). Identification of cells expressing Cx43, Cx30, Cx26, Cx32 and Cx36 in gap junctions of rat brain and spinal cord. Cell Commun Adhes, 8, 315–320.

Reaume, A. G., de Sousa, P. A., Kulkarni, S., Langille, B. L., Zhu, D., Davies, T. C., Juneja, S. C., Kidder, G. M., & Rossant, J. (1995). Cardiac malformation in neonatal mice lacking connexin43. Science, 267, 1831–1834.

Reichenbach, A. & Wolburg, H. (2005). Neuroglia, chap. Astrocytes and ependymal glia., pp. 19–35. (Oxford University Press).

Requardt, R. P., Kaczmarczyk, L., Dublin, P., Wallraff-Beck, A., Mikeska, T., Degen, J., Waha, A., Steinhäuser, C., Willecke, K., & Theis, M. (2009). Quality control of astrocyte-directed cre transgenic mice: the benefits of a direct link between loss of gene expression and reporter activation. Glia, 57, 680–692.

Rivers, L. E., Young, K. M., Rizzi, M., Jamen, F., Psachoulia, K., Wade, A., Kessaris, N., & Richardson, W. D. (2008). PDGFRA/NG2 glia generate myelinating oligodendrocytes and piriform projection neurons in adult mice. Nat Neurosci, 11, 1392–1401.

Rosenbaum, R. S., Priselac, S., Köhler, S., Black, S. E., Gao, F., Nadel, L., & Moscovitch, M. (2000). Remote spatial memory in an amnesic person with extensive bilateral hippocampal lesions. Nat Neurosci, 3, 1044–1048.

Rouach, N., Koulakoff, A., Abudara, V., Willecke, K., & Giaume, C. (2008). Astroglial metabolic networks sustain hippocampal synaptic transmission. Science, 322, 1551–1555.

Sander, J. W. (2003). The epidemiology of epilepsy revisited. Curr Opin Neurol, 16, 165–170.

Sauer, B. & Henderson, N. (1988). Site-specific DNA recombination in mammalian cells by the Cre recombinase of bacteriophage P1. Proc Natl Acad Sci U S A, 85, 5166–5170.

Schulz, T. J., Glaubitz, M., Kuhlow, D., Thierbach, R., Birringer, M., Steinberg, P., Pfeiffer, A. F. H., & Ristow, M. (2007). Variable expression of Cre recombinase transgenes precludes reliable prediction of tissue-specific gene disruption by tail-biopsy genotyping. PLoS One, 2, e1013.

Schutter, D. J. L. G. & van Honk, J. (2005). The cerebellum on the rise in human emotion. Cerebellum, 4, 290–294.

Schwenk, F., Baron, U., & Rajewsky, K. (1995). A Cre-transgenic mouse strain for the ubiquitous deletion of loxP-flanked gene segments including deletion in germ cells. Nucleic Acids Res, 23, 5080–5081.

Sáez, J. C., Connor, J. A., Spray, D. C., & Bennett, M. V. (1989). Hepatocyte gap junctions are permeable to the second messenger, inositol 1,4,5-trisphosphate, and to calcium ions. Proc Natl Acad Sci U S A, 86, 2708–2712.

Shapiro, L. A., Korn, M. J., Shan, Z., & Ribak, C. E. (2005). GFAP-expressing radial glia-like cell bodies are involved in a one-to-one relationship with doublecortin-immunolabeled newborn neurons in the adult dentate gyrus. Brain Res, 1040, 81–91.

Söhl, G. & Willecke, K. (2003). An update on connexin genes and their nomenclature in mouse and man. Cell Commun Adhes, 10, 173–180.

Simard, M. & Nedergaard, M. (2004). The neurobiology of glia in the context of water and ion homeostasis. Neuroscience, 129, 877–896.

Simons, D. J. & Woolsey, T. A. (1984). Morphology of Golgi-Cox-impregnated barrel neurons in rat SmI cortex. J Comp Neurol, 230(1), 119–32.

Simpson, I., Rose, B., & Loewenstein, W. R. (1977). Size limit of molecules permeating the junctional membrane channels. Science, 195, 294–296.

Slepko, N. & Levi, G. (1996). Progressive activation of adult microglial cells in vitro. Glia, 16, 241–246.

Slezak, M., Göritz, C., Niemiec, A., Frisén, J., Chambon, P., Metzger, D., & Pfrieger, F. W. (2007). Transgenic mice for conditional gene manipulation in astroglial cells. Glia, 55, 1565–1576.

Slezak, M. & Pfrieger, F. W. (2003). New roles for astrocytes: regulation of CNS synaptogenesis. Trends Neurosci, 26, 531–535.

Smith, L. (2011). Good planning and serendipity: exploiting the Cre/Lox system in the testis. Reproduction, 141, 151–161.

Soriano, P. (1999). Generalized lacZ expression with the ROSA26 Cre reporter strain. Nat Genet, 21, 70–71.

Squire, L. R. & Zola, S. M. (1997). Amnesia, memory and brain systems. Philos Trans R Soc Lond B Biol Sci, 352, 1663–1673.

Srinivas, S., Watanabe, T., Lin, C. S., William, C. M., Tanabe, Y., Jessell, T. M., & Costantini, F. (2001). Cre reporter strains produced by targeted insertion of EYFP and ECFP into the ROSA26 locus. BMC Dev Biol, 1, 4.

Steiner, B., Zurborg, S., Hörster, H., Fabel, K., & Kempermann, G. (2008). Differential 24 h responsiveness of Prox1-expressing precursor cells in adult hippocampal neurogenesis to physical activity, environmental enrichment, and kainic acid-induced seizures. Neuroscience, 154, 521–529.

Stichel, C. C., Müller, C. M., & Zilles, K. (1991). Distribution of glial fibrillary acidic protein and vimentin immunoreactivity during rat visual cortex development. J Neurocytol, 20, 97–108.

Streit, W. J. (1990). An improved staining method for rat microglial cells using the lectin from Griffonia simplicifolia (GSA I-B4). J Histochem Cytochem, 38, 1683–1686.

Streit, W. J., Graeber, M. B., & Kreutzberg, G. W. (1988). Functional plasticity of microglia: a review. Glia, 1, 301–307.

Syková, E. (1981). K^+ changes in the extracellular space of the spinal cord and their physiological role. J Exp Biol, 95, 93–109.

Syková, E. & Chvátal, A. (1993). Extracellular ionic and volume changes: the role in glia-neuron interaction. J Chem Neuroanat, 6, 247–260.

Szatkowski, M., Barbour, B., & Attwell, D. (1990). Non-vesicular release of glutamate from glial cells by reversed electrogenic glutamate uptake. Nature, 348, 443–446.

Taube, J. S., Muller, R. U., & Ranck, J. B. (1990). Head-direction cells recorded from the postsubiculum in freely moving rats. i. description and quantitative analysis. J Neurosci, 10, 420–435.

Taupin, P. (2008). The Hippocampus: Neurotransmission and Plasticity in the Nervous System, chap. The Hippocampus, pp. 3–12. (Nova Science Publishers).

Teng, E. & Squire, L. R. (1999). Memory for places learned long ago is intact after hippocampal damage. Nature, 400, 675–677.

Teubner, B., Michel, V., Pesch, J., Lautermann, J., Cohen-Salmon, M., Söhl, G., Jahnke, K., Winterhager, E., Herberhold, C., Hardelin, J.-P., Petit, C., & Willecke, K. (2003). Connexin30 (Gjb6)-deficiency causes severe hearing impairment and lack of endocochlear potential. Hum Mol Genet, 12, 13–21.

Theis, M., de Wit, C., Schlaeger, T. M., Eckardt, D., Krüger, O., Döring, B., Risau, W., Deutsch, U., Pohl, U., & Willecke, K. (2001a). Endothelium-specific replacement of the connexin43 coding region by a lacz reporter gene. Genesis, 29, 1–13.

Theis, M., Jauch, R., Zhuo, L., Speidel, D., Wallraff, A., Döring, B., Frisch, C., Söhl, G., Teubner, B., Euwens, C., Huston, J., Steinhäuser, C., Messing, A., Heinemann, U., & Willecke, K. (2003). Accelerated hippocampal spreading depression and enhanced locomotory activity in mice with astrocyte-directed inactivation of connexin43. J Neurosci, 23, 766–776.

Theis, M., Mas, C., Döring, B., Krüger, O., Herrera, P., Meda, P., & Willecke, K. (2001b). General and conditional replacement of connexin43-coding DNA by a lacZ reporter gene for cell-autonomous analysis of expression. Cell Commun Adhes, 8, 383–386.

Theis, M., Söhl, G., Eiberger, J., & Willecke, K. (2005). Emerging complexities in identity and function of glial connexins. Trends Neurosci, 28, 188–195.

Tracey, D. (2004). The Rat Nervous System, Third Edition , chap. Somatosensory System, pp. 797–815. (Academic Press).

Tulving, E. (1972). Organization of Memory, chap. Episodic and semantic memory, pp. 381–402. (New York: Academic Press.).

Ullian, E. M., Sapperstein, S. K., Christopherson, K. S., & Barres, B. A. (2001). Control of synapse number by glia. Science, 291, 657–661.

Unal-Cevik, I., Kilinç, M., Gürsoy-Ozdemir, Y., Gurer, G., & Dalkara, T. (2004). Loss of NeuN immunoreactivity after cerebral ischemia does not indicate neuronal cell loss: a cautionary note. Brain Res, 1015, 169–174.

Vaughan, D. W. & Peters, A. (1974). Neuroglial cells in the cerebral cortex of rats from young adulthood to old age: an electron microscope study. J Neurocytol, 3, 405–429.

Verkhratsky, A. & Kirchhoff, F. (2007). NMDA Receptors in glia. Neuroscientist, 13, 28–37.

Verkhratsky, A. & Steinhäuser, C. (2000). Ion channels in glial cells. Brain Res Brain Res Rev, 32, 380–412.

Verkhratsky, P. A. & Butt, A. (2007). Glial Neurobiology. (Wiley).

Volterra, A. & Steinhäuser, C. (2004). Glial modulation of synaptic transmission in the hippocampus. Glia, 47, 249–257.

von Bohlen Und Halbach, O. (2007). Immunohistological markers for staging neurogenesis in adult hippocampus. Cell Tissue Res, 329, 409–420.

Wallraff, A., Köhling, R., Heinemann, U., Theis, M., Willecke, K., & Steinhäuser, C. (2006). The impact of astrocytic gap junctional coupling on potassium buffering in the hippocampus. J Neurosci, 26, 5438–5447.

Wallraff, A., Odermatt, B., Willecke, K., & Steinhäuser, C. (2004). Distinct types of astroglial cells in the hippocampus differ in gap junction coupling. Glia, 48, 36–43.

Welker, C. & Woolsey, T. A. (1974). Structure of layer iv in the somatosensory neocortex of the rat: description and comparison with the mouse. J Comp Neurol, 158, 437–453.

Wise, S. P. & Jones, E. G. (1978). Developmental studies of thalamocortical and commissural connections in the rat somatic sensory cortex. J Comp Neurol, 178, 187–208.

Woolsey, T. A. & der Loos, H. V. (1970). The structural organization of layer IV in the somatosensory region (SI) of mouse cerebral cortex. The description of a cortical field composed of discrete cytoarchitectonic units. Brain Res, 17, 205–242. barrel cortex.

Woolsey, T. A., Welker, C., & Schwartz, R. H. (1975). Comparative anatomical studies of the SmL face cortex with special reference to the occurrence of "barrels" in layer IV. J Comp Neurol, 164, 79–94. Barrel cortex.

Wu, W.-P., Xu, X.-J., & Hao, J.-X. (2004). Chronic lumbar catheterization of the spinal subarachnoid space in mice. J Neurosci Methods, 133, 65–69.

Yamamoto, T., Ochalski, A., Hertzberg, E. L., & Nagy, J. I. (1990a). LM and EM immunolocalization of the gap junctional protein connexin 43 in rat brain. Brain Res, 508, 313–319.

Yamamoto, T., Ochalski, A., Hertzberg, E. L., & Nagy, J. I. (1990b). On the organization of astrocytic gap junctions in rat brain as suggested by LM and EM immunohistochemistry of connexin43 expression. J Comp Neurol, 302, 853–883.

Yancey, S. B., John, S. A., Lal, R., Austin, B. J., & Revel, J. P. (1989). The 43-kD polypeptide of heart gap junctions: immunolocalization, topology, and functional domains. J Cell Biol, 108, 2241–2254.

Yokoo, H., Nobusawa, S., Takebayashi, H., Ikenaka, K., Isoda, K., Kamiya, M., Sasaki, A., Hirato, J., & Nakazato, Y. (2004). Anti-human Olig2 antibody as a useful immunohistochemical marker of normal oligodendrocytes and gliomas. Am J Pathol, 164, 1717–1725.

Zhuo, L., Theis, M., Alvarez-Maya, I., Brenner, M., Willecke, K., & Messing, A. (2001). hGFAP-cre transgenic mice for manipulation of glial and neuronal function in vivo. Genesis, 31, 85–94.

Zimmer, D. B., Green, C. R., Evans, W. H., & Gilula, N. B. (1987). Topological analysis of the major protein in isolated intact rat liver gap junctions and gap junction-derived single membrane structures. J Biol Chem, 262, 7751–7763.

List of Figures

List of Tables

Appendix B

List of publications

Dominic Gosejacob*, Pavel Dublin*, Peter Bedner, Kerstin Hüttmann, Jiong Zhang, Oliver Tress, Klaus Willecke, Frank Pfrieger, Christian Steinhäuser, and Martin Theis. Role of astroglial connexin30 in hippocampal gap junction coupling. *Glia*, 59(3):511–519, Mar 2011. (*equally contributing first author)

Robert Pascal Requardt, Lech Kaczmarczyk, Pavel Dublin, Anke Wallraff-Beck, Thomas Mikeska, Joachim Degen, Andreas Waha, Christian Steinhäuser, Klaus Willecke, and Martin Theis. Quality control of astrocyte-directed cre transgenic mice: the benefits of a direct link between loss of gene expression and reporter activation.*Glia*, 57(6):680–692, Apr 2009.

Pavel Dublin and Menachem Hanani. Satellite glial cells in sensory ganglia: their possible contribution to inflammatory pain. *Brain Behav Immun*, 21(5):592–598, Jul 2007. (From master thesis)

Joachim Degen*, Pavel Dublin*, Jiong Zhang, Radoslaw Dobrowolski, Melanie Jokwitz, Klaus Willecke, Ronald Jabs, Christian Steinhäuser, Martin Theis, Dual Reporter Approaches for Identification of Cre Efficacy and Astrocyte Heterogeneity. *Submitted* (*equally contributing first author)

Jiong Zhang, Pavel Dublin, Alexandra Klein, Bernd Fleischmann, Christian Steinhäuser, Martin Theis. Ectopic recombination activity of a widely used hGFAP-Cre transgene *Submitted*

Selected Abstracts

Pavel Dublin, Dominic Gosejacob, Peter Bedner, Kerstin Hüttemann, Jiong Zhang, Oliver Tress, Klaus Willecke, Frank W. Pfrieger, Christian Steinhäuser, Martin Theis Comparative analysis of connexin43 and connexin30 expression across brain areas by reporter gene approaches and fate-mapping analysis.

International Gap Junction Conference 2011, Ghent

Pavel Dublin, Joachim Degen, Peter Bedner, Kerstin Hüttmann, Mercedeh Khoshvaghti, Panos Theofilas, Simon Hoeft, Radek Dobrowolski, Melanie Jokwitz, Khalad Karram, Jacqueline Trotter, Gerald Seifert, Ronald Jabs, Amin Derouiche,Christian Steinhäuser, Klaus Willecke, Martin Theis. A new transgenic mouse line expressing the enhanced cyan fluorescent protein (ECFP) instead of Gja1 (Cx43) for in vivo labelling of astrocytes, multiple reporter gene approaches and the study of translational regulation *Bonner Forum Biomedicine,Bonn,2010*

P. Dublin, P. Bedner, K. Hüttmann, C. Steinhäuser, M. Theis Role of glial gap junctional coupling in development and progression of epilepsy *Young neuroscientist Congress,Neuro-Visionen 5,Bochum,2009* Pavel Dublin, Joachim Degen, Peter Bedner, Kerstin Hüttmann, Mercedeh Khoshvaghti, Panos Theofilas, Simon Hoeft, Radek Dobrowolski, Melanie Jokwitz, Khalad Karram, Jacqueline Trotter, Gerald Seifert, Ronald Jabs, Amin Derouiche,Christian Steinhäuser, Klaus Willecke, Martin Theis

A new transgenic mouse line expressing the enhanced cyan fluorescent protein (ECFP) instead of Gja1 (Cx43) for in vivo labelling of astrocytes, multiple reporter gene approaches and the study of translational regulation.*International Gap Junction Conference 2009, Sedona*

Dublin P., Bedner P., Degen J., Kaczmarczyk L., Theofilas P., Derouiche A., Willecke K., Steinhäuser C., Theis M., Comparison of cx43 knock-in reporter mice to investigate translational regulation of Cx43 in the central nervous system. *Meeting of the German Neuroscience Society, Göttingen, 2009*